ENGINEERING LIBRARY

Electrochemical Society

November 1956

LIBRARY
UNIVERSITY OF UTAH
NOV 26 1956
SALT LAKE CITY

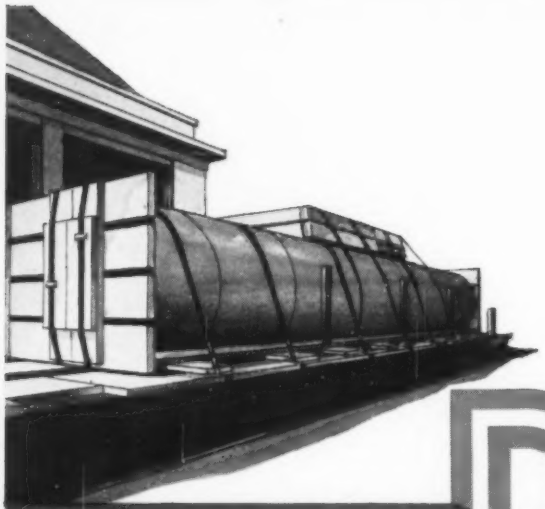

AS PARTNERS IN
YOUR PROGRESS . . .

OUR CAREFUL PACKAGING
– is a *plus* factor!

The painstaking care with which GLC carbon and graphite products are prepared for shipment is typical of the interest taken by our personnel—all along the line—to achieve unsurpassed quality.

The earnestness with which our people tackle their jobs —whether the task be large or small—is a substantial *plus factor* in the dependability of GLC electrodes, anodes, carbon brick and mold stock.

The high degree of integration between discoveries in our research laboratories, refinements in processing raw materials, and improved manufacturing techniques is further assurance of excellent product performance.

ELECTRODE
GLC®
DIVISION

Great Lakes Carbon Corporation

GRAPHITE ELECTRODES, ANODES, MOLDS and SPECIALTIES

ADMINISTRATIVE OFFICE: 18 East 48th Street, New York 17, N.Y. PLANTS: Niagara Falls, N.Y., Morganton, N. C. OTHER OFFICES: Niagara Falls, N.Y. Oak Park, Ill., Pittsburgh, Pa. SALES AGENTS: J. B. Hayes Company, Birmingham, Ala., George O. O'Hara, Wilmington, Cal. SALES AGENTS IN OTHER COUNTRIES: Great Northern Carbon & Chemical Co., Ltd., Montreal, Canada; Great Eastern Carbon & Chemical Co., Inc., Chiyoda-Ku, Tokyo, Japan

EDITORIAL STAFF

R. M. Burns, *Chairman*
Cecil V. King, *Editor*
Norman Hackerman, *Technical Editor*
Ruth G. Sterns, *Managing Editor*
U. B. Thomas, *News Editor*
Natalie Michalski, *Assistant Editor*
Eleanor Blair, *Assistant Editor*

DIVISIONAL EDITORS

W. C. Vosburgh, *Battery*
J. E. Draley, *Corrosion*
John J. Chapman, *Electric Insulation*
Abner Brenner, *Electrodeposition*
H. C. Froelich, *Electronics*
Herbert Bandes, *Electronics—Semiconductors*
Sherlock Swann, Jr., *Electro-Organic*
John M. Blocher, Jr., *Electrothermics and Metallurgy, I*
A. U. Seybolt, *Electrothermics and Metallurgy, II*
W. C. Gardiner, *Industrial Electrolytic*
C. W. Tobias, *Theoretical*

REGIONAL EDITORS

Howard T. Francis, *Chicago*
Joseph Schulein, *Pacific Northwest*
J. C. Schumacher, *Los Angeles*
G. W. Heise, *Cleveland*
G. H. Fetterley, *Niagara Falls*
Oliver Osborn, *Houston*
Earl A. Gulbransen, *Pittsburgh*
A. C. Holm, *Canada*
J. W. Cuthbertson, *Great Britain*
T. L. Rama Char, *India*

ADVERTISING OFFICE

Jack Bain, *Advertising Manager*
545 Fifth Avenue, New York 17, N. Y.

ECS OFFICERS

Hans Thurnauer, *President*
Minnesota Mining & Mfg. Co., St. Paul, Minn.

Norman Hackerman, *Vice-President*
University of Texas, Austin, Texas

Sherlock Swann, Jr., *Vice-President*
University of Illinois, Urbana, Ill.

W. C. Gardiner, *Vice-President*
Olin Mathieson Chemical Corp., Niagara Falls, N. Y.

Lyle I. Gilbertson, *Treasurer*
Air Reduction Co., Murray Hill, N. J.

Henry B. Linford, *Secretary*
Columbia University, New York, N. Y.

Journal of the
Electrochemical Society

NOVEMBER 1956 **VOL. 103 • NO. 11**

CONTENTS

Editorial

Semiconductors. *H. Bandes* 243C

Technical Papers

Depth of Surface Damage Due to Abrasion on Germanium. *T. M. Buck and F. S. McKim* 593

Solid Solubilities and Electrical Properties of Tin in Germanium Single Crystals. *F. A. Trumbore* 597

A Shot Tower for Producing Germanium Doping Pellets of Uniform Composition. *I. A. Lesk* 601

Hydrogen and Oxygen in Single-Crystal Germanium as Determined by Vacuum Fusion Gas Analysis. *C. D. Thurmond, W. G. Guldner, and A. L. Beach* 603

Adsorption of Sodium Ions by Germanium Surfaces. *S. P. Wolsky, P. M. Rodriguez, and Worden Waring* 606

New Semiconductors with the Chalcopyrite Structure. *I. G. Austin, C. H. L. Goodman, and A. E. Pengelly* 609

A Metal-Semiconductor Capacitor. *R. L. Taylor and H. E. Haring* 611

Effect of Oxygen Pressure on the Oxidation Rate of Cobalt. *D. W. Bridges, J. P. Baur, and W. M. Fassell, Jr.* 614

Kinetics of Formation of Porous or Partially Detached Scales. *C. E. Birchenall* 619

Mass Spectrometric Examination of Hydrogen in Chromium-Plated Steel. *Charles Levy and G. A. Consolazio* 624

Formation of Composite Scales Consisting of Oxides of Different Metals. *Carl Wagner* 627

Conductances of Some Acids, Bromides, and Picrates in Dimethylformamide at 25°C. *P. G. Sears, R. K. Wolford, and L. R. Dawson* 633

Technical Review

Rectifying Semiconductor Contacts. *H. K. Henisch* 637

Current Affairs

News Notes in the Electrochemical Field 246C
Section News 248C
New Members 248C
Book Reviews 250C
Announcements from Publishers 252C
Literature from Industry 252C

Published monthly by The Electrochemical Society, Inc., Mount Royal and Guilford Aves., Baltimore 2, Md., combining the JOURNAL and TRANSACTIONS OF THE ELECTROCHEMICAL SOCIETY. Editorial offices: 216 West 102nd Street, New York 25, N. Y. Statements and opinions given in articles and papers in the JOURNAL OF THE ELECTROCHEMICAL SOCIETY are those of the contributors, and The Electrochemical Society assumes no responsibility for them. Nondeductible subscription to members $5.00; subscription to nonmembers $18.00. Single copies $1.25 to members, $1.75 to nonmembers. Copyright 1956 by The Electrochemical Society, Inc. Entered as second-class matter. November 15, 1947, at the Post Office at Baltimore, Md., under the act of August 24, 1912.

Working at the outer boundaries of knowledge

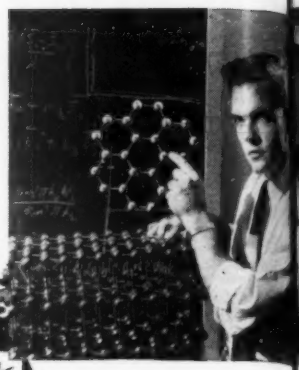

New Research Laboratories in Parma, Ohio. To expand its pioneering work in solid state and chemical physics, National Carbon Company has enlarged its staff of scientists and provided them with an ideal laboratory setup for creative work. Typical of their modern equipment is an *arc radiation furnace* used for work on high-temperature experiments. It can bring light from a carbon arc into focus on a tiny pin-point area, achieving an intensity of several hundred million foot-candles — *approaching the intensity of light near the surface of the sun.*

Mechanized tweezers handle graphite crystal. To make it into a proper experimental guinea pig, the fragile crystal must be painstakingly cut and mounted so that electrical flow can be measured along the unique crystalline directions of graphite. Experiments with pure crystals are important because all materials which we know as carbon and graphite are basically composed of the same graphite crystals being prepared here. Tremendous differences in electrical behavior, thermal conductivity, and other vital properties can be traced to variations in size and arrangement of the graphite crystals in carbon products.

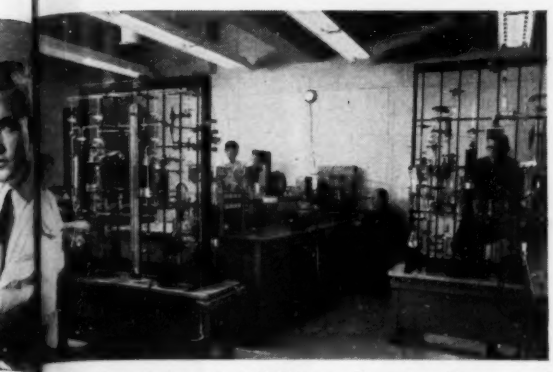

Counting holes of .000004 in. diameter. Control of porosity in original material is important in producing impervious graphite process equipment. Here, liquid mercury under pressure is used to get an accurate count of pores in each size range, down as small as four-millionths of an inch.

Counting noses with Carbon-14 atoms. Relative efficiency of a "tagged" carbon anode material is determined from amount of radioactivity in CO_2 produced by electrolysis. Measuring gas ionization, the vibrating-reed electrometer detects one radioactive molecule in a billion.

reak-through in arbon physics research

promises future advances in carbon and graphite products for the electrochemicals industry

One more barrier is down. And science strides forward in the age-old quest for deeper knowledge of carbon, one of nature's more complex puzzles.

This barrier—the inability to get large graphite crystals pure enough for experimental needs – has now been overcome by researchers of National Carbon Company. Their new annealing techniques, which remove impurities from large graphite crystals, also eliminate imperfections and weaknesses in the crystalline structure.

Several research teams at the new Parma laboratories are exploiting this break-through of science. The purified crystals are being subjected to a variety of experimental tortures—electrical, magnetic and thermal. Fundamental facts about the behavior of the single graphite crystal are being gathered and pieced together like jigsaw cutouts—building up a more complete and systematic picture. In this way, our scientists will be better able to *predict* the properties of new carbon and graphite materials.

The work on single graphite crystals is only one phase of a broad research program in carbon physics. The electrochemicals industry, large user of carbon and graphite products, will share in the gains from this work of science at the outer boundaries of knowledge. Write for a new booklet titled "Research," telling more about the work at the new Parma laboratories.

Look to **NATIONAL CARBON** *for leadership in electrolytic anodes, impervious graphite process equipment, electric furnace electrodes, and primary batteries*

ONAL CARBON COMPANY • A Division of Union Carbide and Carbon Corporation UCC **30 East 42nd Street, New York 17, N. Y.**
Offices: Atlanta, Chicago, Dallas, Kansas City, Los Angeles, New York, Pittsburgh, San Francisco. *In Canada:* Union Carbide Canada Limited, Toronto

WILEY BOOKS

Thorough. . . authoritative

1) PHOTOCONDUCTIVITY CONFERENCE

Edited by R. G. BRECKENRIDGE, National Carbon Research Laboratories, B. R. RUSSELL, The College of Wooster, and the late E. E. HAHN. With 45 contributors.

This symposium thoroughly explores the available information on photoconductivity. It includes thirty papers prepared by 45 internationally recognized authorities in the fields of solid state physics and electronics.

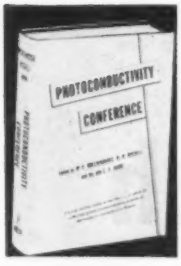

In five sections:

- **Phenomenological Theory of Photoconductivity**
- **Photon Absorption Process**
- **Electron Processes**
- **Photoconducting Materials**
- **Current Topics**

1956 653 pages 216 illus. $13.50

The most advanced information on

3) METALLURGICAL THERMOCHEMISTRY

SECOND EDITION

By O. KUBASCHEWSKI, National Physical Laboratory, Teddington, England; and E. L. L. EVANS, Chemical Research Laboratory, Teddington, England.

An invaluable aid to the research worker and metallurgist, this readable, up-to-date volume includes all the most recent data of thermochemistry organized for practical application. It recounts the latest research and experimental results, including extensive tables of thermochemical data of metal compounds only recently compiled.

Chapter by chapter, the headings are:

- **The Theoretical Basis**
- **Experimental Methods**
- **The Estimation of Thermochemical Data**
- **Thermochemical Data**
- **Examples of Thermochemical Treatment of Metallurgical Problems**

1956 410 pages Illus. $10.00

Basic, yet comprehensive

2) Introduction to SOLID STATE PHYSICS

SECOND EDITION

By CHARLES KITTEL, University of California

The new edition of this well-known work includes fuller explanations of the basic concepts, particularly in the areas of crystal symmetry and energy band theory. As before, the book offers a concise discussion of representative areas of the physics of solids, stressing elementary physical models. Numerous graphs and tables of experimental data are provided. New material is included on: diffusion, dislocations, alloys, semiconductors, photoconductivity, luminescence, and imperfections in solids. This is the first publication in a new Wiley series in the Science and Technology of Materials, J. H. Hollomon, Advisory Editor.

1956 617 pages 363 illus. $12.00

Just published

4) The VACUUM DEPOSITION of THIN FILMS

By L. HOLLAND, W. Edwards & Co., London

This is the first comprehensive work to deal with both physical properties of thin films and deposition procedures. The author, a leading researcher in this field, covers such topics as: design features of vacuum evaporation-apparatus, equipment for sputtering, the use of heater materials other than tungsten spirals, vapor intensity distribution, metal alloy evaporation, and many others.

1956 541 pages Illus. $10.00

Mail this coupon today for ON-APPROVAL copies of these valuable books!

JOHN WILEY & SONS, Inc. **JES-116**
440 Fourth Ave., New York 16, N. Y.

Please send me the book(s) circled below. In 10 days I will return the book(s) and owe nothing, or I will remit the full purchase prices, plus postage.

1 2 3 4

Name .....

Address .....

City ..... Zone.... State.....

☐ SAVE POSTAGE! Check here if you ENCLOSE payment, in which case we pay postage. Same return privilege, of course.

A dependable source of DEPENDABLE ANODES

(Plain or Treated Types)

STACKPOLE

CARBON COMPANY • *St. Marys, Pa.*

THIS IS OUR 50th Year
STACKPOLE
FOUNDED 1906

BRUSHES for all rotating electrical equipment • CONTACTS (carbon-graphite and metal powder types) • TUBE ANODES • CATHODIC PROTECTION ANODES • VOLTAGE REGULATOR DISCS • WATER HEATER and PASTEURIZATION ELECTRODES • BEARINGS • WELDING CARBONS • MOLDS and DIES SPECTROGRAPHITE • POROUS CARBON • SALT BATH RECTIFICATION RODS • SEAL RINGS • FRICTION SEGMENTS • CLUTCH RINGS • ELECTRIC FURNACE HEATING ELEMENTS • PUMP VANES . . . and many others.

DOW

Dow high temperature magnesium alloys have excellent fabrication characteristics

Lightweight structural metals with high strength, stiffness and elasticity at elevated temperatures! A new group of Dow magnesium alloys offers a great combination of these properties without the fabricating difficulties normally experienced with other high temperature materials.

Specially developed for use in airframes, missile and engine structures, the new alloys are already making weight reductions possible for several manufacturers. These alloys show advantages at temperatures up to 700°F. Limited test data on properties up to 800°F. are available for some of them.

FABRICATION: Fabrication characteristics are equal to those of standard magnesium alloys.

WELDABILITY: 95 to 100% weld efficiency at elevated temperatures.

FORMABILITY: Single deep draws can be easily accomplished.

MACHINABILITY: Best machining characteristics of any structural metal.

One of the new alloys is magnesium-thorium composition HK31A. It is now available in rolled form from stock. Castings and sheet in mill quantities are also readily available. A companion alloy for extruded shapes and forgings will soon be in production.

For more information about the new high temperature magnesium alloys, contact your nearest Dow Sales Office or write to THE DOW CHEMICAL COMPANY, Magnesium Sales Department MA 362F, Midland, Michigan.

EASILY FORMED. These HK31A parts were drawn using production dies and processes for standard magnesium alloys. The parts retained a higher percentage of original properties than standard alloys.

you can depend on DOW MAGNESIUM DOW

Editorial

Semiconductors

THE FUNCTIONS of a technical society are many but among the most important is the publication of a periodical in which the results of new researches may be presented. Some journals, of course, are highly specialized—others are more catholic. But why Semiconductors in The Electrochemical Society?

First, let it be said that this JOURNAL has published many semiconductor papers. The selenium and other "metallic" rectifiers, photocells, the oxide cathode, and luminescence have all been discussed in the JOURNAL. In the context of this Semiconductor Issue, it is clear that two semiconducting materials, germanium and silicon, are of greatest interest at present.

Second, and to still the concerns of the theoretical electrochemist, let it be mentioned that germanium may be considered an ionizing solvent of reasonably high dielectric constant.

The foregoing points, while valid, are relatively unimportant in explaining why this Society shall open its meetings and its JOURNAL to the practitioners of a new field. The principal reason is that this Society has long consisted of men who, regardless of the name of their special discipline, have been concerned with the interaction of electricity and matter. (The fact that this is The Electrochemical Society and not the Electrophysical Society is, I feel, a historical accident. The British have begged this question in the Faraday Society, their counterpart of this organization.)

While the use of semiconductors as rectifiers dates back at least to Wehnelt's discovery of the oxide cathode, the term semiconductor is barely 25 years old. The first "metallic" rectifier to enjoy any wide-scale use in this country, selenium, is barely 20 years old. The silicon rectifier is somewhat younger, first attaining prominence in the early days of World War II. With the discovery of the transistor only eight years ago, new emphasis was placed on semiconductors in general and on the rare element germanium in particular.

Semiconductors, in the form of crystal diodes and transistors, are altering modern technology. Important as the transistorized hearing aid and portable radio may be, they are insignificant with regard to what is to come: computers, industrial controls and automation, vehicles, communication equipment, guided missiles, will all rely on transistors for their operation. The high rectification efficiency of germanium and silicon will make for tremendous power economies. Solar energy converters to replace fossil fuels and electronic refrigerators relying on semiconducting Peltier effect cells are realities today. The potential applications of semiconductors are limited only by man's imagination.

To be sure, many of the applications listed above can be fulfilled by the vacuum tube. The special features that make semiconductors so attractive, their relatively small size and the fact that they consume no heater or cathode power, make it certain that semiconductors will replace vacuum tubes for many functions.

To attain their full potential, semiconductor devices must both be improved and reduced in cost. The improvement will come about as the physical metallurgy of silicon is better understood; as the extractive metallurgy of silicon progresses to the point that so abundant an element is not considered, at least in its ultrapure form, a rare metal; as new semiconductor materials, such as the intermetallic compounds, are developed with due regard to stoichiometric purity and crystal perfection. With new knowledge will come the improved devices; with new materials will come the new devices. Reduction in cost will follow as the materials themselves are reduced in cost and as production becomes automated. In order to achieve these objectives, there must be the dissemination of new knowledge through discussion at technical society meetings and prompt publication in reputable scientific journals.

The disciplines of solid state physics, chemistry, metallurgy, and electrical engineering have all contributed to the development of the semiconductor art. Papers dealing with semiconductors are published in the journals of the physicist, the chemist, the metallurgist, and the electrical engineer. Because of the electrochemists' special emphasis on the interaction between matter and electricity, it is inevitable that the JOURNAL of The Electrochemical Society will become one of the leading semiconductor journals.

—H. BANDES

Hyperpure Silicon . . .

During the four years Du Pont Hyperpure Silicon has been available for devices manufactured and used by the electronics industry, this material has surpassed selenium in a number of important electronics applications . . . has proven its superiority over germanium in others.

Today many devices made with Du Pont Hyperpure Silicon are available for electronic, electrical and industrial applications.

Power rectifiers made with Du Pont semiconductor-grade Silicon are competitive in price with conventional rectifiers. These units rectify power at efficiencies greater than 98% and can operate reliably at temperatures as high as 350°F. for brief periods of time, allowing a temperature leeway to carry a current overload.

The size-weight-capacity advantage of silicon devices is an important consideration where space requirements are critical.

To the electronics components manufacturer, Du Pont offers both semiconductor and solar grade silicon. For further information write: Silicon Development Group, Pigments Department, E. I. du Pont de Nemours & Co. (Inc.), Wilmington 98, Delaware.

Pioneer and first commercial producer of Hyperpure Silicon

DU PONT
REG. U. S. PAT. OFF.

BETTER THINGS FOR BETTER LIVING . . . *THROUGH CHEMISTRY*

Depth of Surface Damage Due to Abrasion on Germanium

T. M. Buck and F. S. McKim

Bell Telephone Laboratories, Inc., Murray Hill, New Jersey

ABSTRACT

The approximate depth of surface damage on Ge as it influences surface recombination velocity has been measured for a variety of abrasive treatments by etching, weighing, and making two types of photomagnetoelectric measurements. Values range from 1μ or less for fine polishes to 35μ for heavy sandblasting. Close correlation is found with changes in reverse characteristics of grown junction p-n diodes treated in the same manner.

The drastic effect of mechanical surface damage, produced by sawing and abrasive shaping, was one of the earliest surface effects recognized in Ge transistor research. Various chemical etchants, CP-4 for example (1), were developed for removing damaged material.

The aim of the present work was to measure the depth of damage, as shown by surface recombination velocity, when Ge was subjected to a variety of abrasive treatments including very fine polishes. Such information may be useful in device fabrication, as smaller and more critical physical dimensions become necessary. It should also contribute to a more complete description and definition of surface effects on semiconductors.

The principal technique employed was one involving measurement of open-circuit photomagnetoelectric (PME) voltage, simply to determine qualitatively whether recombination velocity was increased or decreased by a given treatment. In addition to this, a method based on the recently developed theory of the PME effect by van Roosbroeck (2) was used to test a few of the same abrasive treatments and to follow the values of recombination velocity quantitatively. Abrasive treatments were further investigated in regard to their effect on the reverse characteristics of grown junction p-n diodes.

Some work on abrasion damage has been published recently. Clarke and Hopkins (3) found that sand-blasting a thin rod of Ge produced a high-conductivity surface layer which they estimated to be about 0.7×10^{-4} cm (0.7 μ) thick. In etching-rate experiments Camp (4) found the depth of the disturbed layer for several abrasive treatments to be in the range 2–10 μ. McKelvey and Longini (5) found that a Ge surface lapped with 800 grit Alundum required removal of about 5 μ to bring S (surface recombination velocity) down to the order of magnitude associated with etched surfaces. Uhlir (6) has found greater depths than these, 20–50 μ even for fine polishes, in studies of voltage-current curves of electrolyte-Ge barriers.

Qualitative PME Method

A method for determining surface recombination velocity from a simple measurement of open-circuit PME voltage was proposed by Moss, Pincherle, and Woodward (7). This method has been used to test a variety of surface treatments on Ge (8, 9) and gave a convenient qualitative indication of recombination velocity. Most of the data in the present work was obtained by a similar method, but with treatments applied to the illuminated surface rather than to the dark surface. The principle is illustrated in Fig. 1. A thin slab of Ge is illuminated on one large surface by water-filtered light which is highly absorbed at the surface. A magnetic field is applied perpendicular to the direction of illumination and to the long edge of the specimen. The dark surface of the slab is sand-blasted, and remains in that condition, to provide a high-recombination sink for carriers diffusing from the illuminated surface. Electrons and holes in the photodiffusion current are deflected in opposite directions by the magnetic field and this sets up the PME open-circuit voltage normal to both the magnetic field and the diffusion current across the slab. After an abrasive treatment on the front surface PME voltage is very low, perhaps a few tenths of a millivolt, since in this situation most of the carriers created by the nonpenetrating light recombine at the illuminated surface so that concentration gradient and diffusion current are small. As the front surface is given a series of etching treatments, PME voltage increases, since S at the illuminated surface decreases, causing larger concentration gradient and diffusion current. With continued etching V_x eventually levels off, at 200 mv for example, and in this region it is assumed that the disturbed material has been removed, at least insofar as recombination velocity is concerned. The height of the plateau is not of particular interest here; in general it depends on resistivity, volume lifetime, recombination at both surfaces, light intensity, and specimen thickness. All of these are taken into account directly or indirectly when actual values of S are determined (2) and quantitative measurements of this sort are mentioned later. In the simple open-circuit voltage measurements, however, S is not determined, but rather the depth at which PME voltage ceases to change, which is taken as the depth of damage.

The specimen mounting for the open-circuit PME voltage studies is pictured in Fig. 2. The Ge specimens used were p-type, 5.5 ohm-cm slabs 3.17 cm long, 0.635 cm wide, and about 0.127 cm thick initially. The large surfaces were (100) crystal faces. The dark surface was sand-blasted, leads were soldered about 1.9 cm apart, and the whole assembly was cast in Araldite resin with a glass backing so that only the front surface and the ends of the

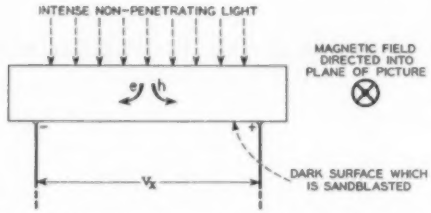

FIG. 1. Photomagnetoelectric method of investigating surface recombination velocity; open-circuit voltage measurements; treatments on illuminated surface.

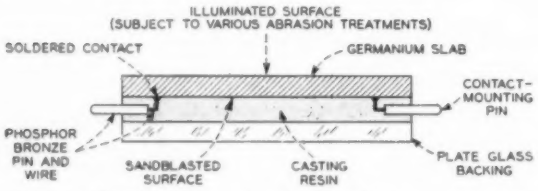

FIG. 2. Specimen mounting for abrasion treatments and PME measurements.

leads were exposed, as shown in Fig. 2. The specimen could then be cemented to a holder for lapping or polishing.

After an abrasive treatment the progressive etching was performed by dipping the front surface into diluted CP-4.[1] The slab was moved about gently to obtain uniform etching. Etching was followed by rinsing in a stream of distilled water and blotting on filter paper. PME measurements were made with the specimen in an atmosphere of dry nitrogen. The specimen was exposed to light for only brief intervals to avoid heating; balance on the type K-2 potentiometer was reached by trial and error which can be accomplished with good precision.

The magnetic field, supplied by a permanent magnet, was 6400 gauss. Light from a 300-watt projection lamp was filtered through a 1.7 cm water filter. Intensity was fairly high, about 10^{18} quanta/cm^2 sec.

The depth of material removed by etching was determined from weight loss. Uniform etching over the surface was assumed. For the specimens used, 1 mg corresponded to about 1-μ change in thickness. Checks with a micrometer at various convenient times during the series agreed fairly well with the weight loss values, within about 10–15%. Weight loss values are inherently more precise and it is felt that if there is an error it is caused by a slight tendency to etch more toward the edges so that the apparent values from weight loss may be too high by a few per cent.

Results of Open-Circuit PME Voltage Measurements

Fig. 3 shows that all the abrasive treatments tested caused high surface recombination velocity (low V_x) but that the amount of etching required for recovery varied widely and in a reproducible manner with the type of abrasive treatment. Thus, a surface which was sandblasted with 180 mesh SiC required removal of 32–34 μ, compared with 1–2 μ for a fine diamond polish. Some details on these

[1] 15 ml glacial CH_3COOH, 15 ml conc. HF, 25 ml conc. HNO_3, 2 drops Br_2, 15 ml H_2O.

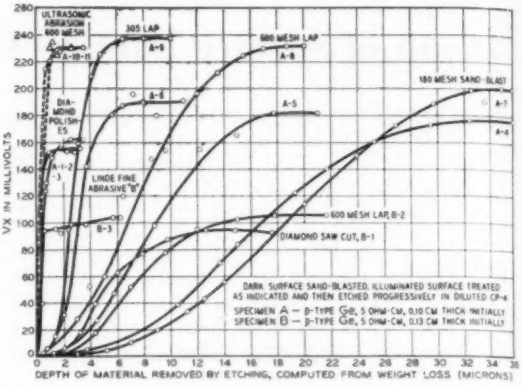
ULTRASONIC ABRASION 600 MESH
305 LAP
600 MESH LAP
180 MESH SAND-BLAST
DIAMOND POLISH
LINDE FINE ABRASIVE "B"
600 MESH LAP, B-2
DIAMOND SAW CUT, B-1
DARK SURFACE SAND-BLASTED, ILLUMINATED SURFACE TREATED AS INDICATED AND THEN ETCHED PROGRESSIVELY IN DILUTED CP-4
SPECIMEN A — p-TYPE Ge, 5 OHM-CM, 0.10 CM THICK INITIALLY
SPECIMEN B — p-TYPE Ge, 5 OHM-CM, 0.13 CM THICK INITIALLY
VX IN MILLIVOLTS
DEPTH OF MATERIAL REMOVED BY ETCHING, COMPUTED FROM WEIGHT LOSS (MICRONS)

FIG. 3. Change of open-circuit PME voltage with etching, after various abrasive treatments.

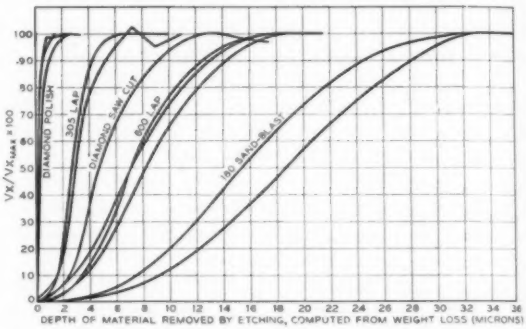

FIG. 4. Change of PME voltage with etching; normalized curves.

TABLE I. *Approximate depth of damage for various treatments on* Ge

Treatment	Depth of damage (μ)	Nominal particle size of abrasive (μ)
Linde fine abrasive "B" polish	1	0.1
Ultrasonic abrasion (600 mesh SiC in water ultrasonically agitated)	1–2	25
Diamond polish	1–2	0.5
No. 305 lap	6–7	5
Diamond saw cut	12–13	
600 Mesh SiC lap	17–18	25
180 Mesh sandblast	32–34	125

treatments are given below. Differences in height of curves for a given treatment are due to gross differences in thickness of the specimen at these particular points in the complete series. In Fig. 4 the curves have been normalized. These results together with those for several other treatments are shown in Table I. As this table shows, an interesting correlation of depth of damage with particle size of abrasive in the lapping treatments was observed.

Five separate applications of the 600 mesh lap, three of which are shown in the curves, yielded approximately the same depth of damage although the total amount of material removed varied from 0.7 to 5 mils. Several times the freshly lapped or polished surfaces were carefully

washed in alcohol, toluene, water, etc., to determine whether any cleaning action short of actual removal of material would raise V_x. None of these attempts was successful; it appeared that the high recombination velocities were indeed due to mechanical damage even with the very finest abrasive treatment.

Remarks on Abrasive Treatments

180 Mesh sandblast.—180 mesh silicon carbide was blown through a 5/16 in. tube under 25 lb/in.² air pressure.

600 Mesh lap.—The 600 mesh SiC was slurried in water and the lapping done by hand on a glass plate with moderate pressure.

Diamond saw cut.—Cutting was done with a new Norton diamond wheel D220-N100 M1/8. It was surprising to find that sawing caused slightly less damage than the 600 mesh lap. Only one test was made, but there seemed to be no reason to believe it was misleading

#305 Lap.—Lapping was done by hand on glass with a water slurry of American Optical Co. #305 abrasive after preliminary laps with 600 mesh SiC and #303½. The depth of damage is in good agreement with the value of 6 μ obtained by Camp (4) from etching rates for the same abrasive on the same crystal face (100).

Diamond polish and Linde fine abrasive B.—Buehler diamond dust or Linde fine abrasive B (Alumina) was held in Buehler microcloth on a power driven wheel. Fine polishes usually involve several steps in which progressively finer abrasive materials are used. The coarsest material (600 mesh SiC) is used first in order to arrive quickly at a fairly true surface. The last step with the fine abrasive must of course go far enough to remove disturbed material left by preceding steps. The same depth of damage was obtained, however, by using the fine abrasive directly on an etched surface.

Ultrasonic abrasion (600 mesh).—The specimen which had been thoroughly etched in CP-4 was immersed for 5–10 min in a suspension of 600 mesh SiC in water which was ultrasonically agitated in a Brush hypersonic generator. Surface recombination velocity was increased drastically even though there was no visible appearance of any change on the etched surface under a low-powered microscope.

Quantitative PME Measurements

As a check on the qualitative open-circuit PME voltage measurements, two representative treatments were tested by a PME method which permits quantitative determination of recombination velocity (2). Results for fine polishes and the 600 mesh lap are shown in Fig. 5. In this method values of S on the dark surface of the specimen are determined from measurement of short-circuit PME current and of relative conductance increase, $\Delta G/Go$, at the same light intensity but with no magnetic field. The ratio of these quantities multiplied by a factor containing constants for the material is used to compute S (2). Introduction of relative conductance increase makes it unnecessary to know either light intensity or S at the illuminated surface explicitly. Specimens were mounted as in Fig. 2 except that two additional current leads were attached at the ends and the dark surface received abrasive treatments and etching while the other large surface with leads attached was etched and was exposed to the illumination through the glass and Araldite resin.

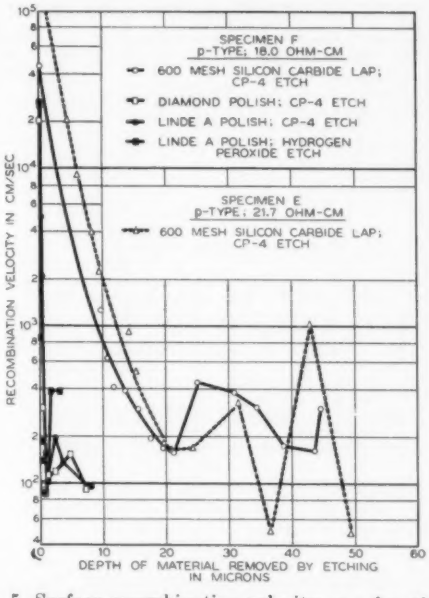
SPECIMEN F
p-TYPE; 18.0 OHM-CM
600 MESH SILICON CARBIDE LAP; CP-4 ETCH
DIAMOND POLISH; CP-4 ETCH
LINDE A POLISH; CP-4 ETCH
LINDE A POLISH; HYDROGEN PEROXIDE ETCH
SPECIMEN E
p-TYPE; 21.7 OHM-CM
600 MESH SILICON CARBIDE LAP; CP-4 ETCH
RECOMBINATION VELOCITY IN CM/SEC
DEPTH OF MATERIAL REMOVED BY ETCHING IN MICRONS

FIG. 5. Surface recombination velocity as a function of depth of material removed by etching. S determined from short-circuit PME current and relative conductance increase.

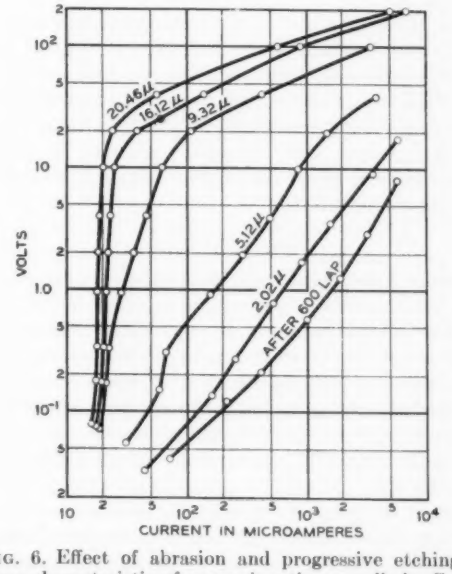

FIG. 6. Effect of abrasion and progressive etching on reverse characteristic of grown-junction p-n diode. Ge p-n diode; n-side 3.5 ohm-cm, p-side 0.2 ohm-cm; volume lifetime 100-300 μsec; dimensions = 0.238 cm x 0.238 cm x 1.25 cm; 600 mesh lap.

It is seen in Fig. 5 that the measurements by the new method show recombination velocities of 30,000 cm/sec and larger for polished or lapped surfaces. The damage appears to be removed at about 20 μ for the 600-mesh lap and at a micron or less for the fine polishes. After that,

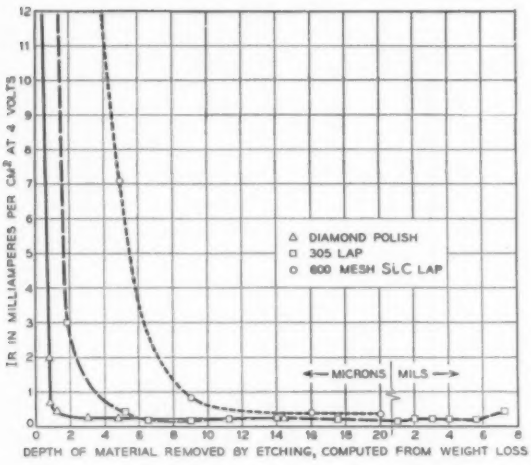
IR IN MILLIAMPERES PER CM² AT 4 VOLTS
DEPTH OF MATERIAL REMOVED BY ETCHING, COMPUTED FROM WEIGHT LOSS
△ DIAMOND POLISH
□ 305 LAP
○ 600 MESH SiC LAP
← MICRONS | MILS →

FIG. 7. Change of reverse dark current (at 4 v) with etching, after abrasion by three different methods. Ge grown-junction p-n diode.

random fluctuations appear with further etching. Presumably these are due to subtle differences in etching and atmosphere. Random fluctuations do not appear in the open-circuit voltage measurements presumably because that method is not so sensitive to small changes at low levels of S.

The physical picture of the abrasion damage seems to be one of a thin layer of very low lifetime material which excess carriers diffuse into as if encountering a surface of very high recombination velocity. Lifetime in this layer is probably lower toward the true outer surface. A considerable amount of the damaged layer must be removed before chemical effects on the true outer surface begin to influence S very strongly.

Diode Studies

Three of the abrasive treatments were given to two large grown junction p-n diodes in order to determine whether differences shown by the PME measurements would appear also in treatment of a junction device. Diodes were lapped or polished on all four sides and then put through the etching and weighing procedure. After etching and washing, a diode was allowed to stand over silica gel in a bottle for 24 hr before measurement of the reverse characteristic.

Results are shown in Fig. 6 and 7. Correlation of the recovery points with the PME data is quite close. [Data on the diodes, however, pertain to the (110) crystal face while PME results were obtained on (100) faces.]

However, the behavior of reverse characteristic, after abrasion, cannot be explained on the basis of surface recombination alone by existing theoretical treatments of p-n junctions. From the equation (10)

$$I_s = A\,\frac{kTb\sigma_i^2}{q(1+b)^2}\left(\frac{1}{\sigma_n L_p}+\frac{1}{\sigma_p L_n}\right) \qquad \text{(I)}$$

I_s = reverse saturation current, A = area of junction, b = ratio of electron mobility to hole mobility, q = electron charge, σ_i = intrinsic conductivity, σ_n = conductivity on n-side, L_p = diffusion length of holes on the n-side = $\sqrt{D_p\tau_p}$; D_p is diffusion constant for holes and τ_p is the effective or filament lifetime, which depends on volume lifetime and S (11). For the case shown in Fig. 6, one obtains $I_s = 7.32$ μamp for $\rho_n = 3.5$; $\rho_p = 0.2$; $A = 0.0558$ cm²; body lifetime = 100 μsec; $S = 100$ cm/sec.

Allowing S to approach infinity would lower the filament ("effective") lifetime (11) from 100 μsec to 40 μsec on the n-side and to 24 μsec on the p-side, not a very large decrease since the cross section is so large. This would then increase I_s to only 11.7 μamp and would not, of course, account for the slopes of the curves.

However, as Shockley (10) has pointed out, equation (I) is not expected to hold for very large values of S, in which case the junction may be expected to become substantially ohmic.

Two alternative explanations of the diode behavior are: (A) the effect of abrasion is due entirely to surface recombination in a manner not yet quantitatively explained (10); (B) the effect may be due to a conductive layer across the junction of the type found by Clarke and Hopkins (3) on a sandblasted filament.

In any event, the PME measurements are evidently revealing surface "damage" of some sort which is detrimental to junctions, and the depth of this damage appears to be the same in both types of measurement.

Greater depths of damage for fine polishes have been found by Uhlir (6) in studies of the reverse characteristics of electrolyte-Ge barriers. He suggests that the discrepancy between PME measurements of S and the Ge-electrolyte studies may be due to the fact that the latter method is more sensitive to local spots of damage whereas the PME method determines an average over a relatively large surface. Undoubtedly in device work it would be safer generally to remove an excess of material, say 2–3 mils, but in situations where dimensions are critical and only very slight etching can be tolerated the fine polishes appear to offer a possible advantage.

Acknowledgment

The authors gratefully acknowledge the help of J. Andrus, E. Berry, and W. L. Bond who developed and administered the fine polishing treatments; the availability of these polishes was responsible for initiation of this work. D. R. Mason performed the ultrasonic abrasion treatment. Thanks are also due to W. van Roosbroeck and W. H. Brattain for helpful discussions.

Manuscript received May 12, 1956. This paper was prepared for delivery before the Cincinnati Meeting, May 1 to 5, 1955.

Any discussion of this paper will appear in a Discussion Section to be published in the June 1957 JOURNAL.

REFERENCES

1. R. D. HEIDENREICH, U.S. Pat. 2,619,414, Nov. 25, 1952.
2. W. VAN ROOSBROECK, *Phys. Rev.*, **101**, 1713 (1956). Additional experimental details of the method to be published by T. M. Buck and F. S. McKim.

3. E. N. Clarke and R. L. Hopkins, *Phys. Rev.*, **91**, 1566 (1953).
4. P. R. Camp, *This Journal*, **102**, 586 (1955).
5. J. P. McKelvey and R. L. Longini, *J. Appl. Phys.*, **25**, 634 (1954).
6. A. Uhlir, *Bell System Tech. J.*, **35**, 333 (1956).
7. T. S. Moss, L. Pincherle, and A. M. Woodward, *Proc. Phys. Soc. (London)*, **66B**, 743 (1953).
8. T. S. Moss, *ibid.*, **66B**, 993 (1953); *Physica*, **20**, 989 (1954).
9. T. M. Buck and W. H. Brattain, *This Journal*, **102**, 636 (1955).
10. W. Shockley, *Bell System Tech. J.*, **28**, 435 (1949).
11. W. Shockley, "Electrons and Holes in Semiconductors," pp. 322–323, D. Van Nostrand and Co., New York (1950).

Solid Solubilities and Electrical Properties of Tin in Germanium Single Crystals

F. A. Trumbore

Bell Telephone Laboratories, Inc., Murray Hill, New Jersey

ABSTRACT

The solid solubility of Sn in Ge has been determined in the range from 400°C to the melting point of Ge using conventional crystal pulling techniques and crystal growth from melts in a thermal gradient. The distribution coefficient changes from 0.020 ± 0.003 at the melting point of Ge to 0.012 ± 0.002 at the lower temperatures, corresponding to solid solubilities of up to about 5×10^{20} at./cc. X-ray measurements substantiate the conclusion that these relatively large amounts of Sn are in solid solution. In spite of the presence of between 10^{19} and 10^{20} at./cc of Sn in the pulled crystals, resistivities as high as 40–50 ohm-cm and minority carrier lifetimes as high as 100–200 μsec were obtained. These results confirm the electrical neutrality of Sn in Ge.

Although Sn is assumed generally to have neither donor nor acceptor properties in Ge, no systematic study appears in the literature. In the present work Ge single crystals were grown from melts containing relatively large amounts of very pure Sn. The results of resistivity, lifetime, x-ray, and solid solubility measurements on these crystals provide a conclusive answer to the question of the electrical neutrality of Sn in Ge.

Experimental

Crystal pulling experiments.—A conventional crystal pulling machine (1) was used to grow Ge single crystals from 100-g melts initially containing from 1 to 5 at. % Sn. The crystals were grown under a hydrogen atmosphere in the <100> direction at pull rates of 3 and 0.5 cm/hr and a rotation rate of 60 rpm. Ge[1] was zone-refined material from which single crystals of resistivities greater than 40 ohm-cm could be grown. Analyses of three different samples of high purity Sn[2] are shown in Table I. Two of these samples were taken from zone-refined lots and, as is evident from the table, were of exceptional purity.

Thermal gradient crystal growth.—With melts containing more than a few atom per cent Sn the crystal pulling method was found to be unsatisfactory. For these melts, which contained up to about 90% Sn, a technique was employed which made use of the fact that the solubility of Ge in Sn increases with temperature. In this method Ge was dissolved in Sn at a given temperature and then precipitated or grown on a seed crystal at a lower temperature.

As shown in Fig. 1 a vertical, doubly wound furnace was used in these experiments. By regulating the current independently in the two windings a controlled thermal gradient could be established. The furnace was mounted on a swivel support so that it could be inverted with the sample tube in place. A number of different seed and melt arrangements were used in these experiments. The most successful design is shown schematically in Fig. 1. A Ge single-crystal seed is held by a constriction in one end of a sealed evacuated vitreous silica tube. The Sn, together with Ge in excess of that needed for saturation, is placed in the other end. The Sn used in these experiments was the "super-pure" material (*see* Table I).

After mounting in the furnace as shown in Fig. 1, Sn and excess Ge were heated out of contact with the seed crystal in order to saturate the Sn with Ge. This was done to minimize solution of the seed crystal when the furnace was inverted. The molten metal was saturated at a temperature slightly lower than that of the seed crystal to prevent spurious crystals from forming on the seed crystal when the furnace was inverted into the growing position. After inversion into the growing position the thermal gradient was adjusted to that the hottest part of the solution was at the top in order that any spurious crystals not grown on the seed would float to the top of the melt. As measured with the thermocouple outside the silica tube, essentially linear

[1] Obtained from the Western Electric Co.
[2] Obtained from the Vulcan Detinning Co.

TABLE I. *Analyses of* Sn *samples*

Sample designation	Impurities
[1] Vulcan "super-pure"	<0.001% Ag, Al, Ca, Cu, Fe, Mg, Na, Pb
[2] Vulcan #1466	<0.00003% Fe; <0.00002% Pb; <0.0005% Sb[a]
[3] Vulcan #VS27SP	<0.00001% Fe, Pb; <0.0005% Sb[a]

[a] Actually no Sb was detected. The figure 0.0005% represents the upper limit of detection for the analytical method

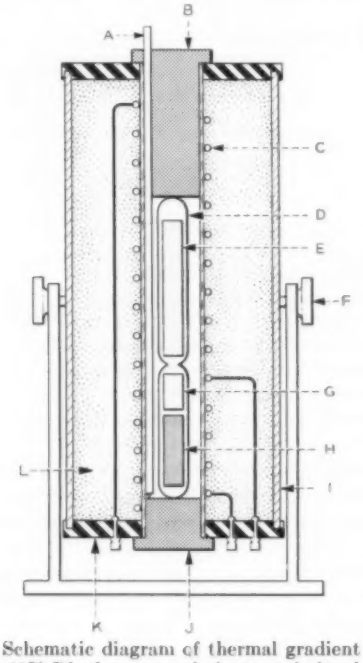

FIG. 1. Schematic diagram of thermal gradient furnace: (A) Pt-Pt 10% Rh thermocouple in ceramic insulator; (B) alundum plug; (C) nichrome heating element; (D) vitreous silica tube; (E) Ge seed crystal; (F) swivel support; (G) excess Ge; (H) Sn; (I) steel furnace shell; (J) alundum plug; (K) transite; (L) silocel insulation.

thermal gradients averaging about 5°C/cm were maintained during growth of the crystals. The total gradient varied with the lengths of the seed crystals which ranged up to 10 cm. The periods of growth varied from about 2 to 4 weeks. At the end of this time the furnace was again inverted to drain off most of the molten alloy, following which the tube was removed from the furnace and quenched in water to minimize further growth on the Ge crystals. Excess Sn then was removed by digesting the sample in hot concentrated HCl. A sketch of the type of growth, typical of this particular geometry, found in these experiments is shown in Fig. 2. In most cases the dimensions of the grown crystals were on the order of 1–3 mm. Growth temperatures were determined by comparison of the positions of the crystals in the tube and the temperature profile in the furnace.

Chemical analyses.—The crystals were analyzed for Sn using spectrochemical techniques. In the case of crystals grown by the thermal gradient method it was found necessary to crush and digest the crystals in HCl in order to remove any occluded Sn. The analyses are believed to be accurate to about ±10% of the total concentration of Sn in the crystals.

Electrical measurements.—Almost all of the electrical measurements reported in this paper were performed on the crystals grown by the pulling technique since the samples grown in a thermal gradient were in general either polycrystalline, too small, and (or) irregular in shape for accurate measurements to be made. Resistivities were determined using the conventional four-point probe technique (2) and are accurate to better than ±10%. Minority carrier lifetimes were determined by observing the decay in photoconductivity as described by Hornbeck and Haynes (3) and are believed to be accurate to better than ±25%. In addition to the photoconductivity decay measurements, a few diffusion length measurements were made using the Goucher technique (4). Results of the two methods were generally in good agreement.

FIG. 2. Schematic diagram of crystal growth: (A) vitreous silica tube; (B) excess Ge; (C) Sn-Ge melt; (D) original seed crystal; (E) grown crystals.

X-ray measurements.—The lattice constants of pure Ge, one pulled crystal, and two crystals grown in a thermal gradient were determined by x-ray diffraction measurements with a precision cell camera.

RESULTS AND DISCUSSION

Solid Solubility of Sn *in* Ge

Results of the crystal pulling experiments are discussed first. Because of the relatively high concentrations of Sn in the melts difficulty was encountered in obtaining equilibrium between the bulk of the melt and the growing crystal. For example, the effect of constitutional supercooling (5) is of more importance where the solute element is present in larger concentrations. In addition, polycrystalline growth and the presence of occluded Sn presented problems. A crystal pulled at the rate of 3 cm/hr contained numerous patches of occluded Sn about 0.05 mm in diameter. With a pull rate of 0.5 cm/hr little or no microscopic evidence of occlusions was observed in the crystals In order to determine whether the observed distribution

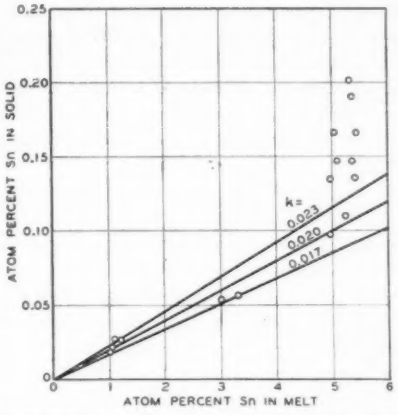

FIG. 3. Solid solubility of Sn in Ge as a function of melt concentration in the crystal pulling experiments.

TABLE II. *Analyses of thermal gradient crystals*

T (°C)	N^s_{Sn}	k
401	0.0111	0.011_5
619	0.0088	0.011_5
637	0.0093	0.012_6
759	0.0056	0.011_9

coefficients corresponded to equilibrium values, a study of the effect of melt concentration on the observed distribution coefficient at a pull rate of 0.5 cm/hr was carried out. Results of these experiments are shown in Fig. 3 where the observed solid solubility is plotted against the concentration of Sn in the melt. The points correspond to individual analyses on sections of eight different crystals. Straight lines, corresponding to three values of the distribution coefficient, k, are also plotted. The best fit to the data is seen to be the line corresponding to a value of k equal to 0.020 with an estimated error of ± 0.003. An obvious scatter or upward trend in the data is observed in the region of 5–6 at. % Sn. It is in this region that difficulty was encountered with polycrystalline growth, occlusions, and undoubtedly with constitutional supercooling. It should be noted that all sources of error (other than the analytical error) lead to high values of the solid solubility. The limiting value of 0.020 is in agreement with a value of 0.02 near the melting point of Ge determined by Struthers (6) using radiotracers and growing crystals from melts much more dilute with respect to Sn.

Results of chemical analyses for Sn in the thermal gradient crystals are summarized in Table II where N^s_{Sn} and k are the atom fraction of Sn in the crystal and the distribution coefficient of Sn in Ge, respectively. In calculating k, the liquidus compositions of Thurmond, Hassion, and Kowalchik (7) were used. Temperatures quoted in Table II must be regarded as being uncertain to perhaps ± 10°C since, due to the relatively high thermal conductivity of the melt, the thermal gradient in the melt probably differed from the gradient measured by the thermocouple outside the sample tube. In addition to any inherent errors, the values for k and N^s_{Sn} are subject to an error

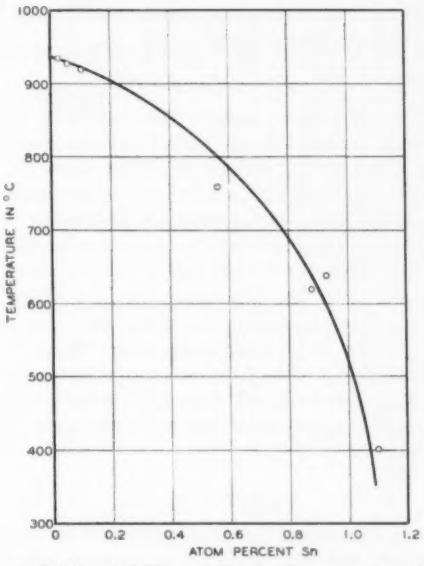

FIG. 4. Solid solubility of Sn in Ge as a function of temperature. The three points above 900°C are from analyses on pulled crystals, while the points at lower temperatures are from thermal gradient experiments.

TABLE III. *Lattice parameters*

N^s_{Sn}	d (observed)	d (calculated)
0 (Ge)	5.6574 ± 0.0003	5.6576[a]
0.0012	5.6576 ± 0.0004	5.6586
0.0066	5.6639 ± 0.0003	5.6631
0.0105	5.6667 ± 0.0014	5.6663
1.00 (Sn)		6.489[a]

[a] ASTM values. The value for Sn is that corresponding to the diamond structure of gray Sn.

TABLE IV. *Electrical properties*

Crystal[a]	Resistivity[b] (ohm-cm)	Lifetime (μsec)	C_{Sn} (atoms/cc)
1[5]	11–12(n)	15	7×10^{19}
2[5]	9–17(n)	10	7.5×10^{19}
3[5]Ga	30–34(n)	45	6×10^{19}
3[5]Sb	0.5–0.6(n)	5	6×10^{19}
3[3]	35–46(n)	>140	3×10^{19}
3[1]	42 (p)–46(n)	185(p)	2×10^{19}

[a] The number outside the brackets refers to the source of Sn (corresponding to the numbers in Table I) used in the growth of the crystal. The number inside the bracket refers to the initial concentration (in atom per cent) of Sn in the melt. Two crystals, 3[5]Ga and 3[5]Sb, were deliberately doped with Ga and Sb, respectively. The amount of Ga added was insufficient to convert crystal 3[5]Ga to p-type.

[b] The resistivities quoted here are the values found near the top and the bottom of the crystal.

of about $\pm 10\%$ because of uncertainties in the chemical analyses.

The solidus curve based on both the crystal pulling and thermal gradient data is plotted in Fig. 4. Near the melting point of Ge the curve is drawn with a slope corresponding to $k = 0.020$ assuming a freezing point lowering constant

of 3.6°C/at. % Sn obtained from a value for the heat of fusion of Ge of 8.1 kcal/g-atom (8).

X-ray Measurements

Results of lattice constant determinations are summarized in Table III. In this table N^s_{Sn} is the atom fraction of Sn in the crystal, d(observed) is the measured lattice parameter in Angstroms at 25°C, and d(calculated) is the value of the lattice parameter assuming a linear variation of the lattice constant over the entire composition range from 0 to 100% Sn. Within the rather wide limits of experimental error, the expansion of the Ge lattice by Sn is in agreement with the assumption that Vegard's law holds over the entire composition range. While the measurements are not sufficiently precise to determine whether this assumption is strictly true, the results do show that Sn is truly in solid solution and is not present as occluded material.

Electrical Properties

Results of electrical measurements on the pulled crystals are summarized in Table IV. As expected, the crystals grown from melts containing the purer Sn samples (and no added impurities) had the higher resistivities. Resistivities of these crystals correspond to differences on the order of 10^{13}–10^{14} at./cc in donor-acceptor concentrations (9) even though Sn concentrations were between 10^{19} and 10^{20} at./cc. Furthermore, qualitative spectrochemical analyses excluded the presence of other detectable impurities at concentrations higher than about 10^{17}–10^{18} at./cc. In addition, low temperature resistivity measurements on one sample gave a resistivity vs. temperature curve typical of ordinary donors and acceptors. These observations indicate that impurities other than Sn are responsible for the observed resistivities.

Minority carrier lifetimes in certain crystals are seen to be relatively high and comparable in magnitude with lifetimes obtained in undoped crystals. There does appear to be a rough correlation between the resistivity and the lifetime which does not depend on the concentration of Sn in the crystal. An explanation of the lower lifetimes found for crystals with low resistivities may be found in the effect of the Fermi level on lifetime as discussed by Hall (10) and by Shockley and Read (11). In addition, there are probably more impurity recombination centers in the lower resistivity samples where the more impure Sn was used. However, a knowledge of both the identity and concentration of the impurity or impurities acting as recombination centers is lacking so that no quantitative calculations will be attempted here.

Rough resistivity measurements were made on some of the thermal gradient crystals containing as much as 1 at. % Sn. Values ranging from 1 to 20 ohm-cm, n-type, were found. However, since the samples were either polycrystalline or too small for accurate measurement, it is possible that these values could be too high by a factor of about ten. Even allowing for an error of a factor of 100 the resistivities obtained correspond to N_D-N_A values of only about 10^{18} at./cc compared to Sn concentrations of more than 10^{20} at./cc.

Conclusions

The presence of near-intrinsic resistivities in conjunction with such large solid solubilities of Sn in Ge is taken as conclusive proof that at concentrations of Sn as high as 10^{20} at./cc Sn is truly neutral insofar as its effect on the conductivity of Ge is concerned. The high lifetimes also show that at these concentration levels Sn is definitely not an effective recombination center for holes and electrons in Ge. These results confirm the conclusions of Woodbury and Tyler (12) who, assuming Struther's value for k at the melting point of Ge, deduced that they had grown crystals containing more than 10^{18} at./cc of Sn without affecting resistivity or lifetime.

Acknowledgments

The author gratefully acknowledges the contributions of many members of the Bell Telephone Laboratories to this work. He especially wishes to thank W. H. Richards for the growth of the pulled crystals, Mrs. M. H. Read for the x-ray measurements, C. R. Isenberg for technical assistance and the Analytical Chemistry Department for the spectrochemical analyses. Helpful discussions with C. D. Thurmond and C. R. Landgren are also acknowledged.

Manuscript received April 18, 1956. This paper was prepared, in part, for delivery before the Pittsburgh Meeting, October 9 to 13, 1955.

Any discussion of this paper will appear in a Discussion Section to be published in the June 1957 Journal.

REFERENCES

1. J. A. Burton, G. W. Hull, F. J. Morin, and J. C. Severiens, *J. Phys. Chem.*, **57**, 853 (1953).
2. L. Valdes, *Proc. I.R.E.*, **42**, 420 (1954).
3. J. A. Hornbeck and J. R. Haynes, *Phys. Rev.*, **97**, 311 (1955).
4. F. S. Goucher, *ibid.*, **81**, 475 (1951).
5. J. W. Rutter and B. Chalmers, *Can. J. Phys.*, **31**, 15 (1953).
6. J. D. Struthers, quoted by J. A. Burton, *Physica*, **20**, 845 (1954).
7. C. D. Thurmond, F. X. Hassion, and M. Kowalchik, to be published.
8. E. S. Greiner, *J. Metals*, **4**, 1044 (1952).
9. M. B. Prince, *Phys. Rev.*, **92**, 681 (1953).
10. R. N. Hall, *ibid.*, **83**, 228 (1951); **87**, 387 (1952).
11. W. Shockley and W. T. Read, *ibid.*, **87**, 835 (1952).
12. H. H. Woodbury and W. W. Tyler, *ibid.*, **100**, 659 (1955).

A Shot Tower for Producing Germanium Doping Pellets of Uniform Composition

I. A. Lesk

General Electric Company, Syracuse, New York

ABSTRACT

A shot tower may be used as a convenient and accurate way to obtain uniform mixtures of Ge and an impurity in a finely divided form. This shot may be used as master alloys for controlled impurity addition during growth of Ge crystals. This method gives convenient small pellets with the impurity fraction in each pellet (in a given batch) the same. The impurity fraction in a given batch of shot is easily controlled. The size range can be controlled, facilitating subsequent weighing procedures. Insoluble materials in the melt, e.g., carbon dust, are left behind, and there is no need to etch the shot.

Present day techniques for producing Ge crystals include zone refining to a high level of purity and doping during crystal pulling with selected impurities to the desired resistivity range. Since resistivity of Ge is dependent on the impurity content, and since, for many practical cases, very small amounts of impurity are required, accurate weighings of elements in amounts of the order of milligrams are necessary. The difficulties associated with such weight determinations have led to the use of master doping alloys, consisting of Ge and an impurity. By using these alloys, only larger doping samples need be weighed, greatly facilitating this procedure. Doping alloys are usually prepared by melting the two elements together, and then rapidly quenching in order to produce a uniform solid solution. However, due to segregation and grain boundary effects, large samples prepared in this way tend to be nonhomogeneous Also, since they must be broken into small pieces for use, the possibility of contamination is introduced

The production and use of Ge shot (for making point contact rectifiers) was first described by Dunlap (1). If a master doping alloy is blown into shot instead of being cooled as one piece, each drop should contain constituents in exactly the same ratio as in the total melt, although the ratio may vary from point to point in the drop. If the shot are made small enough and cover a range of sizes, an integral number of them may be used for any doping application. (Broken shot should not be used because of the impurity variation from point to point in the sphere.) In this way, successive doping samples chosen from a master doping alloy in shot form should be uniform in content of doping element.

The production and use of Ge master doping alloys in the form of shot are described in this paper.

Germanium Shot Tower

The tower for producing Ge master doping alloys in shot form was designed to be versatile, easily disassembled, permit easy viewing of the molten Ge and solid shot, and to consist of few specially made parts. Fig. 1 shows a sectional view.

The tower, of 150 ml capacity, was made gas-tight by means of ground butt joints, under slight pressure vertically by means of a rod pressing down on the rubber stopper at the top. Components were held in position by means of clamps fastened to a large vertical stand. Argon was used as an inert atmosphere, the relative amounts of flow to top and bottom of the tower being controlled by the needle valve. With the needle valve closed, the entire gas flow was into the upper chamber. A pressure of 15 cm Hg could easily be obtained in the upper chamber in this way. With the needle valve fully open, most of the argon flow was into the lower chamber. This produced an agitation of the silicone oil which continued even with the needle valve almost closed. Small grooves were cut in the bottom of the carbon crucible to permit easy access of the argon in the lower chamber to the atmosphere. Hence, the lower chamber always remained at essentially room pressure.

The Ge and impurity were melted in the carbon boat under an argon pressure $\lesssim 1$ cm Hg by means of energy coupled from the r.f. heater coil. A pressure difference of about 2 cm Hg between top and bottom of the carbon crucible was sufficient to overcome surface tension and force the molten constituents through the 0.010 in. hole in the form of droplets.

Care had to be taken in construction and assembly of the tower to make sure that the components were vertical and lined up with each other. Otherwise, during descent, the shot would strike the sides of the tower and splatter.

After a fall of 4 ft, the shot were still mostly molten. Hence, a cooling liquid was required to prevent the shot from sticking together. Allowing the shot to fall into a silicone oil bath worked very well. Shot towers with larger drop distances might be used, where practicable, so that no cooling liquid would be required.

Because of the height of the tower and its support from only one stand it swayed easily. This caused small pressure fluctuations, which resulted in a range of shot sizes being produced during a single run, since the particle size depends on the pressure with which it is blown.

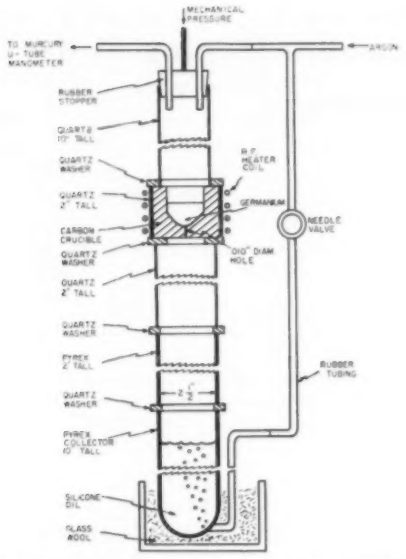

FIG. 1. Germanium shot tower, sectional view

TABLE I

Impurity	Mass % of impurity in alloy		
As	1	0.1	0.02
Sb	10	1.0	0.1
Ga	1	0.1	0.02

Operation

The amount of each element used in a master doping alloy depends on the amount of shot and the ratio of impurity to Ge in the shot that are desired. Some useful alloy compositions that have been made using common doping elements are shown in Table I.

A mass of impurity element of approximately the desired size was weighed accurately. Then, the amount of Ge required to form the correct ratio was weighed. In cases involving impurity elements that are not very volatile at high temperatures, i.e., Ga, Sb, the constituents were simply melted together in the carbon crucible in the shot tower. The short melting time, about 4 min for a 100 g charge, insured little loss of these materials (or the Ge) by vaporization during the melting period. In cases involving impurities that are volatile at high temperatures, i.e., As, it is desirable to melt the constituents together before putting them in the tower. This was done with little loss due to vaporization by plunging the impurity into molten Ge in a quartz tube, such that any vapor from the doping element bubbled into the molten Ge and hence had a good chance of dissolving. It was also necessary to use this apparatus to mix Ge and doping element in cases of heavy doping where the impurity has a lower melting point and surface tension than Ge. In such cases, i.e., 10% Sb, 90% Ge, the doping element melts first and may be blown through the crucible opening by the (low) pressure before the Ge has a chance to melt and dissolve it.

It should be emphasized that since relatively large amounts of doping elements are involved in the production of shot, adequate ventilation facilities should be present when toxic materials are used. If they are dissolved in Ge first, as for volatile impurities, they are less dangerous.

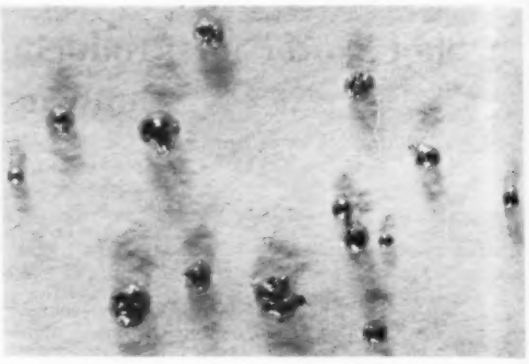

FIG. 2 (*a*). 99% Ge: 1% Sb shot. 6× before reduction for publication.

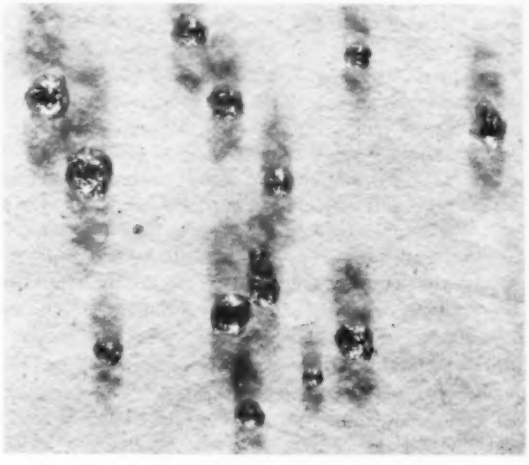

FIG. 2 (*b*). 90% Ge: 10% Sb shot. 6× before reduction for publication.

Before melting alloys in the tower crucible, the needle valve was opened sufficiently so that the pressure in the upper chamber was less than that required to force molten material through the hole ($\lesssim$1 cm Hg).

The mixture should be kept in the molten state in the shot tower carbon crucible long enough to insure complete mixing, but not so long that appreciable evaporation of the impurity or Ge takes place; a few minutes is a reasonable time. The temperature of the molten alloy should not be much above the melting point when the shot are blown; otherwise, the shot will be difficult to cool quickly, and agglomeration in the collector may result.

To blow the shot the needle valve was closed until the upper chamber pressure was sufficient to force the liquid through the hole in the carbon crucible ($\gtrsim$2 cm Hg). It emerged as a fine stream of droplets, which fell into the oil bath and settled to the bottom in a pile. There was no sign of smoke or fumes arising from the silicone oil bath when the red hot droplets entered.

After each run, a small amount of slag composed partially of carbon dust and Ge remained in the carbon crucible. Hence, a further advantage of this method is that the slag is separated from the doping material.

After the run was completed, the shot were removed from the collector, given several washes in CCl_4, and allowed to dry. No stickiness of pellets was observed if the CCl_4 washings were thorough. The shot were not etched, since this would change the impurity concentration.

Results

Fig. 2(*a*) shows a photomicrograph of some typical shot, in this case 1% Sb, 99% Ge. Fig. 2(*b*) shows some 10% Sb, 90% Ge shot, the wrinkled appearance being due to the large Sb content. In each case, the sizes of the particles range from a few tenths of a milligram to about 10 mg.

Doping pellets produced in the shot tower have been used to dope several dozen Ge crystals, grouped according to amount of shot added and crystal growth conditions. Reproducibility of resistivity among crystals pulled under the same conditions with the same amount of doping shot was in all cases about ±10%. However, largely because of limitations of experimental accuracy, distributions with distance down the crystals varied in most cases with that predicted from theory (2) by factors of this order. Hence, shot consistency could be much better than 10%. In any case, this accuracy of crystal resistivity is well within that required for fabrication of most transistors and other Ge devices. The shot composition for doping to a particular resistivity was chosen so that neither very small nor very large quantities of shot are required. A suggested amount of shot is between 10 and 100 mg.

A possible source of contamination is from decomposition products or impurities in the silicone oil bath. Trouble from this source, however, has not been observed. The pure silicone oil used[1] has no known third of fifth group contaminants.

The shot tower should also be useful for producing conveniently sized doping alloys of other materials. The number of constituents need not be limited to two.

Acknowledgment

This work has been supported by the U.S.A.F. Air Research and Development Command, U.S.A.F. Air Material Command, Army Signal Corps, and Navy Bureau of Ships, under Contract AF 33(600)17793.

The help of A. C. Sheckler, W. E. Engeler, and R. E. Shepp is greatly appreciated.

Manuscript received April 20, 1956. This paper was prepared for delivery before the Cleveland Meeting, September 30 to October 4, 1956.

Any discussion of this paper will appear in a Discussion Section to be published in the June 1957 Journal.

References

1. W. C. Dunlap, Jr., *J. Appl. Phys.*, **24**, 448 (1954).
2. W. G. Pfann, *J. Metals*, **4**, 747 (1952).

[1] G.E. SF-81(4D).

Hydrogen and Oxygen in Single-Crystal Germanium as Determined by Vacuum Fusion Gas Analysis

C. D. Thurmond, W. G. Guldner, and A. L. Beach

Bell Telephone Laboratories, Inc., Murray Hill, New Jersey

Abstract

Concentrations of hydrogen from 3 to 4 × 10^{18} at./cc have been found by vacuum fusion gas analysis in specially prepared single crystals of Ge. In these same crystals oxygen concentrations of 1 to 2 × 10^{18} at./cc were also found.

Three special preparations of Ge were made by the hydrogen reduction of GeO_2 in graphite. In the first, Ge was melted once under hydrogen, in the second, 12 times, and in the third, 42 times. Single crystals were grown from portions of these ingots in graphite crucibles under an atmosphere of hydrogen. Resistivities of the *n*-type crystals were in the range 1–10 ohm cm, and lifetimes of several hundred microseconds were observed. There was no significant variation in hydrogen and oxygen concentration from one crystal to the other. Since the ratio of hydrogen to oxygen is around two, the possibility exists that these elements may be present in the crystal as H_2O.

Vacuum crystal growing lowered the hydrogen and oxygen content 20–30 fold.

It has been reported (1) that hydrogen dissolves in Ge to the extent of 0.186 ml (room temperature and atmospheric pressure) per gram of Ge. This was determined by collecting and analyzing the gas evolved when a sample of Ge was melted under vacuum after it had been melted and solidified under an atmosphere of hydrogen. This amount of hydrogen corresponds to about 5 × 10^{19} at./cc of Ge.

Present day, high purity single crystals of Ge are grown frequently under an atmosphere of hydrogen. The presence

of such high concentrations of hydrogen could be expected to influence the electrical properties of the crystals although such evidence has not been reported in the literature. Recently, however, Reiss (2) has suggested that interstitial hydrogen would not be expected to ionize in Ge since the volume of the interstice is large compared to the volume of a hydrogen atom, and consequently the hydrogen atom would be in a medium having a dielectric constant which is essentially unity rather than the bulk dielectric constant of germanium which is 16.

Kaiser, Keck, and Lange (3) concluded that oxygen may be present in Ge crystals and at concentrations as high as an estimated 10^{16} at./cc when grown from silica crucibles. They concluded that less than 10^{15} at./cc were present when Ge crystals were grown from graphite crucibles.

The following work is presented as evidence that both hydrogen and oxygen can be present at concentrations as high as several times 10^{18} at./cc in single crystals of Ge, although the presence of these impurities is not reflected in the electrical properties of the crystals in any known way.

Experimental

Three 300–400 g lots of Ge were prepared by hydrogen reduction of GeO_2 in a graphite crucible. Portions of each polycrystalline preparation were analyzed for hydrogen and oxygen by vacuum fusion gas analysis. Single crystals of Ge were then grown under an atmosphere of hydrogen and portions of the crystals again subjected to vacuum fusion gas analysis. The resistivity and minority carrier lifetime were determined for each of the single crystals.

Materials.—Eagle-Picher Company GeO_2 was used. Reductions were carried out in standard equipment frequently used for such reductions. Tank hydrogen was used without further purification both for the reduction and crystal growth.

Multifusions.—Each of the three lots of Ge obtained from the oxide reduction was treated differently. After the initial reduction to sponge Ge (3 hr at 675°C) the first lot was fused by raising the temperature to 1020°C for 1½ hr, and then removed from the furnace. The second lot was heated to 1020°C for 1½ hr, cooled to 800°C for ½ hr, then reheated to 1020°C. This cycle was repeated twelve times before the Ge was removed from the furnace. The third lot was cycled 42 times before removal from the furnace.

Single crystal preparation.—A single crystal of Ge weighing about 100 g was grown from each of the three lots of Ge by the crystal pulling technique (4). Growth rates of approximately 2 mils/sec were used, and the seed was rotated at 60 rpm. The melt was contained in a graphite crucible and the hydrogen stream at atmospheric pressure was taken directly from the tank.

After cutting samples for vacuum fusion gas analysis from the single crystal grown from the 12-cycle lot of Ge, the remainder of this crystal was regrown under vacuum. Growing conditions were essentially the same as before except that the melt was held for 30 min about 50° above the melting point of Ge under a pressure of about 10^{-4} mm Hg, prior to growth at this pressure.

Resistivity and lifetime measurements.—Resistivities were measured by the standard 4-point probe technique (5). Lifetimes were measured by the photodecay technique described by Valdes (6).

Vacuum fusion gas analysis.—The principle of this method is based on the fusion of Ge in a graphite crucible resulting in the evolution of oxygen as CO and hydrogen and nitrogen in elementary form. The high temperature furnace designed for this work has been described (7). The graphite crucible is outgassed in vacuum for 2 hr at 2500°C. After this treatment, the temperature of the crucible is lowered to the fusion temperature, 1650°C, and the gas evolved in 30 min from the furnace assembly is collected in a capillary pipet. This is accomplished by means of a high-speed two-stage mercury diffusion pump working in combination with an automatic Toepler pump. This gas can be analyzed and constitutes the correction made on the gases evolved from the sample subsequently dropped into the furnace. For this work, 3–11 g samples of Ge were loaded in the glass side-arms and were injected at will into the crucible by a magnetic pusher. During a 30-min fusion period the gases evolved were collected in a capillary pipet to determine the quantity of gas evolved. Composition of the gas mixture was determined by circulating the gas mixture over a selective reagent or group

TABLE I

Polycrystalline Ge	1 cycle	12 cycles	42 cycles
Wt. of sample, g	4.577	2.851	10.954
Total gases, blank, cc mm	13	13	7
Total gases, sample, cc mm	114	124	256
Residual gases, cc mm	8	8	1
Hydrogen, at./cc	$2.8 \pm 0.1 \times 10^{18}$	$7.8 \pm 0.1 \times 10^{18}$	$5.2 \pm 0.1 \times 10^{18}$
Oxygen, at./cc	$2.6 \pm 0.1 \times 10^{18}$	$2.9 \pm 0.1 \times 10^{18}$	$1.1 \pm 0.1 \times 10^{18}$
Single-crystal Ge			
Resistivity, ohm cm	2–7	1–4	2–10
Lifetime, microsec	65	230	350–500
Wt. of samples, g	5.593	5.711	5.124
Total gases, blank, cc mm	8	8	8
Total gases, sample, cc mm	100	106	93
Residual gases, cc mm	0	0	0
Hydrogen, at./cc	$3.3 \pm 0.1 \times 10^{18}$	$3.7 \pm 0.1 \times 10^{18}$	$3.8 \pm 0.1 \times 10^{18}$
Oxygen, at./cc	$1.3 \pm 0.1 \times 10^{18}$	$1.8 \pm 0.1 \times 10^{18}$	$0.9 \pm 0.1 \times 10^{18}$

TABLE II

Single-crystal, vacuum-grown Ge (*12 cycle*)

	A	B
Resistivity, ohm cm	4	4
Lifetime, microsec	65	65
Wt. of sample, g	7.637	6.967
Total gases, blank, cc mm	0	0
Total gases, sample, cc mm	4	5
Residual gases, cc mm	2	1
Hydrogen, at./cc	$1 \pm 1 \times 10^{17}$	$1 \pm 1 \times 10^{17}$
Oxygen, at./cc	$6 \pm 6 \times 10^{16}$	$6 \pm 6 \times 10^{16}$

of reagents to remove a specific gas. The gas is collected again in the pipet to measure the pressure-volume drop. In this work, the gas is circulated over copper oxide which converts the hydrogen to water and then over magnesium perchlorate which removes the water. The pressure-volume drop is a quantitative measure of the hydrogen. Likewise, during this operation CO has been converted to CO_2 with no pressure-volume change. Then, the gas is recirculated over copper oxide to ensure oxidation of the CO, and circulated over Ascarite to remove CO_2. From this pressure-volume drop the quantity of CO present is obtained. The residual gas which did not react with the reagents is a measure of nitrogen and noble gases. This scheme of analysis is similar to standard Orsat procedures except that micro low-pressure techniques have been applied.

Results

The three polycrystalline preparations of Ge were *n*-type and exhibited resistivities in the range 1–10 ohm cm. Cubes, approximately ¼ in. on an edge, were cut from each ingot for vacuum fusion gas analysis and etched in a mixture of HNO_3, HF, and $C_2H_4O_2$ containing Br. Voids could be seen in these cubes. Four or five cubes were analyzed at a time. Results of analyses are given in Table I.

Three single crystals of Ge, grown under an atmosphere of hydrogen, were also *n*-type. Vacuum fusion gas analyses, resistivities, and lifetimes are included in Table I.

The 12-cycle crystal, regrown under vacuum, was *n*-type and two portions were reanalyzed for hydrogen and oxygen. These results are given in Table II.

Discussion

Multifusions of Ge under hydrogen were carried out in an effort to study several effects. It had been reported that the melting point of Ge could be changed by repeated fusions under hydrogen (8, 9) and a recent paper (10) reports that the melting point of the 42-cycle Ge, which is included in Table I, was not detectably different from the starting material. The possibility existed, however, that the hydrogen content of the crystals was sufficiently high (1) to be measured by vacuum fusion gas analysis techniques. In addition, multifusions would indicate if the rate of solution of hydrogen was slow and also might give information as to how effectively oxygen could be removed by such hydrogen treatment.

The constancy of the hydrogen concentration in the three Ge single crystals shows that the multifusions under hydrogen did not add additional hydrogen. Hydrogen concentrations in the polycrystalline samples were not as reproducible as in the single-crystal samples which is consistent with the observation that voids were present in the polycrystalline ingots.

Oxygen analyses have given surprisingly constant results in view of the treatment given the Ge. It is believed that this oxygen is dissolved in the crystal and cannot be accounted for as surface oxygen.

Analyses of the vacuum-grown Ge provide proof that oxygen and hydrogen are both present in the body of the single crystals of Ge. Since the surfaces of the samples from the vacuum-grown crystal received the same treatment as the other crystal samples, it is concluded that the amount of GeO_2 and adsorbed H_2O on the surfaces should be about the same. The vacuum fusion gas analysis of the vacuum-grown crystal puts an upper limit on the amount of oxygen and hydrogen coming from the sample surfaces.

The variation in lifetime shown in Table I is apparently unrelated to the hydrogen and oxygen in the crystals. It is possible that a recombination center such as Cu was removed during repeated fusions under H_2.

Conclusions

It is concluded that hydrogen and oxygen can be present in single crystals of Ge at concentrations around 10^{18} at./cc. The molecular state of these impurities is such that ionization does not occur to give conduction electrons or holes in significant concentrations. This is in agreement with the conclusion of Reiss (2) pertaining to hydrogen, although it has not yet been established that hydrogen is present as an interstitial proton. The fact that the ratio of hydrogen to oxygen is around two in these crystals suggests that either the molecular state of these elements in the crystal may be principally molecular H_2O, or that the source of the hydrogen and oxygen is principally water vapor.

Acknowledgments

The authors wish to thank K. M. Olsen for the special GeO_2 reductions and M. Kowalchik for technical assistance.

Manuscript received May 1, 1956. This paper was prepared for delivery before the San Francisco Meeting, April 29 to May 3, 1956.

Any discussion of this paper will appear in a Discussion Section to be published in the June 1957 Journal.

REFERENCES

1. J. A. Müller, E. F. Pike, and A. K. Graham, *Proc. Am. Phil. Soc.*, **65**, 15 (1926).
2. H. Reiss, *Bull. Am. Phys. Soc.*, Dec. 1955, Los Angeles Meeting.
3. W. Kaiser, P. H. Keck, and C. F. Lange, *Phys. Rev.*, **101**, 1264 (1956).
4. J. A. Burton, E. D. Kolb, W. P. Slichter, and J. D. Struthers, *J. Chem. Phys.*, **21**, 1991 (1953).
5. L. B. Valdes, *Proc. I.R.E.*, **42**, 420 (1954).
6. L. B. Valdes, *ibid.*, **40**, 1420 (1952).
7. W. G. Guldner and A. L. Beach, *Anal. Chem.*, **22**, 366 (1950).
8. T. R. Briggs, R. O. McDuffie, and L. H. Willisford, *J. Phys. Chem.*, **33**, 1080 (1929).
9. F. H. Roninger, *ibid.*, **33**, 1086 (1929).
10. F. X. Hassion, C. D. Thurmond, and F. A. Trumbore, *ibid.*, **59**, 1076 (1955).

Adsorption of Sodium Ions by Germanium Surfaces

SUMNER P. WOLSKY AND PATRIA M. RODRIGUEZ

Research Division, Raytheon Manufacturing Company, Waltham, Massachusetts

AND

WORDEN WARING

Semiconductor Division, Raytheon Manufacturing Company, Newton, Massachusetts

ABSTRACT

Sodium ions are adsorbed from a NaOH solution by Ge surfaces during an electrolytic etching process. Techniques for determining approximate quantities and location of the adsorbed ions using radioactive tracers have been developed. Alloyed junction *p-n-p* transistors, grown junction diodes, and *p*-type and *n*-type Ge bars were studied. Results show approximately 10^{15} Na ions/cm^2 to be adsorbed with some concentration at the junction region and at surface cracks.

The effect of surface characteristics on the behavior of Ge devices has been well recognized. Consequently, the behavior of Ge surfaces has been widely studied. For the most part the experiments have been designed to observe the electrical properties of the semiconductor surface. More recently, the physical behavior of Ge surfaces in various gaseous ambients has been studied. Experiments dealing with the adsorption and kinetic behavior of Ge in various ambients have yielded interesting information. This paper deals with the physical behavior of Ge surfaces in an etch solution, more specifically, with adsorption of Na ions from NaOH solution during electrolytic etching.

The only previous attempt to determine the type and number of impurity ions present on a Ge surface was that reported by Law (1). In that instance the mass spectrograph was used to analyze the materials produced by passing a spark between two Ge electrodes. Approximately 10^{14} ions/cm^2 were present, consisting mainly of Ca, Na, and K. No detailed description was given of the etching and washing procedure used on the Ge studied.

EXPERIMENTAL PROCEDURE

The experimental method used in this research involved the use of radioactive tracers and a scintillation counter. The process of following the adsorption of ions from a solution in which many ions are present was simplified by making only one ion radioactive and by choosing an etch solution in which the ion being observed was one of the major constituents. Radioactive Na (Na^{24}, with a half life of 14.8 hr) in the form of $Na_2{}^{24}CO_3$ was used in a 1% NaOH etch solution. Two counting standards of different dilutions, prepared from the $Na_2{}^{24}CO_3$ for each experiment, were checked against each other. Na residues on the various samples were calculated on the basis of the standards. A Co^{60} standard was used to check the scaler for instrumental fluctuations at frequent intervals during each experiment. The background count was also closely observed.

The experimental procedure was as follows. The Ge unit (transistor, diode, or bar) was electrolytically etched in a solution usually consisting of 0.1 cc of 7% by weight $Na_2{}^{24}CO_3$ and 0.4 cc of 1% by weight NaOH. Total volume of the etch solution was 0.5 cc. Etching conditions for the various units are described below. After etching, the unit was given a controlled wash consisting of the following steps: (*a*) three rinses in deionized water at room temperature (requiring only a few seconds total time), (*b*) a 10-min dip in deionized water maintained at 65°C, (*c*) a rinse with C.P. acetone, and (*d*) drying in a stream of dry nitrogen. In general, these steps were followed in all experiments. After etching, washing, and drying, the activity on the units was counted. In several cases autoradiographs were prepared. These were made by placing the Ge unit on a film plate for several days.

RESULTS AND DISCUSSION

A large number of alloyed type *p-n-p* transistors were studied. In was used as the alloying material. All transistors were etched in the same manner: the emitter, base, and collector leads were tied together and a current of 250 ma was passed for 10 sec. After etching, the unit was washed and counted as described above. The transistor is a rather complicated device containing other adsorbing materials in addition to Ge. The glass stem, for example, would be expected to show a high Na count caused by adsorption and exchange. Therefore, an adsorption figure obtained for the transistor as a whole has little significance. In order to determine the quantity of Na adsorbed by the various sections of the unit, the transistor was carefully dissected into three or four parts. These parts, shown in Fig. 1, were the Ge chip and dot section, the tab, the leads, and the stem. Because of the construction of the transistor, the leads usually retained some In and solder, and the tab usually held a small piece of the Ge chip. Care was taken in the sectioning process to prevent contamination of one unit or section by the prior unit or section. The sum of the parts was checked against the original count of the undissected unit; in general the agreement was quite good. The dissection technique made it possible to obtain quantitative data on the amount of Na actually present on the

chip and dot section. Some typical results are shown in Table I. The numbers in parentheses are values from later readings on the same samples; they give some indication of the precision of the counting process.

The techniques of autoradiography were used to locate the Na adsorbed by the Ge chip and dot section. After cutting the emitter and collector dots flat and parallel to the base of the chip, the section was placed on photographic film. Fig. 2 is an example of an autoradiograph obtained from a transistor. The dark areas in the center represent the In dots. No activity is shown there since, as mentioned above, the major portions of the emitter and collector dots above the surface of the chip were removed. Because the radiation emitted by Na is highly penetrating, the autoradiographs are really composites of the radiation emitted from both sides of the chip. Information was obtained from the autoradiographs by superimposing the negative on the actual chip and dot section. From Fig. 2 it can be seen that Na was present at the junction region and on the chip itself. The electrolytic etching process outlines the junction region quite sharply, forming a well-defined Ge-In interface. Greater adsorption or trapping at this region is consistent with the results of other experiments described below.

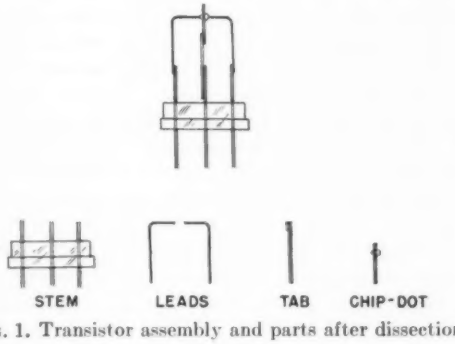

FIG. 1. Transistor assembly and parts after dissection

TABLE I. *Distribution of retained* Na

Unit No.	Parts	Na (μg)	
307	Entire	0.10	
	Total of parts	0.10	
	Chip-dot and tab sections	0.01	
	Leads	0.06	
	Stem	0.03	
406	Entire	1.60	
	Total of parts	1.58	
	Chip-dot section	0.07	
	Tab	0.02	
	Leads	0.19	
	Stem	1.30	
408	Entire	0.84	
	Total of parts	0.73	
	Chip-dot section	0.05	
	Tab	0.02	
	Leads	0.04	(0.02)
	Stem	0.62	(0.58)
409	Entire	0.50	
	Total of parts	0.41	
	Chip-dot section	0.09	(0.06)
	Tab	0.04	
	Leads	0.05	
	Stem	0.23	(0.23)

FIG. 2. Autoradiograph of transistor chip and dot section.

The results in Table I show 0.01–0.1 μg Na is adsorbed by the chip and dot section. Assuming that Na is held only by the Ge surface, there are approximately 10^{15} to 10^{16} ions/cm² present. Some Na is held on the In dot and this must be considered as a maximum value. However, on the basis of some preliminary experiments on the adsorption of Na by In dots, it is believed that most of the Na on the chip and dot section was on the Ge surface.

Similar experiments were performed using *p-n* grown junction diodes and *p*-type and *n*-type Ge bars. The bars, all having very nearly the same dimensions, were cut quite small so as to fit into the small volume of etch solution. Only one lead was attached to a bar. The diode bars were prepared with leads on either the *n* or the *p* side; the junction was usually near the other end of the bar. Solder was used for attaching the leads to the end of the Ge bar. The solder was not dipped into the etch solution; because of splashing during the etching and washing processes, the solder usually picked up Na, but not always. The unit as a whole was biased anodic and etched under the same conditions as were the transistors. Each unit was counted after the standard washing procedure. Results obtained are shown in Table II. Except for unit number 415, there is excellent agreement in the amount of Na retained. Also, there does not appear to be any appreciable difference in the adsorption of Na by *p-n* grown junction diodes, *n*-type bars, and *p*-type bars.

The amount of Na retained by the Ge bars generally was about 0.15–0.25 μg. This is equivalent to approximately 10^{15}–10^{16} ions/cm². For example, bars 416, 417, and 418 showed approximately 1×10^{16}, 1×10^{16}, and 2.5×10^{15} ions/cm², respectively. Again, these amounts must be considered as maximum values, for there is usually some Na held by the solder used to join the lead to the end of the bar. However, in those instances in which the autoradiographs showed little, if any, Na on the solder, there were approximately 10^{15} ions/cm² present on the Ge surface.

Autoradiographs were made of a number of the Ge bars in an effort to determine the distribution of Na on the bar. A typical autoradiograph of a Ge *p-n* grown junction diode is shown in Fig. 3. The bright areas indicate the loca-

TABLE II. *Retention of* Na *on bars*

Unit No.	Type	Lead on	Na (μg)
414	*n-p*	*n*	0.22
415	*n-p*	*p*	4.40
416	*n-p*	*p*	0.23
417	*n-p*	*p*	0.25
418	*n*		0.13
420	*p*		0.16
421	*p*		0.21
1	*n-p*	*p*	0.16
2	*n-p*	*n*	0.39
3	*n-p*	*p*	0.13
4	*n-p*	*n*	0.06

FIG. 3. Autoradiograph of *p-n* grown junction diode bar

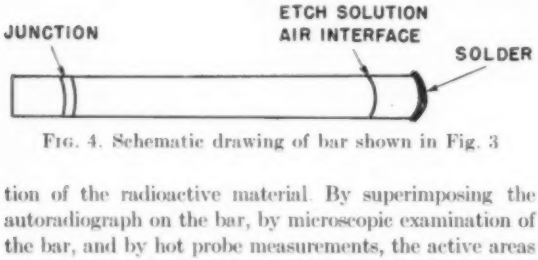

FIG. 4. Schematic drawing of bar shown in Fig. 3

tion of the radioactive material. By superimposing the autoradiograph on the bar, by microscopic examination of the bar, and by hot probe measurements, the active areas were found to be at (*a*) the solder connection to the bar, (*b*) the position of the interface between etch solution and air when the bar is in the process of being etched, and (*c*) the junction of the bar. The autoradiograph of Fig. 3 is shown schematically in Fig. 4. Other bright regions shown in Fig. 3 have been correlated with surface cracks and scratches. One bar which had been cracked so as to expose a very rough and jagged surface showed considerable adsorption at the broken areas. Adsorption at such surface irregularities accounts for the excessive amount of sodium retained by units such as No. 415. Microscopic examination of all the bars revealed considerable erosion at the solution-air interface. Also, the electrolytic etch outlined the junction on all diodes. The *p*-type and *n*-type bars showed activity only at the solution-air interface and occasionally at the solder connection.

The results, therefore, indicate that: (*a*) adsorbed Na is not distributed homogeneously on the germanium surface; certain areas have a greater tendency to retain more of the impurity ions; (*b*) with any differential etch that outlines the junction, there is a probability of adsorption and concentration of the ions at the junction region; (*c*) eroded, cracked, or scratched surfaces tend to hold Na ions; and (*d*) although the result obviously depends somewhat on the treatment of the surface prior to the etching process, as well as on the etching and washing procedure, there appear to be about 10^{15} ions/cm^2 adsorbed on the Ge surfaces.

Data obtained from the alloy-type transistors and Ge bars are generally in good agreement. Considering the assumptions that have been made, the value of approximately 10^{15} ions/cm^2 can also be considered to be in general agreement with the figure of 10^{14} ions/cm^2 found by Law to be present on Ge surfaces after a CP-4 etch. Neither Law's experiments nor these could detect the presence of anions.

No detailed study has been made yet of the effect of adsorbed Na ions on device properties. The only experiment performed in this direction consisted of taking some electrical data on a group of transistors that had been etched, washed, and counted in the usual manner and then were placed in a desiccant box. Collector to base amplification factors of the several units were from 30 to 80, and collector currents on reverse bias were around 10 μamp at low voltages, which are normal for such units treated as these were. From this experiment it appears that in a dry atmosphere electrical properties are not affected by the presence of impurity ions on the surface. Experiments are planned to study the impurity ion effect on device properties in various humidities and ambients. However, changes caused by impurity ions may be of such small magnitude or occur so rapidly as not to be easily observable.

Although these experiments were carried out using Na, it is probable that the results can be extrapolated to other ions. Since there is a substantial number of foreign ions present on the Ge surface at or near the junction region, one must consider their effect on the surface properties. It has been recognized that a sizable portion of the surface conduction observed for Ge, especially in the presence of water vapor, is "ionic." However, the simple "ionic" conduction in an adsorbed water film proposed by Law (1, 2) seems unlikely. It requires either many more ions than can be present, or else some unspecified ionic regeneration process. Other interpretations of the "ionic" process are possible (3, 4), one of them having been proposed since Kingston's review of the surface phenomena on Ge (5).

In considering the effect of impurity ions one must consider their location with respect to the oxide film, which is probably always present on the Ge surface. If the ions are located at the oxide-air interface, they probably influence the adsorption of such materials as water. For example, Law (1) found indications that more adsorption occurred at lower humidities on units previously exposed to NaCl solution or HCl gas than on cleaner units. On the other hand, if the ions are located at the germanium-germanium oxide interface, they may act as trapping centers thereby influencing the surface recombination rate. No experiments has been carried out yet to test these alternatives. It is possible that impurity ions are present both at the oxide-air and at the germanium-germanium oxide interfaces, so their contributions to the observed surface properties may be quite complex.

ACKNOWLEDGMENT

The authors thank Professor John W. Irvine, Jr., of M. I. T., for the radioactive Na and for discussions with them during the course of this work.

Manuscript received February 3, 1956. This paper was prepared for delivery before the Pittsburgh Meeting, October 9 to 13, 1956.

Any discussion of this paper will appear in a Discussion Section to be published in the June 1957 JOURNAL.

REFERENCES

1. J. T. LAW, *Proc. Inst. Radio Engrs.*, **42**, 1367 (1954).
2. J. T. LAW AND P. S. MEIGS, *J. Appl. Phys.*, **26**, 1265 (1955).
3. E. N. CLARKE, *Phys. Rev.*, **99**, 1899 (1955).
4. H. STATZ, W. ERIKSEN, AND G. DEMARS, paper presented at the Institute of Radio Engineers' Semiconductor Device Conference, Purdue University, June 25–27, 1956.
5. R. H. KINGSTON, *J. Appl. Phys.*, **27**, 101 (1956).

New Semiconductors with the Chalcopyrite Structure

I. G. AUSTIN, C. H. L. GOODMAN, AND A. E. PENGELLY

Research Laboratories, The General Electric Company, Ltd., Wembley, England

ABSTRACT

Compounds of the chalcopyrite group are related to well-known semiconductors such as Ge and the zinc blende compounds. This relationship is discussed briefly and some new data are presented regarding the preparation and properties of five chalcopyrite compounds $AgInS_2$, $AgInSe_2$, $CuInSe_2$, $AgInTe_2$, and $CuInTe_2$.

Compounds of the chalcopyrite type are of considerable interest as they are closely related to the well-known semiconductors with diamond and zinc blende structures.

The general formula for chalcopyrite type compounds is ABX_2, where A is Cu or Ag, B is Al, Ga, In, or, in some cases, Fe or Tl, and X is S, Se, or Te (1). They can be considered as being derived from II–VI zinc blende type compounds by replacing a pair of Group II atoms by one from each of Groups I and III (tervalent Fe belongs formally to Group III). Thus silver indium telluride, $AgInTe_2$, is, in this sense, derived from cadmium telluride, CdTe. It is found that, like the related zinc blende-type compounds, chalcopyrite type compounds are semiconductors with a wide range of energy gap (2). The present communication gives limited information on five such compounds with energy gaps close to 1 ev; these are $CuInS_2$, $AgInSe_2$, $CuInSe_2$, $AgInTe_2$, and $CuInTe_2$; some information on chalcopyrite itself, $CuFeS_2$, is also given.

It may be noted that an analogous group of semiconducting compounds derived from III–V zinc blende compounds, may also exist, e.g., InSb would give $CdSnSb_2$. Sufficient work has not been done to establish this definitely.

EXPERIMENTAL PROCEDURES AND RESULTS

All compounds except $CuFeS_2$ were prepared directly from the elements. Starting materials of high purity were used (Cu and Ag, Johnson Matthey spectroscopically pure; S, recrystallized, with traces of Mn, Fe, Si at the 1–10 ppm level; Te, zone melted, with no spectroscopically detectable impurities; Se, 99.995%; In, 99.95%). Synthesis was carried out in sealed evacuated silica tubes, usually heated in an argon-filled furnace. Large ingots (50–100 g) were prepared of all except $CuInS_2$, usually by directional freezing. Zone melting was also used, particularly for $CuInSe_2$.[1] All ingots as prepared were polycrystalline and showed numerous cracks. Attempts to grow large crack-free crystals by directional freezing, zone-melting, or pulling techniques were quite unsuccessful, in marked contrast to experiments with related zinc blende compounds. This difficulty is probably connected with the slight distortion of the diamond-type lattice present in all chalcopyrite compounds, which gives rise to a small degree of anisotropy and with it a differential thermal expansion. For example a differential thermal expansion of 3×10^{-6}/deg (for a and c directions) was found for $CuInSe_2$.

The information obtained for the compounds investigated is summarized in Table I. Energy gaps E_g were calculated from infrared measurements and are values for minimum detectable transmission in polycrystalline specimens. Except for $CuInSe_2$, which was studied in greatest detail, temperature coefficients of the energy gaps dE_g/dT are mean values based on only a few readings between 90° and 300°K. Mobilities are given in cases where it proved possible to obtain crack-free specimens for measurement of Hall effect. Results for chalcopyrite itself were obtained with mineral specimens.

Over 50 ingots of $CuInSe_2$ were prepared. The best n-type samples had a carrier concentration rather less than 10^{16}/cm^3 and showed good point contact rectification (3). The specimens used showed twinning and, although crack-free, were probably appreciably strained since they were cut from ingots which showed many cracks. X-ray examination of crystal structure gave some evidence of thermal disordering above 700°C, an effect similar to that observed in $CuFeS_2$ (4). Zone melting or directional freezing of $CuInSe_2$ appeared to bring about slight changes in the lattice constants along the length of the ingot, as

[1] Zone-melting was carried out using a sealed tube in a high temperature ambient.

TABLE I

Material	Optical gap E_g (ev)	$\frac{dE_g}{dT} \times 10^4$ ev/deg C	μ_e (cm²/v sec)	μ_h (cm²/v sec)	Melting point (°C)
$CuInS_2$	1.2				
$AgInSe_2$	1.18	−1.2			~1000
$CuInSe_2$	0.92	−1.5	300	26	990
$AgInTe_2$	0.96	−2.3			675
$CuInTe_2$	0.95	−3.2			~700
$CuFeS_2$	0.53	−2.2		32	

did additions of Se and Cu. This behavior suggests that an appreciable range of composition is possible; however, infrared transmissions of samples of differing lattice constant were very similar. Transmission beyond the absorption edge was high and at least comparable with that of Ge. Variation of absorption edge with temperature was -1.5×10^{-4} ev/deg at low temperatures, gradually changing to -5×10^{-4} ev/deg above room temperature.

It was found that the vapor pressure of $CuInSe_2$ is high near the melting point. It was not possible to compensate for the loss of a volatile component by the method of van den Boomgaard and co-workers (5) as the vapor appeared to be of complex composition. X-ray analysis of condensed deposits usually indicated the presence of a well-defined but unidentified phase. Comparisons with known structures showed that this was not a known binary compound between In, Cu, Se, or oxygen.

$AgInTe_2$ showed less cracking than $CuInSe_2$ even though it has a much greater differential thermal expansion, more than 9×10^{-6}/°C. This may be connected with the fact that the crystal size in the ingots investigated, zone melted at about 1 in./hr, did not exceed 0.1 mm compared with several centimeters for $CuInSe_2$ grown under similar conditions. $AgInTe_2$, like $CuInSe_2$, had an appreciable vapor pressure at the melting point. X-ray analysis of deposits condensed from the vapor revealed the presence of a complex mixture of phases including In_2Te_3. Some variation in lattice constants could be observed along a zone-melted bar. There was also evidence of thermal disordering above about 400°C. Some material of high resistivity was obtained, but the difficulty of making good contacts prevented electrical measurements being made.

Only a brief study was made of the other compounds. Both $AgInSe_2$ and $CuInTe_2$ have high vapor pressures above their melting points. *n*-type specimens having resistivity of the order of 1 ohm cm gave good point contact rectification. As with $CuInSe_2$, crystal size tended to be large, of the order of 1 cm or more. However, all ingots were badly flawed by cracks.

Only small specimens of $CuInS_2$ were prepared. No attempt was made to zone melt this material because of its high vapor pressure. Photoconductive effects were observed with high resistivity material, with response maxima near 1 μ.

It may be noted that for synthetic chalcopyrite Boltaks and Tarnovskii (6) recently made resistivity measurements and deduced values of thermal activation energy ranging from 0.18 to 0.58 ev for different samples. However, it is not clear from their paper how these values are to be interpreted for comparison with the present value of 0.53 ev for the optical gap for natural chalcopyrite.

The melting point of $CuFeS_2$ was not determined here, but Schlegel and Schüller (7) obtained a value of 950°C.

Summary

1. The pairs $CuInS_2$-$CuInSe_2$ and $AgInSe_2$-$AgInTe_2$ show differences in energy gap in much the same way as do the related zinc blende compounds CdS-CdSe and CdSe-CdTe, but no such difference is found for the pair $CuInSe_2$-$CuInTe_2$. There is no simple explanation of this behavior.

2. The energy gap and melting point of a chalcopyrite-type compound appear to be lower than those for the related II-VI compound.

3. The mobility values measured were low, as shown in the Table I. This may be due in part to crystalline imperfection. Arguing from general views about bonding in diamond-type crystal lattices (8), a "neutral bond" is less likely to be found with ternary compounds of this type than with the related II-VI zinc blende structures. The possible relationship between high mobility and near-neutral bonding would then indicate that very large mobilities are unlikely in compounds of the chalcopyrite type.

Acknowledgments

Thanks are due to Dr. E. A. D. White and Mr. M. H. Francombe for x-ray measurements, and to Dr. L. Ainsworth and Mr. A. West for preparing some of the compounds.

Manuscript received April 2, 1956. This paper was prepared for delivery before the San Francisco Meeting, April 29 to May 3, 1956.

Any discussion of this paper will appear in a Discussion Section to be published in the June 1957 JOURNAL.

REFERENCES

1. H. HAHN, *et al.*, *Z. anorg. u. allgem. Chem.*, **271**, 153 (1953).
2. C. H. L. GOODMAN AND R. W. DOUGLAS, *Physica*, **20**, 1107 (1954).
3. R. W. DOUGLAS AND C. H. L. GOODMAN, *G.E.C. Journal*, **21**, No. 4, 3 (1954).
4. A. J. FRUEH, *J. Am. Mineralogist*, **35**, 282 (1950).
5. J. VAN DEN BOOMGAARD, *et al.*, *J. Electronics*, **1**, 212 (1955).
6. B. I. BOLTAKS AND N. N. TARNOVSKII, *Zhur. Tekh. Fiz.*, **25**, 402 (1955).
7. H. SCHLEGEL AND A. SCHÜLLER, *Z. Metallkunde*, **43**, 421 (1952).
8. C. H. L. GOODMAN, *J. Electronics*, **1**, 115 (1955).

A Metal-Semiconductor Capacitor

R. L. Taylor and H. E. Haring

Bell Telephone Laboratories, Inc., Murray Hill, New Jersey

ABSTRACT

A porous $Ta/Ta_2O_5/MnO_2$ capacitor is described. This capacitor, which might be termed a solid electrolytic capacitor, provides a higher capacitance per unit of volume than can be obtained with any other capacitor heretofore available. Its small size makes it extremely attractive for use in transistor circuits and in other low voltage circuits requiring the ultimate in miniaturization. Construction, characteristics, and advantages of the new electronic device are discussed.

Invention of the transistor and related semiconductor devices has served to emphasize the rapidly growing need for miniaturization of all varieties of electrical circuit components.

The electrolytic capacitor is known for its extremely high capacitance per unit of volume, and for this reason it has become increasingly popular with circuit designers (1, 2). Nevertheless it has several disadvantages, most of which result from the use of an aqueous electrolyte. For example, the tendency of the electrolyte to dry out is always a problem, and the use of a tight seal to prevent this also prevents the necessary venting of gas that may be generated. Also, aqueous electrolytes impose severe limitations because of the relatively narrow operating range between freezing and boiling points. Furthermore, the large temperature coefficients of capacitance and power factor associated with the electrolytic capacitor, particularly in the low temperature region, are largely properties of the aqueous electrolyte. Shelf life, too, is dependent principally on the stability of the oxide film in the liquid electrolyte.

Recognition of the limitation imposed on the electrolytic capacitor by the use of a liquid electrolyte led to the conclusion that a solid "electrolyte" might be substituted for the liquid electrolyte, thus eliminating the disadvantages of the conventional form of electrolytic capacitor without sacrificing its advantages. The purpose of this paper is to describe the "all-solid" electrolytic capacitor developed in three laboratories.

General Description

This solid electrolytic capacitor consists essentially of a porous Ta electrolytic capacitor in which the conventional liquid electrolyte has been replaced by MnO_2, an electronically conductings emiconductor. A schematic cross-sectional view of the device is shown in Fig. 1.

Ta powder sintered to form a porous slug is coated anodically with a current-blocking film of Ta_2O_5 over the entire surface of its porous body. Over the oxide film, and in intimate contact with it, is deposited a layer of an electronically conducting semiconductor, such as MnO_2. Improved electrical contact to the semiconductor is obtained with a coating of graphite followed by a layer of lead-alloy or copper which may be applied by spraying.

The new capacitor retains most characteristics common to electrolytic capacitors. Its capacitance is proportional to the dielectric constant of the oxide film and inversely proportional to film thickness. The film thickness is proportional to and controlled by the forming voltage. The unit has rectifying properties, blocking current when the filmed electrode is made anode and passing current when it is made cathode. The power factor is comparable in magnitude to that of conventional electrolytic capacitors, but superior in respect to temperature and frequency variation. Except for the absence of an initial current surge, the leakage current in the all-solid electrolytic capacitor follows the pattern for electrolytic capacitors with regard to temperature and voltage variation.

Although any of the film-forming metals may be used as anode, Ta was selected because of the excellent quality of its oxide film, its outstanding resistance to corrosion, and because the metal is available in the porous, sintered form. The porous type of electrode represents the most efficient use of Ta metal, yielding a large usable area within a small compact space, approximately 1000 cm^2 of area/cm^3 of porous Ta. Fig. 2 shows some experimental porous Ta electrodes illustrating the variety of shapes and sizes in which porous Ta can be supplied.

Dielectric Film

The heart of any electrolytic capacitor is the electrolytically formed film which serves as the dielectric. The Ta_2O_5 film is formed by the outward movement of Ta ions, under the influence of a high field, through the oxide film already present to combine with oxygen which is held on its outer surface as a further consequence of this same high field. Under the circumstances it is generally assumed that the resulting Ta_2O_5 film cannot be stoichiometric Ta_2O_5 but must be Ta_2O_5 containing a slight excess of Ta ions decreasing in concentration toward stoichiometric as the outer surface of the film is approached. This slight excess of Ta ions agrees with the fact that the Ta_2O_5 film is an *n*-type semiconductor. A concentration gradient of the kind which has been described may be regarded as a "frozen electrolytic polarization" which, it has been suggested (3), is part of the rectification barrier in the electrolytically formed film.[1]

The electrolytically formed film which constitutes the dielectric of the electrolytic capacitor is not pore free.

[1] For a more detailed discussion of film formation and rectification see reference (3). In this connection, a recent theoretical consideration of the kinetics of formation of anode films by Dewald also may be of interest (4).

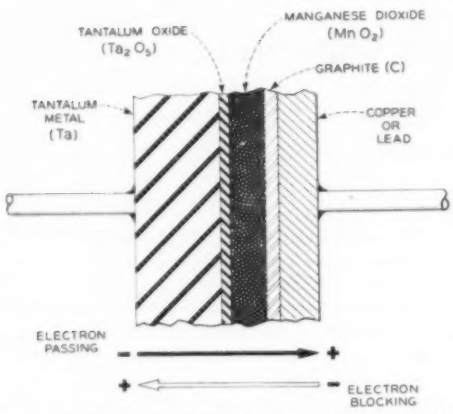

FIG. 1. Enlarged cross section of metal-semiconductor capacitor.

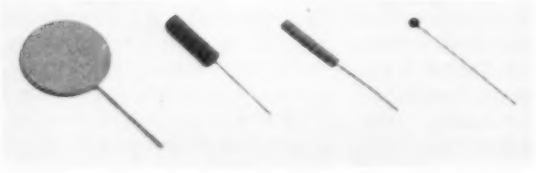

FIG. 2. Experimental porous Ta anodes. Ta metal occupies 60% of volume.

The pores which are present usually result from the inclusion of traces of impurities in the Ta surface and imperfection in the oxide lattice, and are a major cause of leakage current Pores in the oxide film can be detected visually by electroplating Cu on a filmed Ta sheet. Cu plates out at the numerous points of imperfection. Obviously these pores must be effectively blocked or "healed" if the capacitor is to operate successfully. In the liquid electrolytic capacitor, minute oxygen bubbles form within the pores of the film on the anodically charged Ta electrode as a result of the passage of leakage current, and these minute bubbles act as "corks" which make the film sufficiently impervious to be practicable.

In the all-solid electrolytic capacitor there are strong indications that healing of the pores is effected by an irreversible oxidation-reduction reaction which takes place between the Ta or impurity metal which constitutes the pore base and the MnO_2 semiconductor. This reaction, made possible by the extremely high field within the MnO_2 filled pore, must oxidize simultaneously the exposed metal at the base of the pore and reduce the MnO_2 in contact with it, thus forming a permanently nonconducting plug which effectively blocks the leakage current that otherwise would pass through the pores. This permanent healing in the all-solid capacitor eliminates the initial surge of current characteristic of the conventional capacitor with liquid electrolyte.

The fact that a semiconductor, such as MnO_2, can function electronically throughout its bulk, and yet be capable of reacting chemically at the interface with the film-forming metal, may seem incongruous until it is realized that in the healing process only minute localized areas are involved and, in consequence, the field available is tremendous.

As indicated previously, formation of the dielectric film is accomplished ordinarily by the conventional method, viz., by making the film-forming metal anode in aqueous salt solution at temperatures within the boiling range of the electrolyte. However, it is of interest to note that formation also may be accomplished in fused salt electrolytes at comparatively high temperatures. Molten salt formation is of interest because it produces a high quality film in a short time at relatively low voltages. An excellent fused salt electrolyte developed in these laboratories is a eutectic mixture of $NaNO_3$ and $NaNO_2$ operated at a temperature of 250°C, which is slightly above its melting point. A temperature of 300°C is considered maximum for molten salt formation of Ta, because at temperatures above this heat oxidation begins to take place rapidly and a crystalline gray oxide begins to form. Film formation is carried out until the desired oxide film thickness and leakage currents are obtained.

THE SEMICONDUCTOR "ELECTROLYTE"

Preparation of the electrolytically oxidized Ta anode has followed established practice. At this point, however, construction of the all-solid capacitor deviates from the conventional. Use of a semiconductor such as a higher oxide of Pb, Ni, or Mn as an "electrolyte" in combination with a porous type of anode presents many practical problems.

The most obvious problem involves obtaining a uniform coating of the semiconductor over the oxide film throughout the interior of the porous anode. This was solved by dipping the porous electrode into an aqueous solution of manganous nitrate and then heating the wet electrode to evaporate the water and pyrolytically convert the manganous nitrate to MnO_2.

The pyrolytic decomposition of manganous nitrate is accompanied by evolution of steam and other gaseous decomposition products (oxides of nitrogen) which tend to produce minute openings in the MnO_2. In consequence several successive coatings of MnO_2 are applied. The temperature should be higher than that required to convert manganous nitrate to MnO_2, but not high enough to decompose the MnO_2.

Defects in the Ta_2O_5 film which may develop during the pyrolytic process may be repaired by re-anodizing after the first few coatings of MnO_2 have been applied. Re-anodizing involves returning the coated electrode to the forming bath and anodizing as before. Following re-anodizing the final applications of MnO_2 can be made.

PRINCIPLE OF OPERATION

The metal-semiconductor capacitor utilizes the current blocking properties and high capacitance of a thin electrolytically formed film of high resistivity Ta_2O_5 in contact with Ta on one side and MnO_2 on the other. The resistivity of the Ta_2O_5 film in an operating capacitor is extremely high, e.g., 10^{14} ohm-cm; the resistivity of the MnO_2 is relatively low, e.g., 10–100 ohm-cm, depending on its porosity. Both of these materials are *n*-type semiconductors.

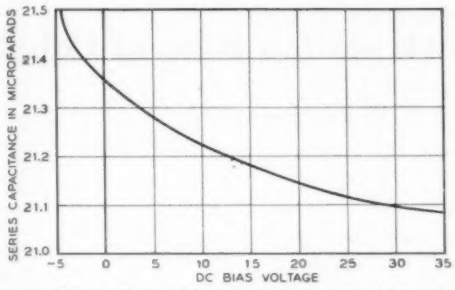

FIG. 3. Effect of d.c. bias on capacitance. (Capacitance measured at 1000 cps and 0.05 v a.c.)

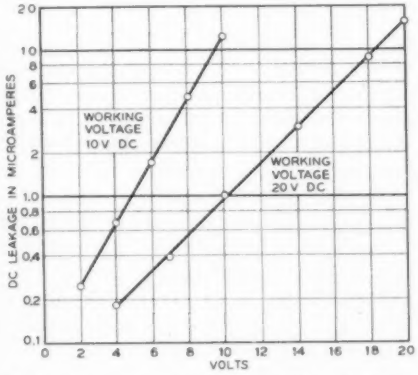

FIG. 4. Leakage current characteristics of 25 μf metal-semiconductor capacitors.

MnO_2 serves not only as an electronically conducting connection with the Ta_2O_5 dielectric but also as an oxidizing "electrolyte" which heals any pores or other defects in the Ta_2O_5 film and thus maintains it in operating condition. In addition to these functions, MnO_2 serves in another extremely important way. MnO_2 must share some of its oxygen with the entire outer surface of the Ta_2O_5 film thus establishing a p/n junction between the n-type Ta_2O_5 and a thin p-type inversion layer induced in the surface region of the Ta_2O_5 by the film of negatively charged oxygen adsorbed on it.

In summary, the rectifying and current blocking barrier which constitutes the dielectric of the solid electrolytic capacitor consists of (*a*) Ta_2O_5 film (containing a decreasing concentration of excess tantalum ions), (*b*) a thin p-type inversion layer at the surface of the Ta_2O_5, and (*c*) the extremely thin film of oxygen (and reduced MnO_2) on the outer surface of this inversion layer. Note that this current blocking system is similar to that previously described (3) as the rectifying and current blocking barrier in the wet electrolytic rectifier and capacitor. In one case the oxygen layer is provided by the incipient decomposition of water (H_2O) in contact with Ta_2O_5; in the other case the oxygen

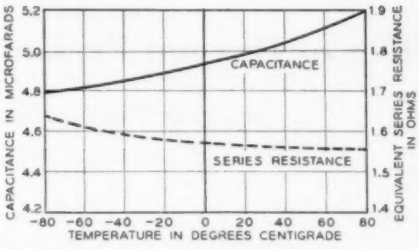

FIG. 5. Effect of temperature on 1000 cps capacitance and series resistance of metal-semiconductor capacitor.

layer is provided by the incipient decomposition (reduction) of MnO_2.

The slight decrease in capacitance with increased bias voltage, shown in Fig. 3, is probably the result of widening of the barrier layer at the p-n junction located at the interface between Ta_2O_5 and MnO_2. This change is experienced not only with the solid electrolytic capacitor but also with the liquid electrolytic capacitor, which is further indication of the close similarity between the current blocking systems in the two cases.

Operating Characteristics

The breakdown voltage in the solid electrolytic capacitor is related to the oxide film thickness The maximum voltage that it may be expected to withstand will not be greater than the formation voltage under comparable temperature conditions. A practical working voltage is roughly one-third the forming voltage.

Typical leakage-current data for capacitors of two voltage ratings are shown in Fig. 4. These curves follow the leakage vs. voltage pattern common to liquid electrolytic capacitors. Steps in the processing for the two ratings differed somewhat.

The effect of temperature on capacitance and series resistance is given in Fig. 5. The temperature range shown, −80° to +80°C, represents considerable improvement over the paste and other liquid-type electrolytic capacitors.

Detailed operating characteristics of the solid electrolytic capacitor are given elsewhere (5).

Manuscript received April 11, 1956. This paper was prepared for delivery before the San Francisco Meeting, April 29 to May 3, 1956.

Any discussion of this paper will appear in a Discussion Section to be published in the June 1957 JOURNAL.

REFERENCES

1. M. WHITEHEAD, *Bell Labs. Record*, **28,** 448 (1950).
2. J. H. HALL AND F. H. BERGHORN, *Elec. Mfg.*, **46,** 82 (1950).
3. H. E. HARING, *This Journal*, **99,** 30 (1952).
4. J. F. DEWALD, *ibid.*, **102,** 1 (1955).
5. D. A. MCLEAN AND F. S. POWER, *Proc. I. R. E.*, **44,** 872 (1956).

Effect of Oxygen Pressure on the Oxidation Rate of Cobalt

DONALD W. BRIDGES,[1] JOHN P. BAUR,[1] AND W. MARTIN FASSELL, JR.[1]

Department of Metallurgy, University of Utah, Salt Lake City, Utah

ABSTRACT

Co was oxidized from 800° to 1200°C in 0.013–27.2 atm O_2. It oxidized in accordance with the parabolic rate law above 950°C and formed the single oxide, CoO, above 900°C. Pressure increase accelerated the rate of oxidation. However, the oxidation rate eventually ceased to increase with increase of oxygen pressure at temperatures below 1150°C. Theoretical considerations employing a vacancy saturation mechanism correlated the data. Photomicrographs of the oxide layer are included. Activation energy for the diffusion process is 58,000 cal.

A review of the oxidation literature for the metal Co is available elsewhere (1). Oxidation of Co above 900°C and 150 mm Hg oxygen pressure involves the single oxide, cobaltous oxide, CoO. CoO is a semiconductor of the metal deficit type (NiO and Cu_2O type) (2). Below 900°C the surface oxide is a thin layer of Co_3O_4, although most of the oxide layer is CoO. The CoO vacancy concentration has been estimated to be 25 times that of NiO (3). The present survey investigates the oxidation behavior of cobalt from 800° to 1200°C over the oxygen pressure range 0.013–27.2 atm; however, theoretical evaluation of the data is limited to temperatures above 900°C where the only oxide present is CoO.

Experimental Procedure

Details of the high-pressure equipment and general procedure have been described (4) as has the low-pressure equipment (5). All rate data were obtained using the quartz spring technique. Two types of Co were employed: (*a*) spectrographically pure Co,[2] and (*b*) high-purity electrolytic Co.[3] Each was rolled to desired thickness, and vacuum annealed prior to oxidation The sample size was: (*a*) 1.3 in. x .37 in. x .01 in.; (*b*) 1.1 in. x .5 in. x .01 in. Spectrographic analysis of sample (*a*) metal is as follows: Si <0.0002%; Fe <0.0005%; Mg <0.0001%; Ag <0.0001%; and a slight trace of Na and Ca. Comparison of the spectrograms of both metals showed sample (*b*) Co to be of comparable purity, with a trace of Ni and Si. Oxidation time varied from 2 hr to 45 min depending on the rate of reaction.

Experimental Results

Above 950°C and at all oxygen pressures investigated the metal rigorously obeyed the parabolic oxidation rate equation, $\Delta W^2 = K_p \cdot t$. At lower temperatures irregularities sometimes occurred as others have noted (1). Table I summarizes the parabolic rate constants for corresponding temperatures and oxygen pressures.

The parabolic constants of Carter and Richardson (2) compare favorably with those obtained in this survey. As no determinations were made at one atmosphere in this study, direct comparison is impossible. However, if the parabolic constants are plotted vs. oxygen pressure, interpolation yields remarkably close agreement. Values thus obtained and those of Carter are as follows: 1000°C, 1 atm, CR, 87.6; BBF, 83; 1148°C, 1 atm, CR, 334.5; BBF, 320; 1148°C, 0.15 atm, CR, 180.1, BBF (0.125 atm), 134.5. The units are those of Table I; the authors' initials are used to designate the investigators.

Due to the proximity of the sample to the furnace winding in the high-pressure furnace, together with the increased current required to maintain the elevated temperature at higher oxygen pressures, 1200°C data are not available above 1 atm. The sample was seized as it entered the magnetic field of the winding and fused to the furnace tube wall. Fusion occurred at the lower guard winding where the temperature is just below the Curie temperature of 1130°C. At high-oxygen pressures the current must be higher in the guard windings than in the center winding in order to maintain a uniform temperature zone adjacent to the sample thermocouple. Seizure did not occur in the low-pressure furnace because the furnace winding is approximately twice the distance from the sample, and the current requirement is not as great. In determinations at lower temperatures in both furnaces, current requirements are less, resulting in a smaller magnetic field and less chance of arrestment during the raising of the sample.

Experimental conditions above 950°C were such as to suppress the decomposition of CoO to Co_3O_4 or the formation of Co_3O_4 as a layer over the CoO substrate when the sample is lowered at the completion of a determination. X-ray diffraction showed the oxide formed at 800°C and 6.8 atm to be a mixture of CoO and Co_3O_4 spinel, but mainly CoO. At 1000°C and 6.8 atm the oxide was predominantly CoO with a slight trace of the spinel possibly due to quenching in an excess of oxygen. The oxide formed at 1200°C and 0.125 atm was entirely CoO. Oxidized samples resembled silvered mirrors in physical appearance. The same type of grain structure and triangular grain boundary shape exist on high-pressure samples as have been observed on copper oxidized to Cu_2O (5). Fig. 1 shows CoO grains formed on Co at 1100°C at various oxygen pressures for a period of 45 min. Photographs are of the *in situ* oxide layer unetched. Grain growth phe-

[1] Present address: Howe Sound Co., Salt Lake City, Utah.

[2] Obtained from Jarrell-Ash Co., manufactured by Johnson-Matthey Co., Ltd.

[3] Prepared by Howe Sound Co Research Lab.

TABLE I. *Compilation of observed parabolic rate constants*

P, atm	K_p, $mg^2cm^{-4}hr^{-1}$								
	800°C	850°C	900°C	950°C	1000°C	1050°C	1100°C	1150°C	1200°C
0.013				8.0*	15.9*	27.7*	46.1*	91.7*	121.0*
0.033				13.0*			56.4*	98.3*	144.3*
0.066				18.1*	18.0*	46.4*	71.3*	116.7*	191.5*
0.092				13.8*					
0.125				19.2*	37.7*	66.3*	107.0*	134.5*	237.8*
0.250				24.7*			129.8*		
0.500				35.1*	63.1*	116.3*	160.4*	229.1*	
1.36	1.5†	4.4*	12.7*	59.4†	96.8*	171.7†	302.3†	531.7†	
		5.3†	14.1†		96.6†				
6.81	2.0†	5.0*	13.0*	56.3†	156.1†	326.5†	536.5*	951.9†	
		5.2†	19.3†		167.9*	323.9†	507.0†		
13.61	2.7†	5.1*	15.5*	55.5†	144.5†	365.6†	822.8*	1049.8†	
		7.4†	21.1†		144.8*		717.8†		
20.41	1.7†	6.0*	16.0*	50.2†	143.8†	306.3†	835.0*	1066.7†	
		8.5†	19.8†		144.1*		809.1†		
27.2							738.2*	1376.1†	
							742.1†		

* Johnson-Matthey cobalt.
† Howe Sound Co. cobalt.

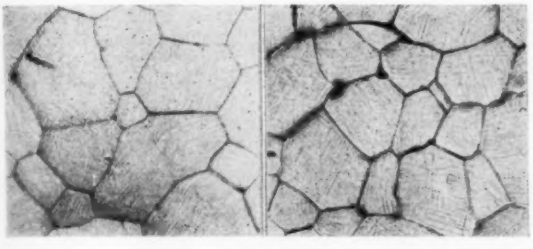

FIG. 1. Photomicrographs of CoO layers formed in 45 min at 1100°C and (*left*) 6.81 atm and (*right*) 20.4 atm. 250× before reduction for publication.

nomena are quite apparent. Grain size is larger as the temperature of oxidation is increased.

DISCUSSION OF RESULTS

No attempt is made to explain the mechanism of oxidation below 900°C where the oxidation process involves two oxides.

According to Mott and Gurney (6), the parabolic constant for oxidation involving a metal deficit type of oxide whose migrating cations are divalent is:

$$K_p = 3\Omega D_o(n_g - n_m) \qquad (I)$$

where K_p is the parabolic constant as defined by $\Delta W^2 = K_p \cdot t$; Ω is the volume of metal oxide containing 1 mole of the cation, and D_o is the temperature dependent part of the diffusion coefficient. n_g is the number of vacancies per unit volume near the oxide-oxygen interface, and n_m is the corresponding quantity for the region near the metal-oxide interface. If the concentration of vacancies at the oxygen interface, n_g, is much greater than the vacancy concentration at the metal-oxide boundary, n_m (i.e., $n_g \gg n_m$), one obtains the expression:

$$K_p = n_g \cdot K_p' \qquad (II)$$

where n_g is a function of the external oxygen concentration and

$$K_p' = 3\Omega D_o = A \cdot \exp(-\Delta H^*/RT) \qquad (III)$$

ΔH^* is the activation energy for the diffusion process. The assumption of temperature invariance of the parabolic constant other than the variation in the exponential term, $\exp(-\Delta H^*/RT)$, is universal but never rigorously correct. The success of this assumption depends on the parameter A containing only factors involving powers of T near unity. For small temperature changes the variation of A will then be negligible compared to that of the exponential term. The explicit form for the factor A depends on the theory of diffusion preferred (7).

For all isotherms except those at 1150° and 1200°C, the parabolic constant reaches a maximum value. This suggests two possible saturation effects: (*A*) The surface sites become saturated with oxygen. This effect is discussed in detail elsewhere (5). (*B*) Alternatively, the vacancy density has obtained a limiting condition. Co oxidation data are correlated through the assumptions of sufficiently low oxygen surface coverage to allow the bulk oxygen gas pressure to be used as the surface oxygen activity, and of equilibrium between the gas phase and the near surface vacancy concentration. Cessation of increase in the parabolic rate constant with increased oxygen pressure is attributed to saturation of the cation vacancies.

The Schottky-Wagner (8) theory of defects, which is the basis of the Wagner (9) theory of parabolic oxidation, assumes that the number of vacancies is much smaller than the number of lattice sites and that interaction between the vacancies (defects) is negligible. Anderson (10) expanded the theory to encompass large defect concentrations with interaction between the pairs of like defects. This theory yields, for oxides of the form MeO, the expression (10–12)

$$\lambda = [p(\theta)]^{1/2} = \frac{\theta}{1-\theta} P^o \cdot \exp(2\theta w/kT) \qquad (IV)$$

where θ the fraction of unoccupied sites is defined by $\theta = n_g/N$, n_g is the number of vacant sites per unit volume,

TABLE II. *Summary of the calculations necessary in the application of Eq. (IX)*

950°C $K_p'' = 55$ $p(1/2) = 0.225$

$p(\theta)$	θ	K_p	$\frac{p(\theta)}{p(1/2)}$	$1/2 \ln \frac{p(\theta)}{p(1/2)}$
0.500	0.637	35.07	2.222	0.399
0.250	0.448	24.65	1.111	0.0525
0.125	0.350	19.22	0.556	−0.294
0.092	0.250	13.77	0.409	−0.446
0.0658	0.329	18.09	0.292	−0.615
0.0329	0.236	12.95	0.146	−0.961
0.0132	0.146	8.04	0.0587	−1.481

1000°C $K_p'' = 144$ $p(1/2) = 0.54$

$p(\theta)$	θ	K_p	$\frac{p(\theta)}{p(1/2)}$	$1/2 \ln \frac{p(\theta)}{p(1/2)}$
1.361	0.672	96.71	2.520	4.606
0.5000	0.438	63.05	0.926	−0.0384
0.1250	0.262	37.70	0.232	−0.731
0.0658	0.125	17.95	0.122	−1.052
0.0132	0.110	15.88	0.0244	−1.858

1050°C $K_p'' = 340$ $p(1/2) = 1.20$

$p(\theta)$	θ	K_p	$\frac{p(\theta)}{p(1/2)}$	$1/2 \ln \frac{p(\theta)}{p(1/2)}$
1.361	0.505	171.67	1.134	0.0629
0.500	0.342	116.25	0.4167	−0.438
0.125	0.195	66.29	0.1042	−1.131
0.0658	0.136	46.36	0.0548	−1.451
0.0132	0.081	27.71	0.0110	−2.255

1100°C $K_p'' = 760$ $p(1/2) = 2.50$

$p(\theta)$	θ	K_p	$\frac{p(\theta)}{p(1/2)}$	$1/2 \ln \frac{p(\theta)}{p(1/2)}$
6.805	0.687	521.75	2.722	0.500
1.361	0.398	302.31	0.544	−0.304
0.500	0.221	160.40	0.200	−0.805
0.250	0.171	129.76	0.100	−1.151
0.125	0.141	107.01	0.050	−1.499
0.0658	0.094	71.26	0.02632	−1.819
0.0329	0.074	56.37	0.01316	−2.165
0.0132	0.061	46.13	0.00528	−2.618

1150°C $K_p'' = 1550$ $p(1/2) = 5.00$

$p(\theta)$	θ	K_p	$\frac{p(\theta)}{p(1/2)}$	$1/2 \ln \frac{p(\theta)}{p(1/2)}$
27.218	0.888	1376.0	5.444	0.8475
20.414	0.688	1066.7	4.083	0.704
13.609	0.676	1049.0	2.722	0.501
6.805	0.614	951.0	1.361	0.154
1.361	0.343	531.0	0.2722	−0.651
0.500	0.148	229.1	0.1000	−1.151
0.125	0.087	134.5	0.0250	−1.841
0.0658	0.075	116.3	0.01316	−2.165
0.0329	0.063	98.3	0.00658	−2.515
0.0132	0.059	91.7	0.00264	−2.965

1200°C $K_p'' = 3200$ $p(1/2) = 9.5$

$p(\theta)$	θ	K_p	$\frac{p(\theta)}{p(1/2)}$	$1/2 \ln \frac{p(\theta)}{p(1/2)}$
0.125	0.0740	237.82	0.01316	−2.165
0.0658	0.0599	191.46	0.00693	−2.485
0.0329	0.0452	144.29	0.00346	−2.818
0.0132	0.0378	120.97	0.00139	−3.285

and N is the total number of sites per unit volume; λ is the absolute activity of the surface oxygen and is assumed to be equal to $[p(\theta)]^{\frac{1}{2}}$, the square root of the oxygen pressure for a particular value of θ; w is the vacancy interaction energy; P^o is determined by the temperature dependent portion of the partition function for the oxygen gas and may be approximated for the purpose of expansion in this paper as,

$$P^o = B \cdot \exp[(E^v + \tfrac{1}{2}E^d)/kT] \qquad (V)$$

B is a function containing the absolute temperature to powers of the order of unity; E^v is the energy required to form a vacancy; and E^d is the dissociation energy for an oxygen molecule.

In applying the theory underlying Eq. (IV) to the oxidation of Co to CoO one must introduce two generalities of the theory as applied to equilibrium monolayers by Fowler (12). It is felt that these modifications are necessary to form a three-dimensional analogy of the two-dimensional monolayer in the immediate neighborhood of the oxide-oxygen interface: (*a*) gross deviations from stoichiometric proportions must be capable of existence near the oxide-oxygen interface so that θ may approach unity while the bulk of the oxide remains of near stoichiometric proportions, and (*b*) concentration of vacancies near the interface must increase sharply over that in the bulk oxide phase.

Multiplication of Eq. (II) by N/N yields the following forms:

$$K_p = \theta \cdot N \cdot K_p' = \theta \cdot K_p'' \qquad (VI)$$

where $K_p'' = N \cdot K_p'$. Eq. (IV) cannot be solved explicitly for θ in terms of p, the oxygen pressure. It is necessary to resort to an indirect method in order to illustrate the closeness of fit between the experimentally observed parabolic rate constants and the theory underlying Eq. (IV). The steps of the method are enumerated below.

Step 1. Approximate values of K_p'' for all temperatures below 1150°C are selected easily from the data of Table I. Compatible K_p'' values for 1150° and 1200°C are found by plotting the logarithm of K_p'' vs. 1/°K and extrapolating to the desired temperature. This extrapolation requires that ΔH^* is constant over the investigated temperature range. Table II lists K_p'' values for all temperatures.

Step 2. Experimental θ values are calculated from division of the observed parabolic rate constant by the compatible K_p''. θ is tabulated in Table II.

Step 3. Substitution of $\theta = \frac{1}{2}$ in Eq. (IV) results in the particular solution,

$$[p(\tfrac{1}{2})]^{\frac{1}{2}} = P^o \cdot \exp(w/kT) = B \cdot \exp[(E^v + \tfrac{1}{2}E^d + w)/kT] \qquad (VII)$$

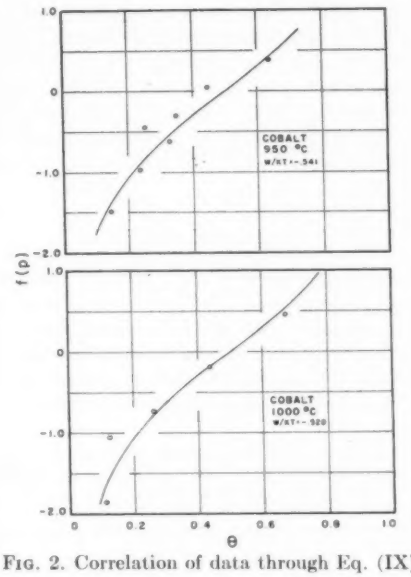

FIG. 2. Correlation of data through Eq. (IX)

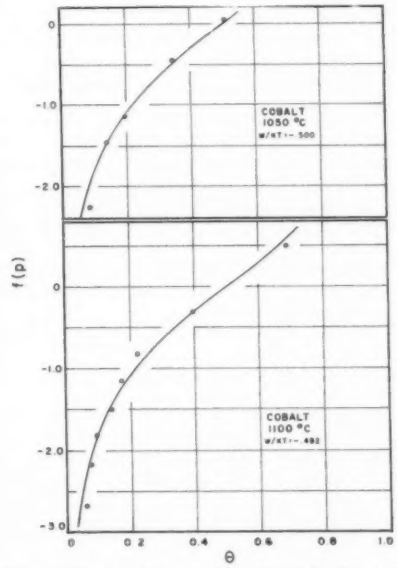

FIG. 3. Correlation of data through Eq. (IX)

Division of Eq. (IV) by Eq. (VII) eliminates the variable P^o and gives the forms:

$$\left[\frac{p(\theta)}{p(\tfrac{1}{2})}\right]^{\frac{1}{2}} = \frac{\theta}{1-\theta}\exp\left[(2\theta-1)w/kT\right] \qquad \text{(VIII)}$$

or

$$f(p) = \tfrac{1}{4}\ln\frac{p(\theta)}{p(\tfrac{1}{2})} = (2\theta-1)w/kT + \ln\frac{\theta}{1-\theta} \qquad \text{(IX)}$$

The left-hand member of Eq. (IX) is a function of oxygen pressure suitable for use in plotting the experimental data of Table I. Table II shows the calculated values of this function for θ values found in Step 2 and $p(\frac{1}{2})$ values (also tabled in Table II) estimated by plotting K_p vs. p and determining the pressure corresponding to $\frac{1}{4}K''_p$.

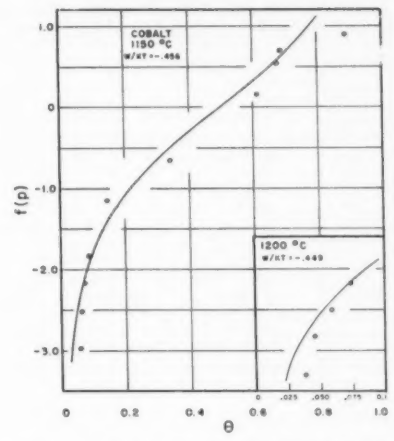

FIG. 4. Correlation of data through Eq. (IX)

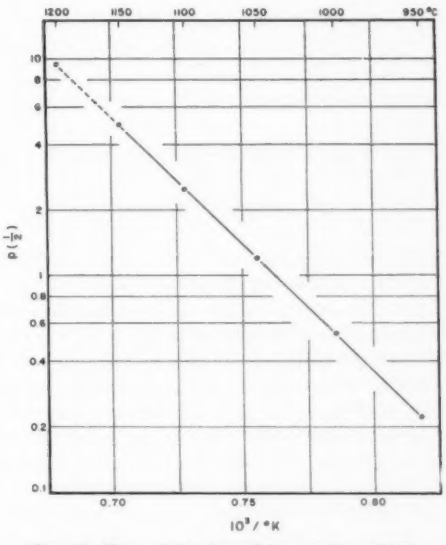

FIG. 5. Plot of the logarithm of Eq. (VII)

Step 4. Theoretical plots of Eq. (IX) vs. θ can be formulated by selection of a value of w and computation of the right-hand side of Eq. (IX) for selected values of θ.

Fig. 2 through 4 are the plots of $f(p)$ of Eq. (IX) vs. θ. The solid theoretical curves were calculated by the method described under Step 4. The assumed values of w/kT used to fit the data vary from -0.541 to -0.449. These values correspond to an interaction energy w of -1324 cal/mole.[4]

Differentiation, with respect to the reciprocal absolute temperature, of the logarithms of both sides of Eq. (VII) yields:

$$\frac{d\ln[p(\tfrac{1}{2})]}{d(1/T)} = 2(E^v + \tfrac{1}{2}E^d + w)/K \qquad \text{(X)}$$

[4] Molar energy quantities can be found from the cited equations by substituting R (2 cal/mole·°K) in place of the Boltzmann constant, k, or alternatively by multiplying the molecular energies of the equations by Avogadro number.

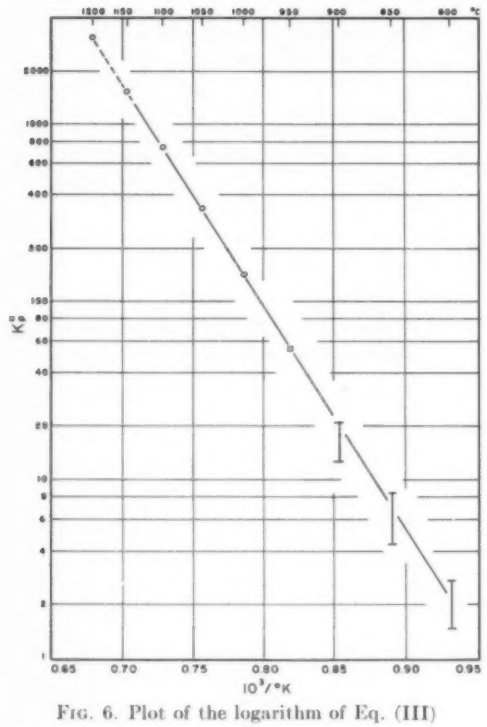

FIG. 6. Plot of the logarithm of Eq. (III)

If each of the energies is reasonably insensitive to temperature in the range of experimental determination, a plot of the logarithm of $p(\frac{1}{4})$ vs. the reciprocal absolute temperature would yield a straight line. Fig. 5 is the curve obtained from the estimates of $p(\frac{1}{4})$ in Table II. From the slope of Fig. 5 the summation of the molar energies of Eq. (X) was found to be $-28{,}300$ cal/mole. The dissociation of oxygen molecules requires an E^d of 117,200 cal/mole (13). Use of the above values of the energies results in an energy of vacancy formation, E^v, of $-85{,}576$ cal/mole or 3.71 ev.[5] No reference could be found for the energy of vacancy formation in an oxide. However, energies are reported for hole formation in silver and alkali metal halides. Halide crystals, as well as oxides, have ionic crystal lattices. E^v for AgCl is 25,000 cal/mole and for AgBr, 20,200 cal/mole (15). For the alkali metal halides the following values are available: NaCl, 1.86 ev; KCl, 2.08 ev; and KBr, 1.92 ev (16).

[5] Literature estimates of involved energies are sometimes reported in electron volts (ev); 1 ev equals 23,052 cal/mole (14).

Fig. 6 is a plot of the limiting parabolic rate constant, K_p'', vs. the reciprocal absolute temperature. The vertical lines at 900°C and lower temperatures are the spread of the parabolic rate constants at these temperatures, which were not analyzed as the oxidation process involved two oxides. The slope of this graph yields an activation energy for the diffusion process, i.e., the diffusion of Co^{++} through CoO of 58 kcal.

ACKNOWLEDGMENTS

The authors are indebted to the Office of Ordnance Research, U. S. Army, and the Watertown Arsenal Laboratory, for the funds necessary for this work. Thanks are due to J. R. Lewis, Head, Department of Metallurgy, for his interest in this work and Mr. Theron Odekirk for his assistance in the numerous calculations involved.

Manuscript received January 23, 1956.
Any discussion of this paper will appear in a Discussion Section to be published in the June 1957 JOURNAL.

REFERENCES

1. O. KUBASCHEWSKI AND B. E. HOPKINS, "Oxidation of Metals and Alloys," p. 176, Academic Press, Inc., New York (1953).
2. R. E. CARTER AND F. D. RICHARDSON, *J. Metals*, **7**, 336 (1955).
3. W. J. MOORE AND J. K. LEE, *J. Chem. Phys.*, **19**, 255 (1951).
4. R. C. PETERSON, W. M. FASSELL, JR., AND M. E. WADSWORTH, *J. Metals*, **6**, 1038 (1954).
5. J. P. BAUR, D. W. BRIDGES, AND W. M. FASSELL, JR., *This Journal*, **103**, 273, (1956).
6. N. F. MOTT AND R. W. GURNEY, "Electronic Processes in Ionic Crystals," 2nd ed., p. 256, Oxford Press, New York (1948).
7. B. CHALMERS, Editor, "Progress in Metal Physics," vol. 4, chap. 6, pp. 265-332, Interscience Publishers, Inc., New York (1953).
8. W. SCHOTTKY AND C. WAGNER, *Z. phys. Chem.*, **B11**, 163 (1930).
9. C. WAGNER, "Atom Movements," p. 153, American Society of Metals, Cleveland (1951).
10. J. S. ANDERSON, *Proc. Roy. Soc.*, **A185**, 69 (1946).
11. A. L. G. REES, "Chemistry of the Defect Solid State," p. 41, Methuen & Co., Ltd., London (1954).
12. R. H. FOWLER AND E. A. GUGGENHEIM, "Statistical Thermodynamics," p. 431, Cambridge (1949).
13. A. G. GAYDON, "Dissociation Energies and Spectra of Diatomic Molecules," p. 212, Dover Publications, Inc., New York (1950).
14. "Handbook of Chemistry and Physics," 30th ed., p. 2634 (1948).
15. W. JOST, "Diffusion in Solids, Liquids, Gases," p. 95, Academic Press, Inc., New York (1952).
16. *Ibid.*, p. 113.

Kinetics of Formation of Porous or Partially Detached Scales

C. Ernest Birchenall

Forrestal Research Center, Princeton University, Princeton, New Jersey

ABSTRACT

Growth of oxide scales on metals is often accompanied by the development of porosity in the oxide or at the metal-oxide interface. These irregularities should affect the kinetics of the reaction and, if ignored, may lead to incorrect conclusions about the mechanism of the reaction. A number of simple models in which pores are assumed to grow in the oxide or at the interface are investigated, and it is shown that a sequence of ranges governed by different kinetics might be found in several cases. Recent experiments which seem to contradict Wagner's theory of scale growth are discussed and an explanation in terms of pore growth is offered.

For the formation of thin oxide films on metals Mott and coworkers (1) have shown how a number of rate laws may arise out of the physical requirements of the metal-oxide composite. These rate equations may be linear, parabolic, cubic, or logarithmic in form. During the oxidation of a single material at constant oxygen pressure and temperature the various rate laws may apply in time sequence due to the thickening of the film. However, when the oxide product is a thick scale without porosity and firmly attached to the metal base the number of possibilities seems to be rather severely limited. Reaction at one of the phase interfaces in the system may be rate controlling, in which case the rate of growth will be constant. Alternatively, diffusion through the oxide layer may be controlling, leading to the familiar parabolic dependence of thickness on time. Although there may be an initial period of linear growth, once the parabolic law is established it should persist indefinitely in the absence of other physical changes in the system. These observations are embodied in the equation

$$\frac{x}{l} + \frac{x^2}{k} = t \qquad \text{(I)}$$

frequently employed in the past (2). The squared term is small at short times and large at long times as required if the rate constants l and k are chosen properly.

A metal or alloy seldom oxidizes precisely according to the parabolic law or a sequence of linear followed by parabolic rates. Sometimes the behavior belongs properly to the thin film range, but often it is simply an indication of the difficulty of providing the ideal conditions postulated above: nonporous and closely adherent oxide. In fact, Dravnieks and MacDonald (3) have given a rather detailed picture of a possible mechanism by which vacancies, halted in their flow by the metal-oxide interface, condense to destroy the metal-oxide contact. They suggest the need for an appreciable oxide ion diffusion contribution. This suggestion is not adopted here because recent experiments in this laboratory seem to rule out this contribution for the growth of wüstite on iron and to show that, when it can, the oxide follows the retreating metal interface by a plastic flow mechanism (4).

It is instructive to examine the variety of rate equations which may be obtained for simple assumptions which are reasonable for oxidizing metals. Consider a metal on which an oxide grows by the diffusion of metallic ions by a cationic vacancy mechanism. The oxide will usually find some coherency relationship with the underlying metal in which a common plane of metallic ions is shared. A continuous barrier of oxide prevents direct access of oxygen gas to the metal surface.

Actual cases will not be as simple as this, since plastic deformation processes can be taken into account in only incomplete fashion and cracking, blistering, and spalling (5) have been disregarded. The nucleation step and the possible irregular shape of the initial oxide are less serious omissions, since this stage is over very quickly in the cases of greatest interest here.

In order for the oxide to form a new layer at the oxide-oxygen interface the appropriate number of metal ions must be removed from the metal and carried across the oxide, and an equal number of vacancies must be carried in the reverse direction. Therefore, the number of vacancies transported across the scale will be proportional to the thickness of the scale if the area remains constant. This means that somewhere in the system, by some mechanism, vacancies must be removed. The two likely mechanisms are plastic deformation, which might prevent porosity growth and interfacial detachment, and condensation and precipitation to form pores within a phase or at an interface. It is recognized that for cations to condense to form pores anions must somehow be removed. In some systems where the anion mobilities are not too much smaller than those of the cations a creep process, like that suggested by Nabarro and Herring for metals, in which anion vacancies arrive by relatively short diffusion paths from grain boundaries may be possible. If anion diffusion is too slow the high concentration of negative charge in the region of cation vacancy supersaturation may promote slip in the anion lattice. This should lead to a preference for nucleation at dislocation lines if more serious disturbances like inclusions are absent. In some oxides anion vacancies may form at the metal-oxide interface and be unable to diffuse far. If porosity develops in this region, as is often observed, the supply of anion vacancies may be no problem.

A number of cases will be examined consisting of simple assumptions about the location at which porosity forms and the form and rate at which it accumulates. Condensation of vacancies to form pores in the underlying metal has been sought several times (4, 6, 7), but has not been observed unequivocally. For this reason the case of pores in the metal phase will be excluded. Copious porosity has been found in the metal during the oxidation of alloys, but this is presumably a consequence of unequal metal atom diffusion rates in the alloy (8).

It should be emphasized that, even though the mechanism assumed for the growth of porosity may not be correct, the effects on the over-all rates of reaction should still apply as long as the growth rates of the pores are approximated adequately. If the pores develop at rates different than those deduced here, the fact of the existence of porosity insures deviations from the simple parabolic rate law.

Calculations

Confine attention to unit area and represent the specific rate constant for interface transport by l_o and that for diffusion transport by k_o where the latter contains as factors $D\,\Delta c$. D is the average diffusion coefficient and Δc the change in concentration of the diffusing species across the thickness of the oxide. In order to show the properties of some of the equations derived below in graphical form the rate constants measured by Wagner and Grünewald (9) for the oxidation of Cu at 1000°C have been substituted (*see* appendix A).

Case 1. If the porosity forms entirely at the metal-oxide interface, as suggested by Dravnieks and MacDonald (3), it will act to decrease the rate of interface transport by an amount corresponding to the decrease in contact area (if transport of ions by vaporization is neglected). For a thick specimen on which a film may grow indefinitely interface control must eventually overcome diffusion control, for there are interfacial sites available only in limited number. Whether this will happen in a reasonable time will depend on the constants of the system.

If all vacancies condense as pancake pores at the metal-oxide interface the loss in area is proportional to Δx. Diffusion remains in control until interface transport is reduced to a comparable rate. That is until

$$l_o A \approx k' D \frac{dc}{dx} A_d \approx k' D \frac{\Delta c}{\Delta x} A_d \approx \frac{k_o}{x} A_d \qquad \text{(II)}$$

where x is distance in the growth direction, A_i is the area for the interfacial reaction, and A_d is the area for diffusive flow. If the effective diffusive area is unchanged and ϕ represents the fraction of the contact area remaining,

$$\frac{k_o}{x_a} = l_o \phi_a \qquad \text{(III)}$$

where the subscripts a indicate that interface control is replacing diffusion control. But $(1 - \phi)$ is proportional to x; or $\phi = 1 - cx$, hence

$$\frac{k_o}{l_o} = x_a(1 - cx_a) \qquad \text{(IV)}$$

If a constant fraction of the vacancies passing through the scale are effective in reducing the area, the remainder being removed by plastic flow, the value of c can be determined from equation (IV). If all vacancies are removed by plastic flow until the scale reaches a critical thickness[1] x_c and then all or some constant fraction become effective, the equation should be modified to the following form:

$$\{1 - c(x_a - x_c)\}x_a = \frac{k_o}{l_o} \qquad \text{(V)}$$

Since enough vacancies to detach the interface should be provided by the growth of a few layers of scale, if all vacancies are effective, loss of contact may be precipitous when the scale becomes thick enough to resist further plastic deformation It is apparent from general experience that c is seldom large, so condensation of vacancies in this fashion must be inefficient or repair processes must be rapid.

Quadratic equations (IV) and (V) yield two roots, the smaller value of x_a indicating approximately the thickness at which the initial linear rate passes to the diffusion-controlled parabolic rate, the larger value of x_a indicating return of interface control. However, if the interface reaction at the oxide-oxygen interface is slower than that at the metal-oxide interface, the former will control the initial stage.

Once the interface is in control with contact area ϕ_a remaining at time t_a the further course of the reaction should be determined there. The appropriate relation is

$$\frac{dx}{dt} = l_o \phi = l_o[1 - c(x - x_c)] \qquad \text{(VI)}$$

which, upon integration, gives

$$\ln \frac{[1 - c(x - x_a)]}{[1 - c(x - x_c)]} = c l_o (t - t_a) \qquad \text{(VII)}$$

where $t > t_a$ and x_a is the thickness of the scale when interface control again becomes effective. For the conditions corresponding to equation (IV), $x_c = o$.

If the metal-oxide interfacial porosity does not form as a very thin layer but condenses as a series of hemispherical voids the contact area will decrease at a rate proportional to $x^{2/3}$ rather than x. Also, inert inclusions accumulating at the interface from the reacted metal volume should correspond to this case. Such effects have been noted in the sulfidation of iron (10), although the rates were not determined precisely enough nor over long enough times to test the equations. Then

$$1 - \phi = c(x - x_c)^{2/3} \qquad \text{(VIII)}$$

Interface control reappears when

$$\frac{k_o}{l_o} = \{1 - c(x_a - x_c)^{2/3}\}x_a \qquad \text{(IX)}$$

The appropriate rate equation is

$$\frac{d_x}{dt} = l_o\{1 - c(x - x_c)^{2/3}\} \qquad \text{(X)}$$

[1] Alternatively, growth to a thickness x_c may be required to produce the vacancy supersaturation required for nucleation of pores.

This integrates to

$$\ln\left[\frac{1 + a(x - x_c)^{1/3}}{1 - a(x - x_c)^{1/3}}\right] - a(x - x_c)^{1/3} = \tfrac{2}{3}a^3 l_o t + \text{const} \quad \text{(XI)}$$

where $a = \sqrt{c}$ and the constant may be determined from the condition $x = x_a$ at $t = t_a$. Letting $z = (x_a - x_c)^{1/3}$, which is fixed for a given set of experimental conditions, and $y = (x - x_c)^{1/3}$

$$\ln\left[\frac{(1 + ay)(1 - az)}{(1 - ay)(1 + az)}\right] + 2az - 2ay = \tfrac{2}{3}a^3 l_o (t - t_a) \quad \text{(XII)}$$

For these conditions of porosity developing at the interface the sequence of rate laws is expected to be linear, parabolic, logarithmic. The growth by solid diffusion primarily must cease when the interface is destroyed, but some other process such as evaporation or dissociation and evaporation may make it possible for the reaction to continue (10). Also the metal must rest against the oxide at some places for support. These regions of contact may become preferred sites for continued reaction (4).

If the metal and oxide are unable to yield plastically and the specimen geometry tends to promote shrinkage of the metal away from the oxide, the formation of porosity at the metal-oxide interface may assist in the start of a crack between the two phases. Thus, the growth rate might diminish faster than predicted by equations (VII) and (XII).

Case 2. If the porosity forms entirely within the oxide it is important to determine how it is distributed, whether generally dispersed in such a way as to reduce the area nearly equally in all cross sections or whether restricted to a narrow region. In either case the pseudosteady-state condition ordinarily assumed for diffusion-controlled scaling will be retained. That is, it will be required that the rate of flow be constant through any cross section in the scale parallel to the interface. The initial period of interface control will be neglected in this section.

If the vacancies condense to form pores uniformly distributed throughout the thickness of scale (the same as oxide forming with uniform porosity) the effective cross-sectional area will be the same in all cross sections at all times; hence a simple parabolic law will be observed, but the diffusion coefficient will be somewhat greater than estimates based on the growth of dense oxides would give.

An induction time prior to the formation of any porosity, that is $\phi = 1$ until $t = t_c$, followed by random distribution of porosity so that $\phi = 1 - c\Delta x$ for $t > t_c$ would yield a parabolic relation until t_c followed by an exponential relationship.

$$\frac{dx}{dt} = \frac{k}{x}\phi \quad \text{(XIII)}$$

integrates to

$$c^2 k_o (t - t_c) = c(x_c - x) - (1 + cx_c)\ln\{1 + c(x_c - x)\} \quad \text{(XIV)}$$

For times large compared with t_c the porosity may become essentially uniform again and the parabolic growth re-established with a smaller rate constant. Thus the sequence—parabolic, logarithmic, parabolic—is conceivable.

For porosity concentrated in the region of width δ, which is considerably smaller than x, the requirement of constant flow rate means that through the region δ the concentration gradient will be steeper than in the remainder of the oxide. Hence the remaining gradient will be less steep than normal, for the concentration extremes at the ends of the scale are determined by equilibria with metal and oxygen, respectively.

In the thickness δ if ϕ_2 is the average nonporous area, assuming that D varies little over the thickness, and since Δc is constant, Δc will be given by

$$\left(\frac{dc}{dx}\right)_1 (x - \delta) + \left(\frac{dc}{dx}\right)_2 \delta = \Delta c \quad \text{(XV)}$$

and the steady-state condition requires that

$$D\left(\frac{dc}{dx}\right)_1 = D\left(\frac{dc}{dx}\right)_2 \phi_2 \quad \text{(XVI)}$$

where $(dc/dx)_1$ and $(dc/dx)_2$ are the concentration gradients outside of and within region δ, respectively.

If, on the other hand, D varies with position in the scale, the usual case, let D_1 be the average value in the sound layer and D_2 the average value in the porous region and m be their ratio defined by

$$m = \frac{D_1}{D_2} \quad \text{(XVII)}$$

Then the steady-state condition becomes

$$mD_1\left(\frac{dc}{dx}\right)_1 = D_1\left(\frac{dc}{dx}\right)_2 \phi_2 \quad \text{(XVIII)}$$

Substituting in the equation for the concentration range yields

$$\left(\frac{dc}{dx}\right)_1 (x - \delta) + m\left(\frac{dc}{dx}\right)_1 \frac{\delta}{\phi_2} = \Delta c \quad \text{(XIX)}$$

The growth rate is proportional to the flow through any cross section, hence to $D_1 (dc/dx)_1$ or

$$\frac{dx}{dt} = \frac{k'\Delta c}{x + \left(\dfrac{m - \phi_2}{\phi_2}\right)\delta} \quad \text{(XX)}$$

For a constant number, n, of roughly spherical pores per unit area, $(1 - \phi_2)$ is proportional to $x^{2/3}$, while δ is approximately proportional to $x^{1/3}$.

$$\begin{aligned} (1 - \phi_2) &= nax^{2/3} \\ \delta &= bx^{1/3} \end{aligned} \quad \text{(XXI)}$$

where $\sqrt{a} = b$ for true spheres. Substituting these expressions in the rate equation yields

$$\frac{dx}{dt} = \frac{k''}{x + \left(\dfrac{nax^{1/3} + m - 1}{1 - nax^{2/3}}\right) bx^{1/3}} \quad \text{(XXII)}$$

which, integrated for $x = o$ at $t = o$, yields

$$x^2 - \tfrac{3}{5}bx^{4/3} - \frac{3mb}{na}x^{2/3} - \frac{3mb}{n^2a^2}\ln(1 - nax^{2/3}) = kt \quad \text{(XXIII)}$$

TABLE I. *Growth rate of cobalt oxide from Eq. (XXIII)*

x (cm)	t (sec)
10^{-6}	14
10^{-5}	67
10^{-4}	580
10^{-3}	1450
10^{-2}	8000
10^{-1}	10^5

This expression would be simplified for spherical pores or for a diffusion coefficient independent of distance through the scale.

It seems likely in the last case that the formation of porosity would be delayed either by plastic deformation or by the difficulty of nucleation. Thus a parabolic law should be established initially, then the rate should drop off as the other terms grow.

These relationships break down when the pores begin to impinge seriously. At this point the reaction should go slightly more rapidly than the equations predict, and complete cessation due to separation of the scale should occur at a later time than predicted. Before this occurs the rate may be determined principally by the rate of the dissociation of oxide on the side of the pores nearest the oxide-oxygen interface, or by vaporization of metal or oxide.

Discussion

It is evident that porosity forming in the locations in the oxide scale in which the rate of growth is controlled can affect the kinetics of growth strongly. The simple cases treated here do not exhaust the possible modes of pore development, but they do give some idea of the sequences of rate laws which might be anticipated, if concurrent cracking and spalling are absent. The idealized cases are not likely to be found without some complication.

No very systematic attempts have been made to investigate the sites at which porosity develops nor the factors controlling its development However, metallographic evidence of its presence is abundant Unfortunately it is impossible to correlate the amount and distribution with measured growth rates for lack of sufficient data on any one case.

Another serious difficulty in studying a rate curve which follows a sequence of rate laws is that the number of points and the precision with which they must be determined far exceeds the current practices and standards. The procedure of fitting the oxide growth rate curve after some arbitrary initial period of deviation with a simple parabola will succeed quite well in almost any case since the procedure has two disposable constants built into it. The need for careful correlation of microstructure with growth rate measurements is obvious.

There is one kind of recent observation which may find its explanation in considerations of this type. Moore (11), in studying the oxidation of Cu and diffusion of Cu ions in cuprous oxide, and Carter and Richardson (12), in similar studies on Co and its oxide, found that they could calculate the growth rate constants reasonably well from diffusion coefficients determined on isolated oxides and the Wagner theory of oxide growth on metals. Himmel, Mehl, and Birchenall also succeeded in this for the iron oxides (13). However, Moore and Carter and Richardson found that they obtained anomalous distributions of radioactive tracers in growing oxides when they performed the experiment first done by Bardeen, Brattain, and Shockley (14)—oxidizing a specimen initially covered with a thin layer of radioisotope of the same element, followed by sectioning of the oxide product to determine the resulting distribution of the tracer. In both cases, instead of finding a distribution corresponding to a steady but gradual decrease of the cation diffusion coefficient from oxide-oxygen to metal-oxide interface, the distribution suggested that the diffusion coefficient was high over most of the thickness then dropped rather abruptly near the metal-oxide interface. An explanation is suggested by a photomicrograph [Fig. 1 in reference (12)] which shows a layer of pores with diameters about 15–20% of the thickness of the cobalt oxide scale near the metal-oxide interface. Taking into account the magnification of the photograph, a rough estimate indicates that δ is about one sixth of the total thickness when the thickness is $\frac{3}{4}$ mm. If the area is reduced to one half in this thickness about 4000 spherical pores are required per cm². (A rough count on the photomicrograph suggested an even larger number than this.) The ratio of diffusion coefficients m would be about 4, and the concentration gradient would be about 8 times as steep in the porous region as in the balance of the scale. Then the concentration gradient in the sound part of the scale would be less than half as steep as the ideal and in the porous region would be almost four times as steep as the ideal (*see* Appendix B). This is illustrated in Fig. 1. Concentration gradients of this type would produce the kind of deviation from the Bardeen, Brattain, and Shockley distribution that has been observed, although a quantitative check would require better data on the pore distribution and kinetics of growth.

Calculations based on equation (XXIII) (*see* Appendix B) indicate that porosity growth such as Carter and Richardson's sample shows should markedly affect the

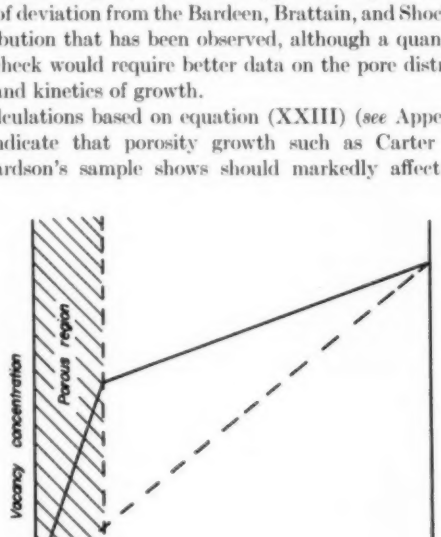

Fig. 1. Schematic diagram of the diffusion gradient of vacancies in an oxide scale with pores concentrated in one region. The gradient in the absence of pores is given by the dashed line. For more detailed discussion, *see* Appendix B.

kinetics of scale growth. Yet strong deviations from the parabolic law are not reported for cobalt. This is probably due to the model chosen here.

Summary

It has been shown by a series of simple models that growth rates of oxide scales on metals may be strongly affected by the development of porosity. The ability of porosity to form must be related to the plastic properties of oxide and metal to some extent. A suggestion is made concerning a recent discrepancy in relating oxide growth rates to cation diffusion processes in cuprous and cobaltous oxides.

Acknowledgment

This research was supported by the United States Air Force, through the Office of Scientific Research of the Air Research and Development Command.

Manuscript received December 12, 1955. This paper was prepared for delivery before the Pittsburgh Meeting, October 9 to 13, 1955.

Any discussion of this paper will appear in a Discussion Section to be published in the June 1957 JOURNAL.

REFERENCES

1. N. CABRERA AND N. F. MOTT, *Repts. Progr. Phys.*, **12,** 163 (1948–49).
2. U. R. EVANS, *Trans. Electrochem. Soc.*, **46,** 247 (1924).
3. A. DRAVNIEKS AND H. J. MCDONALD, *J. (and Trans.) Electrochem. Soc.*, **94,** 139 (1948).
4. D. W. JUENKER, R. A. MEUSSNER, AND C. E. BIRCHENALL, To be published.
5. U. R. EVANS, *Trans. Electrochem. Soc.*, **91,** 547 (1947).
6. C. E. BIRCHENALL AND M. WEINBAUM, Unpublished research.
7. W. J. MOORE, *J. Chem. Phys.*, **21,** 1117 (1953).
8. F. N. RHINES AND B. J. NELSON, *Trans. Am. Inst. Mining Met. Engrs.*, **156,** 171 (1944).
9. C. WAGNER AND K. GRÜNEWALD, *Z. physik. Chem.*, **B40,** 455 (1938).
10. R. A. MEUSSNER AND C. E. BIRCHENALL, To be published.
11. G. W. CASTELLAN AND W. J. MOORE, *J. Chem. Phys.*, **17,** 41 (1949); W. J. MOORE AND B. SELIKSON, *ibid.*, **19,** 1539 (1951).
12. R. E. CARTER AND F. D. RICHARDSON, *Trans. Am. Inst. Mining Met. Engrs.*, **203,** 336 (1955).
13. L. HIMMEL, R. F. MEHL, AND C. E. BIRCHENALL, *ibid.*, **197,** 827 (1953).
14. J. BARDEEN, W. N. BRATTAIN, AND W. SHOCKLEY, *J. Chem. Phys.*, **14,** 714 (1946).

APPENDIX A

Numerical Evaluation of Rate Curves for Interfacial Porosity

For 1000°C and 63 mm Hg pressure of oxygen Wagner and Grünewald (9) found these rate constants for the growth of cuprous oxide on copper: $k_c = 7.37 \times 10^{-8}$ cm²/sec and $l_c = 4.06 \times 10^{-5}$ cm/sec. In Fig. 2 on a log-log plot of thickness against time, which exaggerates the early part of the rate curve and compresses the later part, a number of equations are compared using these values of k_c and l_c and compatibly chosen constants. Reference slopes for simple linear and parabolic growth may be inferred from curve 1 corresponding to Eq. (I), which has a slope appropriate to linear growth at short times and to parabolic growth at long times.

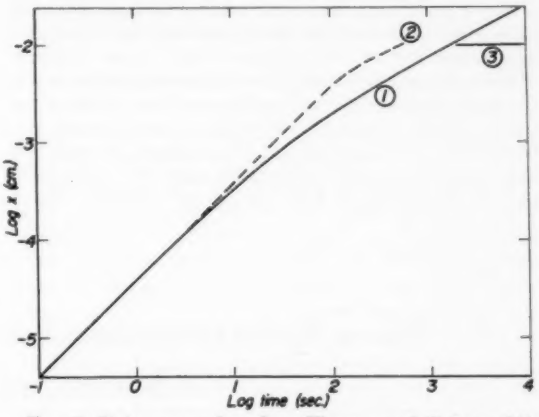

FIG. 2. Rate curves based on Wagner and Grünewald's constants for copper at 1000°C and 63 mm oxygen pressure. Curve 1 is for Eq. (I), curve 2 for Eq. (VII) with x_c equal to zero, and curve 3 for Eq. (VII) with x_c equal to 5×10^{-3} cm.

Eq. (VII) with x_c equal to zero can be solved with these rate constants only for c less than 125. Curve 2 is plotted for c equal to 25. Higher values of c lead to interface control with larger residual areas of contact. The curve terminates at x equal to $1/c$ for very long times. When a critical thickness x_c is postulated, the permissible values of c depend on x_c when x_c is below 3.6×10^{-3} but not above. To avoid the range of restricted c, the value of x_c is taken as 5×10^{-3} cm. Then ϕ_a increases as c increases and x_a approaches x_c asymptotically. For c equal to 125 the thickness increase is only 10^{-3} cm between 400 sec and the end of the reaction at very long times as shown by curve 3. At 1.25×10^{-2} cm $d \log x/d \log t$ is about 1/320.

For Eq. (XII), for $a = 11$ corresponding to $c = 121$ and other constants chosen as before, x increases only from 5.41×10^{-3} to 5.73×10^{-3} as the time goes from 400 sec to very long times. At a thickness of 5.51×10^{-3} and t of 444, $d \log x/d \log t$ is about 1/3, so the rate drops off rapidly once porosity returns interface control.

In all cases it has been assumed that no other transport mechanism capable of moving metal or oxygen across the pore volume intervenes to increase the rate of reaction.

APPENDIX B

Rough Estimate of Concentration Gradients in Porous Scale Layers for Carter and Richardson's Cobalt Oxide Specimen

If the pores are spherical, Eq. (XXI) becomes

$$1 - \phi = n\delta^2$$

For x about 0.067 cm, δ about 0.011 cm, m about 4, ϕ about one half, it is found that

$$n \backsim 4.2 \times 10^3$$
$$a \backsim 7.6 \times 10^{-4}$$

From Eq. (XVIII)

$$\left(\frac{dc}{dx}\right)_2 \Big/ \left(\frac{dc}{dx}\right)_1 = \frac{m}{\phi} \backsim 8$$

And from Eq. (XIX)

$$\frac{\Delta c}{\Delta x} = \frac{13}{6}\left(\frac{dc}{dx}\right)_1 = \frac{13}{48}\left(\frac{dc}{dx}\right)_2$$

Fig. 1 is plotted on this basis to show the large deviation from ideal conditions for these conservatively estimated conditions.

Since the reaction layer does not know the thickness of the underlying metal, the equation need not terminate at the experimental thickness. However, ϕ may approach zero before the metal is consumed. If k is chosen to make the theoretical and experimental values agree at a thickness of 10^{-2} cm, k becomes 4.83×10^{-7} and the growth rate predicted by Eq. (XXIII) is given in the Table I. The last three values correspond to the usual range of experimental measurement of from 1/3 to 36 hr. Since this does not approximate the parabolic slope, it is probable that Carter and Richardson's porosity has a different rate of formation than that postulated, and perhaps a different origin. However, the effect of the porosity on the concentration gradient should be qualitatively as described.

Mass Spectrometric Examination of Hydrogen in Chromium-Plated Steel

CHARLES LEVY AND GEORGE A. CONSOLAZIO[1]

Watertown Arsenal Laboratory, Watertown, Massachusetts

ABSTRACT

Specimens of chromium-plated SAE 1015 steel were examined for hydrogen in the mass spectrometer. The peak heights obtained in arbitrary units were plotted as a function of time. Evolution of hydrogen was studied in the temperature range 100°–800°C. At any given temperature, the amount of hydrogen liberated approached a limit asymptotically over a long period of time. No specimen could be run to complete exhaustion of hydrogen.

Evolution of hydrogen from steel and chromium-plated steel was measured for a constant temperature rise of 2°C/min. In the chromium-plated specimens, it was shown that below 350°C hydrogen was evolved almost exclusively from the chromium plate, while above 490°C evolution occurred primarily from the steel.

Hydrogen evolution at 350°C from a chromium-plated specimen and from a steel specimen was also compared, with time as a parameter. The major portion of the hydrogen available for release in both specimens was liberated after approximately 80 min of heating.

The problem of the concurrent electrodeposition of hydrogen and chromium on various basis metals has been studied by numerous investigators. Most attempted to correlate deposition of hydrogen with hardness, crystal structure of the chromium plate, or the embrittlement of steel basis metal. It has been shown (1–3) that virtually all of the hydrogen is removed from chromium plate at 400°C without any appreciable loss in hardness. A rapid decrease in hardness occurs on heating above 500°C, indicating that there is no direct correlation between the high hardness of the chromium electrodeposit and the hydrogen content. It has been postulated, however, that during deposition, hydrogen enters the chromium lattice and then escapes, leaving the lattice in a state of strain which results in increased hardness.

Snavely (4) states that chromium is normally deposited from the chromic acid bath as unstable hydrides. Being unstable, the hydrides decompose rapidly after deposition into atomic hydrogen and body-centered cubic chromium. The hardness of chromium plate is related to the volume change of 15.6% which accompanies this decomposition. Gaydon (5) and Muro (6) observed evidence for the existence of chromium hydrides by use of the optical spectrograph and x-ray methods, respectively. Brenner (7) believes that oxygen content and fine grain size are the two most important factors which determine the hardness of electrolytic chromium. An excellent summary of work done on gases in chromium is given by Sully (8).

Embrittlement of steels resulting from chromium plating is much more severe than that produced by cathodic pickling under the same conditions of temperature and current density (9). Heating to temperatures above 400°C was necessary to regain completely the original bend value of the unplated steel. In the discussion of reference (9), Snavely states that when the hydrides decompose, the released hydrogen is sparingly soluble in body-centered cubic chromium and tends to diffuse in both directions out of the plate. The diffusion path into the basis metal is greatly favored because of the high concentration of atomic hydrogen in the surface layer of the plate. By contrast, when plating 100% hydrogen on steel (cathodic pickling) the atomic hydrogen available for diffusion into the metal is at the metal-solution interface. It seems likely that a large portion of the hydrogen escapes in molecular form and that this proportion is larger than in the case of chromium plating.

Conventional vacuum methods used for studying gas-metal systems fall into two categories: vacuum fusion and

[1] Present address: Atlantic Gelatin Div., General Foods Corp., Woburn, Mass.

warm vacuum extraction. In both procedures, gases are collected and the pressures are subsequently measured by a McLeod gauge or other pressure measuring device. An inherent disadvantage of these methods is that the total pressure of the system is measured, rather than the partial pressure of the individual gases. Furthermore, it is necessary to analyze for a gas such as hydrogen by combustion or oxidation methods.

The mass spectrometer comprises a sensitive measuring device which is highly selective with regard to ion species. Thus, it is possible to measure a peak height which is proportional to the partial pressure of hydrogen, to the exclusion of the partial pressures of any other gases present. In a similar manner, this technique can also be applied to oxygen, nitrogen, water vapor, or other gases for the chromium-plated steel system being studied.

In this study, absolute hydrogen gas pressures were not measured. This could have been done, however, by incorporating a micromanometer into the modified inlet system. Use of a micromanometer is necessary in order to measure absolute pressures in the micron range. A McLeod gauge or ionization gauge might be used, but difficulty would be encountered in regard to sensitivity of these gauges to gases other than hydrogen, particularly water vapor.

Experimental

The steel specimens used were annealed at 871°–882°C (1600°–1620°F), hardness 59 Rockwell B, and had the following analysis, which corresponds approximately to that of SAE 1015:

C	Mn	S	P
0.17	0.40	0.022	0.008

Specimens were 1.27 cm (½ in.) in diameter and 0.64 cm (¼ in.) in height, and surface ground on all sides. Specimens were cleaned prior to plating by a cycle involving electrolytic alkali treatment for 20 sec anodically, 5 sec cathodically, and a 30 sec 50% HCl dip, with water rinses following each step. Specimens were reverse etched in the plating bath at 15.5 amp/dm² (1 amp/in.²) for 1 min immediately prior to plating. The plating bath consisted of an aqueous solution containing 250 g/l of chromic acid and 2.5 g/l of H_2SO_4. The temperature of the bath was maintained at 55°C and a current density of 31 amp/dm² (2 amp/in.²) was applied, using lead anodes.

After plating over the entire surface, the specimen was rinsed and air-blast dried. In the early experiments, drying was accomplished by immersing in acetone prior to the air blast, and then in liquid nitrogen after the air blast, but subsequently this was found not to be necessary to prevent the escape of hydrogen. The weight of chromium deposited was found to be the major factor controlling the amount of hydrogen produced in the specimen. A weight of 180 ± 9 mg of deposited chromium was chosen since it could be produced in approximately 30 min and the specimen did not evolve more hydrogen than could be handled conveniently in the mass spectrometric analysis. The thickness of chromium deposited was approximately 0.0076 mm.

The mass spectrometer used was a commercially available dual purpose instrument capable of operation in both the isotope ratio and analytical mixture analysis mode. The sample inlet system was somewhat modified from conventional usage. The expansion chamber was replaced by a specimen-containing Vycor tube which was heated to the required temperature by a Nichrome-wound furnace. Temperature measurements were made by means of an external chromel-alumel thermocouple.

Initially, the mass spectrometer was adjusted to "sit" on the hydrogen molecule ion (H_2^+) peak. Before heat was applied to the Vycor tube and specimen, the entire inlet system was evacuated to approximately 10^{-5} mm Hg. The molecules of gas, including hydrogen, which were released from the specimen upon heating were allowed to flow into the ionization chamber where they were bombarded by electrons emitted from a tungsten filament. The beam of positive ions so produced was then accelerated by a controlled potential into the analyzer tube where the moving ions were deflected 180° by a magnetic field according to the equation:

$$m/e = B^2r^2/2\,E$$

where B = magnetic field strength, e = charge on the particle, m = mass of the ion, r = radius of deflection, and E = accelerating potential.

Only ions having an m/e value which satisfied the equation would travel the semicircle of the analyzer tube and emerge through a slit at the far end, where they would be focussed.

Therefore, if B, r, and E were fixed, only one species of ion came to a focus. In this instrument, the radius of the tube r and the accelerating potential E are fixed. The magnetic field was varied until mass position 2, or the hydrogen molecule ion, was located, as noted above.

To obtain each peak on the mass spectrometer recorder chart, gases evolved from the specimen were collected for a period of 5 min, at the end of which time the gases were allowed to flow through a stopcock into the ionization chamber. The signal which resulted exclusively from the ionized hydrogen molecules was amplified and recorded as a peak which is directly proportional to the number of hydrogen molecule ions and also to the partial pressure of hydrogen in the gas system. After the peak was recorded, the entire inlet system was again evacuated. The stopcock leading to the ionization chamber, which was open for 30 sec during recording and evacuation, was then closed and the pressure in the Vycor tube was allowed to build up for another 4.5-min period. The peak height value was adjusted to correct for the 30 sec during which gases were not collected. This procedure was continued until the required data were obtained.

Evolution of hydrogen from chromium-plated steel was studied at 100°, 200°, 300°, 400°, 500°, 600°, 700°, and 800°C. Ten to fifteen minutes were required to reach temperature once the heat was applied. Peak heights obtained were plotted as a function of time in the following manner. For each constant temperature run, the first peak value in arbitrary units was plotted as the first point. The next peak value was added to the first and plotted as the second point. The third peak value was added to the second and plotted as the third point, and so on until all the points were plotted. Thus, the final point in each curve for each tem-

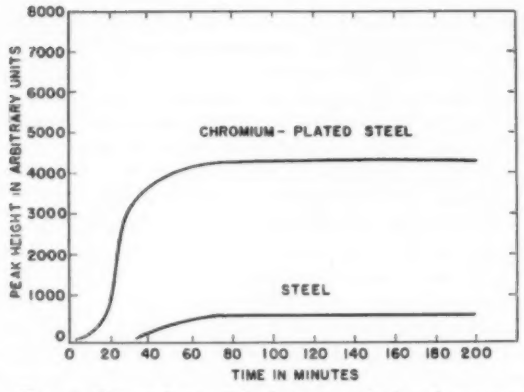

FIG. 1. Comparison of hydrogen evolution from steel and from chromium-plated steel at 350°C.

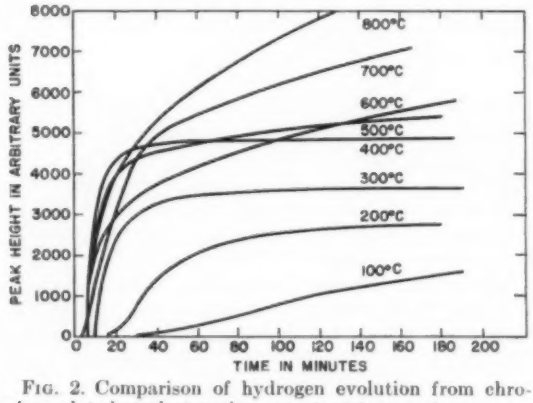

FIG. 2. Comparison of hydrogen evolution from chromium plated steel at various constant temperatures.

perature shows the total hydrogen evolved from the specimen in arbitrary units for the total time of the run.

In another set of experiments, evolution of hydrogen was measured for a constant rise of 2°C/min. Specimens included steel and chromium-plated steel. Peak height data were plotted as a function of time, which is directly related to temperature in this case. Graphical representation of the peak values was achieved in the same manner as above.

Hydrogen evolution at 350°C from a chromium-plated steel specimen and from a steel specimen was also compared, with time as a parameter.

Some hydrogen evolution runs at 350°C were also made after aging chromium-plated steel specimens at room temperature in a desiccator for periods from 1 day to 3 weeks.

Results and Discussion

The comparison of hydrogen evolution from steel and chromium-plated steel at 350°C is shown in Fig. 1. At this temperature the chromium-plated specimen evolved many times more hydrogen than did the steel specimen. The major portion of the hydrogen available for release at this temperature in both specimens was liberated after 80 min of heating.

Fig. 2 gives the constant temperature evolution of hydrogen vs. time. After a heating period of 180 min at the

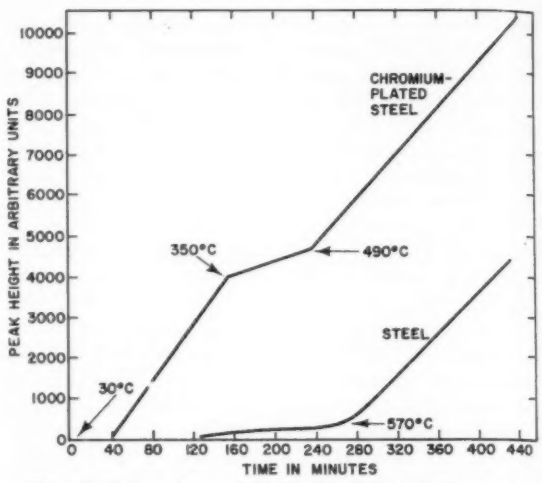

FIG. 3. Comparison of hydrogen evolution from steel and from chromium-plated steel measured at a constant temperature rise of 2°C/min.

given constant temperature, the curves for the 100°, 200°, 300°, 400°, and 500°C runs leveled out, indicating that small amounts of hydrogen were being evolved. Further heating did not release appreciable amounts of hydrogen from these specimens. Above 600°C, extrapolation of the curves in Fig. 2 to a time of 180 min would show no leveling out such as occurs at the lower temperatures.

Since only very small amounts of hydrogen would be liberated on further heating at a given constant temperature, it is apparent that the temperature must be raised in order to release the residual hydrogen in the specimen in a reasonable length of time. For example, at 300°C, after 180 min, 3680 arbitrary units of hydrogen were evolved. At this time, the rate of evolution had decreased to approximately ¼ unit/min. In order to increase appreciably the amount of hydrogen liberated, a higher temperature must be used, such as 400°C, where 4890 arbitrary units of hydrogen were evolved after 180 min. As can be seen from Fig. 2, at each higher temperature the amount of hydrogen evolved is considerably increased.

Hydrogen evolution from steel and from chromium plated steel measured at a constant rise of 2°C/min is shown in Fig. 3. The steel began to evolve appreciable amounts of hydrogen at 570°C and continued at a constant rate. Hydrogen evolved rapidly from the chromium plated steel specimen at an approximately constant rate from 130°C to 350°C, leveled off, and then broke upward at 490°C and continued at a slightly lower constant rate of evolution than at below 350°C.

It appears that hydrogen is virtually exhausted from the chromium plate at 350°C, at which point the curve in Fig. 3 levels out. The curve does not attain a zero slope because slight amounts of hydrogen are still being evolved from the chromium plate and, in addition, the steel is beginning to evolve hydrogen at an appreciable rate. Above 490°C, the hydrogen is apparently being evolved entirely from the steel basis metal. Comparing the slopes of the curves for steel and chromium plated steel at temperatures above approximately 550°C, it may be con-

cluded that chromium plate has little or no effect on the rate of diffusion of hydrogen from steel.

Hydrogen evolution did not vary appreciably in chromium-plated steel specimens which had been aged for periods from 1 day to 3 weeks before heating at 350°C. These data, if plotted, would closely approximate the curve shown for chromium plated steel in Fig. 1. Experimentation in this vein was therefore abandoned since other investigators (1, 7) have found similar results over longer periods of aging time.

It should be noted that no specimen, either steel or chromium plated steel, was completely exhausted of hydrogen in any of the above experiments. An attempt was made to completely exhaust the hydrogen from a chromium-plated steel specimen by heating in the mass spectrometer inlet system at 800°C. After approximately 20 hr appreciable quantities of hydrogen were still being evolved.

Conclusions

1. The mass spectrometer, by virtue of its selectivity, provides a useful technique for the investigation of metal-gas systems.

2. Hydrogen is evolved from both plated and unplated specimens at virtually the same rate at temperatures above approximately 550°C. Apparently chromium plate 0.0076 mm (0.0003 in.) in thickness has no effect on the rate of diffusion of hydrogen from steel in this temperature range.

3. Below 350°C, hydrogen is evolved almost exclusively from the chromium plate, while above 490°C, the evolution occurs primarily from the steel basis metal, with a transition region in the 350°–490°C temperature range.

4. At any given temperature, the amount of hydrogen which can be liberated approaches a limit asymptotically. No specimen could be run to the complete exhaustion of hydrogen, although an attempt was made by heating at 800°C for approximately 20 hr. At the end of this time, appreciable quantities of hydrogen were still being evolved.

5. The major portion of the hydrogen available for release at 350°C in both steel and chromium-plated steel is liberated after approximately 80 min of heating.

Manuscript received April 11, 1955. This paper was prepared for delivery before the Boston Meeting, October 3 to 7, 1954.

Any discussion of this paper will appear in a Discussion Section to be published in the June 1957 Journal.

References

1. S. P. Makariewa and N. D. Birukoff, *Z. Elektrochem.*, **41**, 623, 838 (1935).
2. Guichard, Clausmann, Billon, and Lanthony, *Bull. Soc. chim.*, [5], **1**, 679 (1934).
3. C. A. Snavely and C. L. Faust, *This Journal*, **97**, 466 (1950).
4. C. A. Snavely, *Trans. Electrochem. Soc.*, **92**, 537 (1947).
5. A. G. Gaydon and R. W. B. Pearse, *Nature*, **140**, 110 (1937).
6. Z. Muro, *Oyo Butsuru (Japan)*, **21**, 321 (1952).
7. A. Brenner, P. Burkhead, and C. Jennings, *J. Research Nat. Bur. Standards*, **40**, 31 (1948).
8. A. H. Sully, "Chromium," Metallurgy of the Rarer Metals Series, Vol. I, Academic Press, New York (1954).
9. C. A. Zapffe and M. E. Haslem. *Trans. Am. Soc. Metals*, **39**, 241 (1947).

Formation of Composite Scales Consisting of Oxides of Different Metals

Carl Wagner

Department of Metallurgy, Massachusetts Institute of Technology, Cambridge, Massachusetts

Abstract

This paper presents a theoretical analysis of diffusion processes during the oxidation of an alloy when oxides of different alloying elements are formed concurrently. For idealized conditions it is possible to calculate the decrease in the oxidation rate which results from alloying a base metal, having a relatively high oxidation rate such as Cu or Fe, with less noble metals such as Al, Cr, or Be whose oxides form relatively slowly.

In a previous paper (1) it was shown that high temperature oxidation of an alloy consisting of metals A and B may result in the formation of only one oxide. In particular, on A-rich alloys only oxide AO may be formed, and on B-rich alloys only oxide BO may be formed. At intermediate compositions of the alloy, however, formation of only one oxide does not correspond to a stable state and, therefore, two oxides of different metals are formed simultaneously. Under these conditions, diffusion rates depend decisively on the spatial distribution of the two oxides in the scale. This distribution is not given *a priori* but is the result of simultaneous diffusion processes. In spite of this rather involved situation, a mathematical analysis is possible as is shown below.

Both oxides AO and BO are supposed to have a greater volume per gram-atom of metal than the alloy and to grow by outward migration of cations and electrons. It may be assumed that both oxides are nucleated initially at

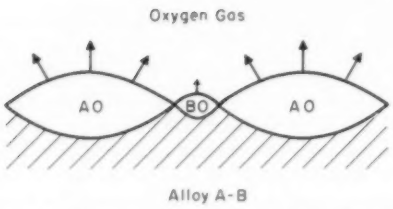

FIG. 1. Initial stage of oxidation of an alloy A-B

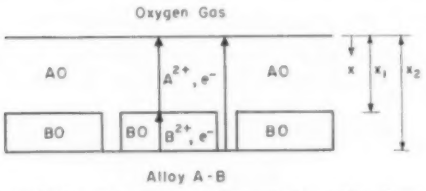

FIG. 2. Schematic cross section of the scale of an alloy A-B with an outer layer of oxide AO and an inner two-phase layer of oxides AO and BO. At the interface of oxides AO and BO, the displacement reaction

$$B^{2+} + 2e^- + AO = A^{2+} + 2e^- + BO$$

is supposed to take place so that oxide BO can grow, although it is not in contact with the oxidizing atmosphere.

different points of the surface of the alloy. Each oxide nucleus grows inward because it fills the space of the metal being oxidized; and grows outward because the volume of the oxide is supposed to be greater than the volume of the metal. If oxide AO grows faster than oxide BO as is shown schematically in Fig. 1, oxide AO will bury oxide BO after some time in the same way as markers of inert material are buried by oxide growing on a pure metal due to outward migration of cations and electrons (2, 3). The final pattern is shown schematically in Fig. 2. Rhines and Nelson (4) have shown that this pattern of a scale is found on Cu-Zn alloys and have discussed qualitatively the various diffusion processes involved. Such a configuration is essentially stable if metal B whose oxide has the lower growth rate has a higher affinity for oxygen than metal A. Although oxide BO is not in direct contact with atmospheric oxygen, oxide BO can continue to grow as is shown in Fig. 2. However, if metal B has a considerably lower affinity for oxygen than metal A, oxide BO is not stable when it is buried near the oxide-alloy interface where the oxygen activity is very low and the displacement reaction

$$BO + A\ (\text{alloy}) = AO + B\ (\text{alloy})$$

may take place unless the concentration of A in the alloy is very low. Diffusion in a scale involving B-rich alloy as a second phase has been considered in another paper (5). Therefore, calculations in the present paper are confined to conditions shown in Fig. 2 where the buried oxide BO is stable. Exclusive diffusion control is assumed. Effects due to space charge layers are disregarded.

Mathematical Analysis

In view of the rather complex situation, it is advisable to introduce simplifying presuppositions.

First, if the molar volumes V_{AO} and V_{BO} of oxides AO and BO, respectively, are equal, the reaction at the BO-AO interface shown in Fig. 2 does not result in a volume change. Under these conditions, oxidation of a plane sample can proceed by virtue of diffusion and phase boundary reactions but without plastic flow of the alloy or the oxide. Therefore, assume that $V_{AO} = V_{BO}$ and plastic flow of each of the phases involved is negligible.

Second, although a protective oxide film is to be expected only if the volume of each of the oxides per gram-atom metal is greater than the molar volume V of the metal (6), in the following equations the limiting case that the volume ratio is equal to unity is assumed. Thus each volume element of the oxides and the alloy contains the same number of metal atoms and there is no expansion of a sample during oxidation.

The first condition, $V_{AO} = V_{BO}$ is essential for neglect of plastic flow. If $V_{AO} \neq V_{BO}$, additional equations accounting for plastic flow are needed. The second condition, $V = V_{AO} = V_{BO}$, however, is chosen only for the sake of mathematical simplification. If $V \neq V_{AO} = V_{BO}$, the following equations would not change basically but become only somewhat more involved.

Under the conditions assumed in Fig. 2, it is necessary to consider diffusion normal and parallel to the surface of the sample. To simplify calculations, it is assumed that the thickness of the two-phase layer is large in comparison to the dimensions of the particles of oxide BO and the width of the channels of oxide AO parallel to the surface of the sample. Hence, diffusion equations are formulated only in the direction normal to the surface and, therefore, correspond to a one-dimensional problem.

The diffusion rate in an individual phase may be expressed in terms of either a concentration or an activity gradient. In the region involving two oxides, it is convenient to use the activity of atomic oxygen, a, as the characteristic variable and to let $a = 1$ at the outer surface, $x = 0$, where the oxygen activity is determined by the oxidizing atmosphere.

x denotes the distance from the outer surface toward the interior of the sample, and x_1 and x_2, respectively, denote the locations of the outer and the inner boundary of the two-oxide region at a given time t (*see* Fig. 2).

Diffusion of cations in oxides may take place either by migration of interstitial ions or via vacancies. The concentration of such lattice defects has been found to be proportional to a fractional power of the oxygen partial pressure of a coexisting atmosphere (7). Consequently, it is assumed that the self-diffusion coefficients D_A and D_B of the metal ions in oxides AO and BO, respectively, as functions of the oxygen activity are given by

$$D_A = D_A^0 a^\alpha \quad [1]$$

$$D_B = D_B^0 a^\beta \quad [2]$$

where α and β are constants, which are positive for oxides involving a metal deficit and negative for oxides with metal excess, e.g., equal to about $-\frac{1}{8}$ for ZnO (8).

Moreover, predominant electronic conduction in the oxides AO and BO is assumed. Thus, transport rates of metals A and B in oxides AO and BO in the x-direction, j_A and j_B, respectively, in moles per unit total area per unit time are (9)

$$j_A = (1 - \psi)(D_A^0/V)a^\alpha \ (\partial \ln a/\partial x) + u(1 - \psi)/V \quad [3]$$

$$j_B = \psi(D_B^0/V)a^\beta \ (\partial \ln a/\partial x) + u\psi/V \quad [4]$$

where $u = dx_2/dt$ is the drift velocity of the oxides toward the bulk alloy due to the recession of the oxide-alloy interface and ψ is the volume fraction of oxide BO at distance x from the surface, which is supposed to be equal to the fraction of the cross section of oxide BO for transport in the x-direction.

Since the molar volumes of the oxides are assumed to be equal to the molar volume of the alloy and, therefore, the outer oxide surface remains at the position of the original surface of the alloy, there is no net transport of metal, i.e., the sum of the transport rates of A and B vanishes,

$$j_A + j_B = 0 \quad [5]$$

Substituting Eqs. [3] and [4] in Eq. [5], one obtains

$$u = dx_2/dt = -[(1 - \psi)D_A^0 a^\alpha + \psi D_B^0 a^\beta] \ (\partial \ln a/\partial x) \quad [6]$$

Since no special assumptions have been made, Eqs. [3] to [6] hold for the outer scale involving only oxide AO with $\psi = 0$, and for the inner scale involving oxides AO and BO with $\psi > 0$.

Substitution of Eq. [6] in Eq. [4] yields

$$j_B = -\psi(1 - \psi)\,[(D_A^0/V)a^\alpha - (D_B^0/V)a^\beta] \ (\partial \ln a/\partial x) \quad [7]$$

Solving Eq. [6] for $(\partial \ln a/\partial x)$ and substituting in Eq. [7]

$$j_B = \frac{\psi(1 - \psi)[D_A^0 a^\alpha - D_B^0 a^\beta]}{V[(1 - \psi)D_A^0 a^\alpha + \psi D_B^0 a^\beta]} \frac{dx_2}{dt} \quad [(8)]$$

The over-all concentration of B in the two-phase region II is equal to ψ/V. From the principle of the conservation of mass, it follows that the rate of change in the concentration of B is equal to the divergence of the transport rate. Thus

$$\partial(\psi/V)/\partial t = -\partial j_B/\partial x \quad [9]$$

Substitution of Eq. [8] in Eq. [9] yields

$$\frac{\partial \psi}{\partial t} = -\frac{dx_2}{dt}\frac{\partial}{\partial x}\left\{\frac{\psi(1 - \psi)[D_A^0 a^\alpha - D_B^0 a^\beta]}{(1 - \psi)D_A^0 a^\alpha + \psi D_B^0 a^\beta}\right\} \quad [10]$$

The rate of transport of B per unit area in the alloy is

$$j_B = -D\partial(N_B/V)/\partial x \quad [11]$$

where N_B is the local mole fraction of B in the alloy, and D is the interdiffusion coefficient in the alloy, which is supposed to be independent of concentration. Then Fick's second law reads

$$\partial N_B/\partial t = D(\partial^2 N_B/\partial x^2) \quad [12]$$

At the oxide-alloy interface, $x = x_2$, equilibrium between the two oxides AO and BO and the alloy is assumed and, therefore, the oxygen activity has a definite value a_2. Likewise, the mole fraction of B in the alloy has a definite value N_{B2}. Thus there are the boundary conditions

$$a = a_2 \text{ at } x = x_2 \quad [13]$$

$$N_B = N_{B2} \text{ at } x = x_2 \quad [14]$$

Integrating Eq. [6] with respect to x at constant time t between the limits $x = 0$, $a = 1$ and $x = x_1$, $a = a_1$ where only phase AO is present, i.e., $\psi = 0$,

$$D_A^0(1 - a_1^\alpha) = \alpha x_1(dx_2/dt) \quad [15]$$

At $x = x_1$, the over-all concentration of B changes discontinuously from 0 to ψ_1/V where ψ_1 is the volume fraction of oxide BO at the outer boundary of the two-oxide region. Since no oxide BO is present at $x < x_1$, only transport of B at $x > x_1$ is to be taken into account. From the principle of the conservation of mass, it follows that

$$-(\psi_1/V)(dx_1/dt) = -j_B(x = x_1 + \epsilon) \quad [16]$$

where ϵ denotes an infinitesimal positive value.

Substitution of Eq. [8] in Eq. [16] yields

$$\frac{dx_1}{dt} = \frac{(1 - \psi_1)(D_A^0 a_1^\alpha - D_B^0 a_1^\beta)}{(1 - \psi_1)D_A^0 a_1^\alpha + \psi_1 D_B^0 a_1^\beta}\frac{dx_2}{dt} \quad [17]$$

The over-all concentration of B also changes quasi-discontinuously at $x = x_2$. From the principle of the conservation of mass it follows that

$$\left[\frac{\psi(x = x_2 - \epsilon)}{V} - \frac{N_B(x = x_2 + \epsilon)}{V}\right]\frac{dx_2}{dt} = j_B(x = x_2 - \epsilon) - j_B(x = x_2 + \epsilon) \quad [18]$$

Substitution of Eqs. [8], [11], and [14] in Eq. [18] yields

$$[\psi_2 - N_{B2}](dx_2/dt) = \frac{\psi_2(1 - \psi_2)\,(D_A^0 a_2^\alpha - D_B^0 a_2^\beta)}{(1 - \psi_2)D_A^0 a_2^\alpha + \psi_2 D_B^0 a_2^\beta}\frac{dx_2}{dt} + D(\partial N_B/\partial x)_{x=x_2+\epsilon} \quad [19]$$

where ψ_2 is the volume fraction of oxide BO at the end of the two-oxide region II ($x = x_2$).

The alloy is supposed to have initially a uniform composition corresponding to the mole fraction N_B^0. Since diffusion into a semi-infinite space with time-independent conditions at the outer surface is considered, it may be assumed that solutions of the foregoing partial differential Eqs. [10] and [12] involve only the combination $x/t^{\frac{1}{2}}$ of the independent variables x and t. Consequently, the dimensionless variable is introduced

$$z = x/2(D_A^0 t)^{\frac{1}{2}} \quad [20]$$

and the constant parameters

$$z_1 = x_1/2(D_A^0 t)^{\frac{1}{2}} \quad [21]$$

$$z_2 = x_2/2(D_A^0 t)^{\frac{1}{2}} \quad [22]$$

In addition,

$$\gamma = \beta - \alpha \quad [23]$$

and introduce the symbols q and r for the ratio of the diffusion coefficients,

$$q = D_B^0/D_A^0 \quad [24]$$

$$r = D/D_A^0 \quad [25]$$

For the mole fraction of B in the alloy, use is made of the particular solution

$$N_B = N_B^0 + C \operatorname{erfc}[x/2(Dt)^{\frac{1}{2}}] \quad [26]$$

which involves the constant C eliminated below and satisfies Eq. [12] and the initial condition $N_B = N_B^0$. Upon substitution of Eqs. [20] and [25], Eq. [26] becomes

$$N_B = N_B^0 + C \operatorname{erfc}(z/r^{1/2}) \quad [27]$$

In view of Eqs. [14] and [22], Eq. [27] may be rewritten as

$$N_B = N_B^0 + (N_{B2} - N_B^0) \operatorname{erfc}(z/r^{1/2})/\operatorname{erfc}(z_2/r^{1/2}) \quad [28]$$

Upon substitution of Eqs. [20] to [25] and [28] in Eqs. [6], [10], [13], [15], [17], and [19] it follows that

$$2z_2 = -[(1-\psi) + \psi q a^\gamma] a^\alpha (d\ln a/dz) \text{ at } z_1 \leqq z \leqq z_2 \quad [29]$$

$$z_2 \frac{d}{dz}\left[\frac{\psi(1-\psi)(1-qa^\gamma)}{(1-\psi)+\psi q a^\gamma}\right] - z(d\psi/dz) = 0 \quad [30]$$

$$\text{at } z_1 \leqq z \leqq z_2$$

$$a = a_2 \text{ at } z = z_2 \quad [31]$$

$$1 - a_1^\alpha = 2\alpha z_1 z_2 \quad [32]$$

$$\frac{z_1}{z_2} = \frac{(1-\psi_1)(1-qa_1^\gamma)}{(1-\psi_1)+\psi_1 q a_1^\gamma} \quad [33]$$

$$z_2(\psi_2 - N_{B2}) = z_2 \frac{\psi_2(1-\psi_2)(1-qa_2^\gamma)}{(1-\psi_2)+\psi_2 q a_2^\gamma} - (N_{B2} - N_B^0)\frac{r^{1/2}}{\pi^{1/2}} \frac{\exp(-z_2^2/r)}{\operatorname{erfc}(z_2/r^{1/2})} \quad [34]$$

For the following discussion it is profitable to transform the two latter equations. Subtracting corresponding sides of Eq. [33] from unity, one obtains

$$\frac{z_2 - z_1}{z_2} = \frac{q a_1^\gamma}{1 - \psi_1 + \psi_1 q a_1^\gamma} \quad [35]$$

Eq. [34] may be rewritten as

$$\frac{(1-\psi_2+\psi_2 q a_2^\gamma)(N_B^0 - N_{B2})}{\psi_2 q a_2^\gamma (1 - N_{B2}) - N_{B2}(1-\psi_2)} = F(z_2/r^{1/2}) \quad [36]$$

where $F(w)$ for w as general argument is defined as

$$F(w) = \pi^{1/2}\, w(1 - \operatorname{erf} w) \exp w^2 \quad [37]$$

For small and large arguments, respectively, the following approximations hold

$$F(w) \cong \pi^{1/2}\, w \text{ if } w \ll 1 \quad [38a]$$

$$F(w) \cong 1 - \tfrac{1}{2}w^{-2} \text{ if } w \gg 1 \quad [38b]$$

Eqs. [28] to [32], [35], and [36] are sufficient in order to calculate the constants z_1 and z_2, and both the oxygen activity a and the volume fraction ψ in the two-phase region as functions of z if the values of the parameters α, β, q, r, a_2, N_{B2}, and N_B^0 are given. The relatively large number of the parameters makes the discussion somewhat difficult but some general conclusions may be drawn.

Discussion

In view of practical situations, it is assumed that the absolute values of the standard free energies of formation of the oxides are much greater than RT and, therefore, the oxygen activity a_2 for coexistence of alloy, oxide AO, and oxide BO, is much smaller than the oxygen activity at the surface, i.e.,

$$a_2 \ll 1 \quad [39]$$

In addition, it is assumed that the difference of the absolute values of the standard free energies of formation of oxides BO and AO is much greater than RT and, therefore,

$$N_{B2} \ll 1 \quad [40]$$

In view of the latter condition, the oxidation rate of the alloy changes gradually from a high value characteristic of pure metal A to a low value characteristic of pure metal B at fairly low concentrations of B in the alloy as is shown below.

Throughout the following discussion, it is assumed that oxide AO involves a metal deficit and, therefore, α is positive. This is true, e.g., for Fe, Ni, and Cu.

If $r \gg 1$, i.e., $D \gg D_A^0$, concentration differences in the alloy are very small as has been discussed previously (1). Thus the composition of the alloy at the alloy-oxide interface is virtually equal to the bulk composition. In essence, only oxide AO is formed if $N_B^0 < N_{B2}$, and, conversely, only oxide BO is formed if $N_B^0 > N_{B2}$.

On the other hand, if $r \ll 1$, a two-oxide scale is expected in a certain range of alloy composition. For the following discussion one assumes, therefore, $r \ll 1$.

A particularly simple case occurs if both oxide AO and oxide BO have a metal deficit and $\alpha = \beta$, i.e.,

$$\gamma = 0 \quad [41]$$

Since it has been assumed above that oxide AO grows much faster than oxide BO, D_A^0 must be much greater than D_B^0 if $\alpha = \beta$, i.e., in view of Eq. [24],

$$q \ll 1 \quad [42]$$

Upon substitution of Eq. [41] in Eq. [30], it follows that the volume fraction of oxide BO in the two-phase region is independent of x,

$$\psi = \psi_1 = \psi_2 \text{ at } z_1 < z < z_2 \quad [43]$$

In view of Eqs. [41] and [43], integration of Eq. [29] between $z = z_1$ and $z = z_2$ yields

$$2\alpha z_2(z_2 - z_1) = (1 - \psi_1 + q\psi_1)(a_1^\alpha - a_2^\alpha) \quad [44]$$

If $\gamma = 0$, Eq. [35] becomes

$$(z_2 - z_1)/z_2 = q/(1 - \psi_1 + q\psi_1) \quad [45]$$

Multiplying corresponding sides of Eq. [44] and Eq. [45], one obtains

$$2\alpha(z_2 - z_1)^2 = q(a_1^\alpha - a_2^\alpha) \quad [46]$$

Substituting Eqs. [41] and [43] in Eq. [36] and solving for ψ_1, one obtains

$$\psi_1 = \frac{N_B^0 - N_{B2}[1 - F(z_2/r^{1/2})]}{(N_B^0 - N_{B2})(1-q) + [q + N_{B2}(1-q)]F(z_2/r^{1/2})} \quad [47]$$

Thus for $\alpha = \beta$, the problem has been reduced to a calculation of the four unknowns ψ_1, a_1, z_1, and z_2 from Eqs. [32], [44], [46], and [47].

The general characteristics of the problem may be obtained from a discussion of the behavior of alloys with gradually increasing concentrations of B.

1. For pure metal A, there is only formation of AO and,

therefore, $z_1 = z_2$, $a_1 = a_2$. For $\alpha > 0$ it follows from Eqs. [32] and [39] that

$$z_1 = z_2 \cong (2\alpha)^{-\frac{1}{2}} \quad [48]$$

2. A-B alloys involving small concentrations of B below a certain limit N_B' also yield only oxide AO according to previous calculations (1). Component B is enriched at the alloy-AO interface and diffuses backward at a sufficient rate so that the concentration of B at the alloy-AO interface does not reach the concentration N_{B2} at which alloy, oxide AO, and oxide BO coexist. The maximum concentration N_B' of the alloy at which only oxide AO is formed is obtained from Eq. [47] with $\psi_1 = 0$ and $N_B^0 = N_B'$. In view of Eqs. [48] and [38*b*] it follows from Eq. [47] that

$$N_B' = N_{B2}\{1 - F[(2\alpha r)^{-1/2}]\} \cong \alpha r N_{B2} \quad [49]$$

3. If the concentration of B in the alloy exceeds the concentration N_B', both oxides AO and BO are formed simultaneously, but a small excess of B will change conditions for diffusion of A only slightly. Therefore, if $N_B^0 \gtrsim N_B'$, one may still use the approximation

$$z_1 \cong z_2 \cong (2\alpha)^{-\frac{1}{2}} \quad [50]$$

Substituting Eqs. [38*b*] and [50] in Eq. [47],

$$\psi_1 = \frac{N_B^0 - \alpha r N_{B2}}{N_B^0 + q - N_B^0 q - \alpha r(N_{B2} + q - N_{B2}\, q)} \quad [51]$$

If $N_B^0 \ll 1$, $q \ll 1$, and $r \ll 1$, the terms $N_B^0 q$ and $N_{B2} q$ in the denominator of Eq. [51] can be neglected and, therefore, Eq. [51] becomes

$$\psi_1 \cong \frac{N_B^0 - \alpha r N_{B2}}{N_B^0 + q - \alpha r(N_{B2} + q)} \cong \frac{N_B^0 - \alpha r N_{B2}}{N_B^0 + q - \alpha r N_{B2}} \quad [52]$$

4. If the concentration of B in the alloy is further increased, the volume fraction of BO will increase. Accordingly, the available cross section for diffusion of A in AO within the two-phase region will decrease, and thereby the growth rate of the AO layer will decrease.

If $N_B^0 < N_{B2}$, i.e., if the concentration of B at the alloy-oxide interface is higher than in the bulk alloy, only a certain fraction of B present in the original alloy is oxidized, whereas another fraction of B diffuses backward from the alloy-oxide interface toward the bulk alloy.

On the other hand, if $N_B^0 > N_{B2}$, conditions are reversed, i.e., B diffuses from the bulk alloy toward the alloy-oxide interface and, therefore, the relative amount of B in the scale is greater than in the original alloy. The excess of B in the scale, however, is small if the over-all oxidation rate of the alloy is of the same order of magnitude as that of pure metal A since diffusion in the alloy is assumed to be slow in comparison to diffusion of A in AO, i.e., $D \ll D_A^0$ or $r \ll 1$.

If the concentration of B remains below a certain limit calculated below in Eq. [62], there results the inequality

$$(2\alpha)^{\frac{1}{2}} > z_2 \gg r^{\frac{1}{2}} \quad [53]$$

where α is supposed to be of the order of unity, and r is much smaller than unity. Under these conditions, the argument of the function F in Eq. [47] is much greater than unity. Therefore, one may use the approximation $F(z_2/r^{\frac{1}{2}}) \cong 1$ according to Eq. [38*b*] in order to calculate ψ_1 from Eq. [47] if $N_B^0 \gtrsim N_{B2}$. Hence

$$\psi_1 \cong \frac{N_B^0}{q + N_B^0 - N_B^0 q} \quad [54]$$

As a further approximation,

$$\psi_1 \cong \frac{N_B^0}{q + N_B^0} \quad [55]$$

5. If $N_B^0 \gg q$, ψ_1 is close to unity, i.e., the two-phase region contains mostly BO and only a small amount of AO.

Upon substitution of Eq. [54] in Eq. [45], it follows that

$$z_2 - z_1 = (q + N_B^0 - N_B^0 q)\, z_2 \cong N_B^0 z_2 \text{ if } N_B^0 \gg q \quad [56]$$

Substitution of Eq. [56] in Eq. [46] yields

$$2\alpha(N_B^0 z_2)^2/q \cong a_1^{\alpha} - a_2^{\alpha} \text{ if } N_B^0 \gg q \quad [57]$$

For $N_B^0 \ll 1$, $q \ll 1$, and $z_2 - z_1 \ll z_2$ according to Eq. [56], Eq. [32] may be rewritten as

$$2\alpha z_2^2 \cong 1 - a_1^{\alpha} \quad [58]$$

Adding corresponding sides of Eq. [57] and [58], letting $1 - a_2^{\alpha} \cong 1$ in view of Eq. [39], and solving for z_2, one obtains

$$z_2 \cong \left[\frac{1}{2\alpha}\frac{q}{q + (N_B^0)^2}\right]^{1/2} \text{ if } N_B^0 \gg q \quad [59]$$

Substitution of Eq. [59] in Eq. [56] yields

$$z_2 - z_1 \cong \left[\frac{1}{2\alpha} \cdot \frac{q(N_B^0)^2}{q + (N_B^0)^2}\right]^{1/2} \text{ if } N_B^0 \gg q \quad [60]$$

The foregoing equations, in particular Eqs. [59] and [60], are only valid if the inequality in Eq. [53] holds.

Substituting Eq. [59] in Eq. [53], one obtains the limiting condition

$$N_B^0 \ll \{q|(2\alpha r)^{-1} - 1|\}^{\frac{1}{2}} \quad [61]$$

Since $\alpha \sim 1$ and $r \ll 1$, Eq. [61] may be rewritten as

$$N_B^0 \ll (q/2\alpha r)^{\frac{1}{2}} \quad [62]$$

The following special relations are noteworthy. If N_B^0 is much greater than $q^{\frac{1}{2}}$ but much smaller than $(q/2\alpha r)^{\frac{1}{2}}$, it follows from Eqs. [59] and [60] that

$$z_2 \cong (q/2\alpha)^{\frac{1}{2}}/N_B^0 \quad [63]$$

$$z_2 - z_1 \cong (q/2\alpha)^{\frac{1}{2}} \quad [64]$$

Thus the thickness $(x_2 - x_1)$ of the two-phase region, which is proportional to $(z_2 - z_1)$ according to Eqs. [21] and [22], tends to a limiting value corresponding to an oxygen activity of a_1 nearly equal to unity at the outer boundary of the two-phase region as follows by a comparison of Eqs. [46] and [64].

6. If the alloy concentration approaches the right-hand member in Eq. [62], N_B^0 is necessarily much greater than q, $\psi_1 \cong 1$ in view of Eq. [55], $a_1 \cong 1$, and Eq. [64] holds. Multiplying corresponding sides of Eqs. [44] and [47], letting $\psi_1 = 1$, $a_1 \cong 1$, and $a_2 \cong 0$, $1 - N_{B2} \cong 1$ and substituting Eq. [64], one obtains

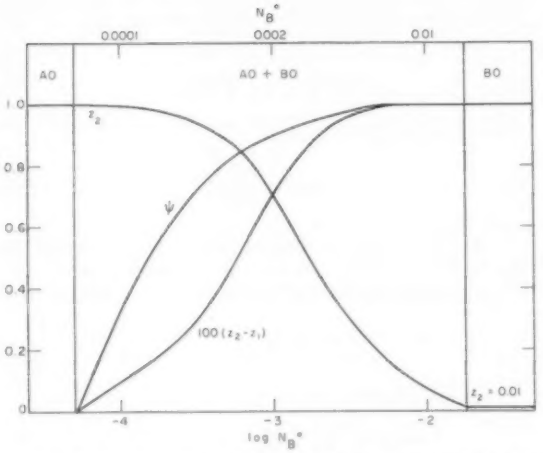

FIG. 3. Oxidation of an alloy A-B as a function of mole fraction N_B^0 for $N_{B2} = 10^{-3}$, $q = D/D_B^0 = 10^{-4}$, $r = D/D_A^0 = 10^{-2}$.

$z_2 = x_2/2(D_A^0 t)^{\frac{1}{2}}$, relative thickness of the entire scale;

$z_1 - z_1 = (x_2 - x_1)/2(D_A^0 t)^{\frac{1}{2}}$, relative thickness of the two-oxide region;

ψ: volume fraction of BO in the two-oxide region.

$$z_2(2\alpha/q)^{\frac{1}{2}}\,(N_B^0 - N_{B2}) = F(z_2/r^{\frac{1}{2}}) \qquad [65]$$

Eq. [65] gives a relation between z_2 and alloy composition N_B^0, which may be evaluated by computing values of N_B^0 for appropriately chosen values of z_2. A limiting value N_B'' is reached if the thickness of the homogeneous AO layer approaches zero, i.e., if $z_1 = 0$, or $z_2 - z_1 = z_2$. Substituting Eq. [64] for $z_2 = z_2 - z_1$ in Eq. [65],

$$N_B'' = N_{B2} + F\,[(q/2\alpha r)^{\frac{1}{2}}] \text{ if } z_1 = 0 \qquad [66]$$

In view of Eq. [38a], Eq. [66] may be rewritten as

$$N_B'' = N_{B2} + (\pi q/2\alpha r)^{\frac{1}{2}} \text{ if } z_1 = 0 \text{ and } (q/2\alpha r)^{\frac{1}{2}} \ll 1 \qquad [67]$$

From Eq. [67] it follows that the minimum concentration for exclusive formation of BO is relatively low if $q \ll r$, i.e., in view of Eqs. [24] and [25], if

$$D \gg D_B^0 \qquad [68]$$

7. If the alloy contains more B than the limiting concentration calculated in Eq. [67], only BO is formed.

Fig. 3 illustrates the dependence of the thickness of the scale, the thickness of the two-oxide region, and the volume fraction ψ on alloy composition for selected values of N_{B2}, q, and r.

Conclusions

In the literature, there are numerous investigations on the oxidation of alloys consisting of a base metal which oxidizes rather rapidly and alloying metals which are less noble and whose oxides form more slowly. In accordance with the foregoing analysis, it has been found that the oxide of the base metals appears preferably in the outer scale, and the oxide of the alloying element in the inner scale (10–17). Moreover, it has been found that the oxidation rate of base metals such as Fe and Cu is considerably decreased by the presence of small amounts of less noble elements such as Al, Cr, Si, and Be (10–21). So far, however, no observations are available to check quantitatively the theoretical calculations for the dependence of the oxidation rates on alloy composition.

Deviations are to be expected since, according to Pilling and Bedworth (22) and Dunn (23), alloys do not always follow the parabolic rate law even under conditions where the pure components obey the parabolic rate law. Observations on Cu-Al alloys by Dennison and Preece (15) are of particular interest. At 850°C, the initial oxidation rate of copper containing from 2–4 wt % Al is relatively high, although much lower than that of pure Cu. After 20 hr the oxidation rate decreases to virtually zero. During the initial stage, both Cu and Al are oxidized, as has also been found by Price and Thomas (19). Calculations based on Eq. [67] indicate that the aforementioned Al concentrations are much higher than the limiting value N_B'' for exclusive formation of Al_2O_3 (1). At present, details of the formation of a two-phase scale under these conditions are not understood. Formation of a two-phase scale on these alloys, however, seems to represent only a transient state. Finally, steady-state conditions presupposed in the foregoing analysis are presumably approached, i.e., a coherent layer of Al_2O_3 is formed. Slow attainment of steady-state conditions confines the applicability of the foregoing theoretical analysis but does not make it worthless. Oxidation rates calculated above may be considered as lower limiting values which are attainable either after long times or after appropriate pretreatment in order to shorten an induction period of rapid oxidation (19).

To obtain results which can be applied directly to practical situations, a more sophisticated approach seems to be needed with due regard to finite lateral dimensions of the grains of the constituent phases, diffusion normal and parallel to the surface of a sample, internal oxidation, and the occurrence of plastic deformation. The latter must definitely be taken into account if the condition $V_{AO} = V_{BO}$ is not satisfied as has been pointed out above.

If oxides of different metals have a noticeable mutual solubility, cations of metal A may also diffuse in oxide BO, and conversely. Moreover, mutual solubility of oxides of metals having different valences may change the number of lattice defects and thereby diffusion coefficients (24). On some alloys, ternary oxide phases such as $NiCr_2O_4$ are formed. Theoretical and experimental work on diffusion and lattice defects in ternary oxides is still almost completely missing but is prerequisite for a better understanding of the oxidation of such alloys.

It would be rather impractical to deal with all these problems in a "unified theory." Instead, it seems appropriate to consider relatively simple limiting cases. The choice of the special presuppositions introduced above is somewhat arbitrary. Its usefulness can be shown only by future experimental investigations on a variety of systems. None of these may satisfy all presuppositions, but deviations may be minor for some systems so that the foregoing considerations apply at least semiquantitatively.

Acknowledgment

This investigation was sponsored by Office of Ordnance Research under Contract DA-19-020-ORD-2244, Project TB2-0001 (779).

Manuscript received October 17, 1955.
Any discussion of this paper will appear in a Discussion Section to be published in the June 1947 JOURNAL.

REFERENCES

1. C. WAGNER, *This Journal*, **99**, 369 (1952).
2. L. B. PFEIL, *J. Iron Steel Inst.*, **119**, 501 (1929).
3. M. H. DAVIES, M. T. SIMNAD, AND C. E. BIRCHENALL, *Trans. Am. Inst. Mining Met. Engrs.*, **191**, 889 (1951).
4. F. N. RHINES AND B. J. NELSON, *ibid.*, **156**, 171 (1944).
5. C. WAGNER, *This Journal*, **103**, 571 (1956).
6. N. B. PILLING AND R. E. BEDWORTH, *J. Inst. Metals*, **29**, 529 (1923).
7. H. DÜNWALD AND C. WAGNER, *Z. physik. Chem.*, **B22**, 212 (1933); J. GUNDERMANN AND C. WAGNER, *ibid.*, **B37**, 155 (1937); C. WAGNER AND K. GRÜNEWALD, *ibid.*, **B40**, 455 (1938).
8. E. A. SECCO AND W. J. MOORE, *J. Chem. Phys.*, **23**, 1170 (1955).
9. C. WAGNER, "Diffusion and High Temperature Oxidation of Alloys" in "Atom Movements", p. 153, American Society for Metals, Cleveland (1951).
10. A. PORTEVIN, E. PRÉTET, AND H. JOLIVET, *Rev. mét.*, **31**, 101, 186, 219 (1934); *J. Iron Steel Inst.*, **130**, 219 (1934).
11. E. SCHEIL AND E. KIWIT, *Arch. Eisenhüttenw.*, **9**, 405 (1935/36).
12. E. SCHEIL, *Z. Metallkunde*, **29**, 209 (1937).
13. K. W. FROEHLICH, *ibid.*, **28**, 368 (1936).
14. A. PREECE AND G. LUCAS, *J. Inst. Metals*, **81**, 219 (1952/53).
15. J. P. DENNISON AND A. PREECE, *ibid.*, **81**, 229 (1952/53).
16. J. MOREAU, *Compt. rend.*, **236**, 85 (1952); *Publs. inst. recherches siderurg.*, **A49**, 7 (1953); J. MOREAU AND J. BÉNARD, *Compt. rend.*, **237**, 1417 (1953).
17. H. J. YEARIAN, "Investigations of the Oxidation of Chromium and Chromium-nickel Steels," Report Contract N7onr-39419 (1954).
18. E. SCHEIL AND E. H. SCHULZ, *Arch. Eisenhüttenw.*, **6**, 155 (1932/33).
19. L. E. PRICE AND G. J. THOMAS, *J. Inst. Metals*, **63**, 21, 29 (1938).
20. A. DES. BRASUNAS, J. T. GOW, AND O. E. HARDER, *Proc. Am. Soc. Testing Materials*, **46**, 870 (1946).
21. L. DE BROUCKÈRE AND L. HUBRECHT, *Bull. soc. chim. Belges*, **61**, 101 (1952); L. HUBRECHT, *ibid.*, **61**, 205 (1952).
22. N. B. PILLING AND R. E. BEDWORTH, *Ind. Eng. Chem.*, **17**, 372 (1925).
23. J. S. DUNN, *J. Inst. Metals*, **45**, 25 (1931).
24. C. WAGNER AND K. E. ZIMEN, *Acta Chem. Scand.*, **1**, 547 (1947); W. HIMMLER, *Z. physik. Chem.*, **195**, 129 (1950); K. HAUFFE AND C. GENSCH, *Z. physik. Chem.*, **195**, 116 (1950); C. GENSCH AND K. HAUFFE, *ibid.*, **195**, 386 (1950); **196**, 427 (1951); K. HAUFFE AND H. PFEIFFER, *Z. Elektrochem.*, **56**, 390 (1952); H. PFEIFFER AND K. HAUFFE, *Z. Metallkunde*, **43**, 364 (1952); K. HAUFFE, *Werkstoffe u. Korrosion*, **1**, 131, 221, 243 (1951); "The Mechanism of Oxidation of Metals and Alloys at High Temperatures" in "Progress in Metal Physics", edited by B. Chalmers, Vol. 4, p. 71 (1953)

Conductances of Some Acids, Bromides, and Picrates in Dimethylformamide at 25°C

PAUL G. SEARS, RICHARD K. WOLFORD, AND LYLE R. DAWSON

Department of Chemistry, University of Kentucky, Lexington, Kentucky

ABSTRACT

Conductances of five acids, three partially substituted ammonium salts, and three alkali metal and quaternary ammonium picrates in dimethylformamide have been investigated at 25° for solute concentrations in the range 1–50 × 10^{-4} *N*. Results indicate that dimethylformamide exhibits differentiating properties toward the acids and the partially substituted ammonium salts and also that the picrates are completely dissociated.

Previous studies which have been reported from this laboratory (1–3) indicate that dimethylformamide (DMF) is a potentially useful electrolytic solvent. Na, K, and quaternary aminonium salts have been found to be appreciably soluble and also apparently completely dissociated in dilute DMF solutions. The purpose of this study has been to examine the leveling or differentiating properties of DMF toward acids and some partially substituted ammonium salts and also to investigate the conductance behavior of several picrates.

EXPERIMENTAL

Commercial grade DMF which had been dried for several days over KOH pellets was fractionated at atmospheric pressure and then redistilled at 5 mm pressure. The middle fractions which were retained had conductivities of 2 × 10^{-7} ohm^{-1} cm^{-1} or less.

Picric acid ('Baker Analyzed' Reagent) was recrystallized three times from ethanol. From this acid, K, Na, triethylammonium and tetramethylammonium picrates were synthesized by reacting with the proper base. Each product was recrystallized several times from water-ethanol mixtures.

HBr was prepared by dropping Br_2 into tetrahydronaphthalene. The evolved gas was passed through three towers containing tetrahydronaphthalene in order to remove any gaseous Br which may have been carried from the reaction flask into the gas stream.

Reagent grade glacial acetic acid was distilled at atmospheric pressure and a small middle fraction was retained.

TABLE I. *Equivalent conductances of some electrolytes in dimethylformamide at 25°C*

$C \times 10^4$	Λ	$C \times 10^4$	Λ	$C \times 10^4$	Λ
(*a*) Picric acid		(*e*) Acetic acid		(*i*) Monoethylammonium bromide	
2.326	69.39	1.751	24.73	2.593	87.00
3.852	68.56	3.744	19.20	4.380	85.16
6.111	67.65	5.871	16.39	7.411	82.28
8.978	66.79	9.544	13.67	13.63	77.55
16.65	65.05	14.91	11.48	18.92	74.05
18.29	64.76	20.35	10.08	37.07	66.56
		41.56	7.34		
(*b*) Hydrobromic acid		(*f*) Potassium picrate		(*j*) Triethylammonium bromide	
0.7748	86.69	1.468	66.81	0.8966	85.68
1.133	86.18	3.104	66.11	2.245	82.32
3.048	84.02	6.689	65.02	4.163	78.50
6.300	82.13	9.910	64.27	6.741	74.54
10.08	80.51	13.94	63.54	10.43	70.06
14.76	78.12	19.00	62.74	16.29	64.76
		34.61	60.91		
(*c*) Trichloroacetic acid		(*g*) Sodium picrate		(*k*) Triethylammonium picrate	
0.8852	33.33	1.172	65.84	0.8069	71.59
2.753	23.65	2.373	65.11	2.085	70.89
6.167	20.46	4.762	64.15	3.609	70.32
10.06	19.96	6.967	63.53	5.920	69.59
14.21	19.74	12.18	62.36	14.35	67.73
22.99	19.28	23.81	60.60	22.58	66.87
(*d*) Hydrochloric acid		(*h*) Tetramethylammonium picrate			
1.568	72.07	0.6171	75.29		
2.979	59.01	1.920	74.48		
4.829	49.93	3.308	73.82		
7.240	42.94	5.468	72.91		
12.78	34.35	9.118	72.15		
20.98	28.16	14.59	71.05		
44.17	20.74				

Trichloroacetic acid (Eastman White Label) was fractionated also at atmospheric pressure. The middle fraction which boiled at 194°–195° was retained.

Triethylammonium and monoethylammonium bromides (Fisher Reagent) were recrystallized three times from ethanol.

Prior to using, all salts were dried to constant weight in a vacuum oven. Approximately 0.01*N* stock solutions were prepared on a weight basis and all other solutions were prepared from these by a weight-addition technique. Transfers were made in a dry box under a positive pressure of nitrogen. All weights were corrected to vacuum. In converting concentrations from a weight basis to a volume basis, it was assumed that densities of the solutions were equal to that of DMF at 25°C. Conductivity of an electrolyte was obtained by subtracting the conductivity of the solvent from that of the solution.

The bridge assembly, conductance cells, constant temperature bath, and other aspects of the experimental procedure have been described previously (1, 2).

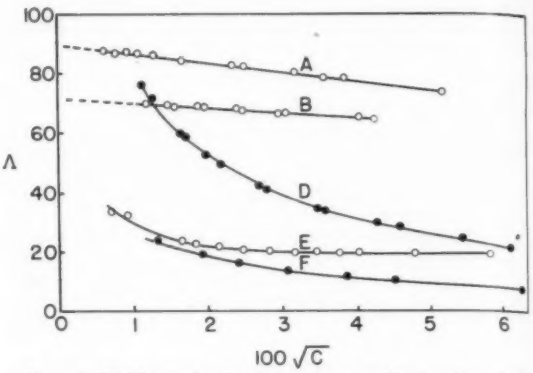

FIG. 1. Kohlrausch plots for some acids in dimethylformamide. A—HBr; B—HPi; D—HCl; E—CCl_3COOH; F—CH_2COOH.

TABLE II. *Data pertinent to experimental and theoretical slopes of Kohlrausch plots for some electrolytes in DMF*

Electrolyte	Experimental slope (S_E)	Theoretical slope (S_T)	$\frac{S_E - S_T}{S_T}$ 100
HBr	−313	−163	91
HPi*	−169	−151	12
Et_2NHBr	−672	−165	308
Et_2NHPi	−128	−151	−16
$EtNH_2Br$	−478	−167	186
Me_4NPi	−138	−154	−10
NaPi	−133	−145	−9
KPi	−130	−148	−12

* Pi is symbol used for picrate.

The following data for DMF at 25°C were used in the calculations: density, 0.9443 g/ml; viscosity, 0.00796 poise; dielectric constant, 36.71 (4). Values of the fundamental constants which were used in the evaluation of the Onsager constants were taken from a recent report of the Subcommittee on Fundamental Constants (5).

RESULTS

Corresponding values of the equivalent conductance, Λ, and the concentration in gram equivalents of solute per liter of solution, *C*, for each salt are presented in Table I. Confirmatory data for another series of solutions for each electrolyte have been omitted from Table I for conciseness. In each case, however, results for the two series of solutions agreed within an estimated error of 0.2%.

DISCUSSION

Plots of the equivalent conductances of several acids in DMF as a function of the square root of the concentration are shown in Fig. 1. Those for acetic and trichloroacetic acids in DMF are similar to plots which are characteristic of weak electrolytes in water. Nevertheless, the nature of the two plots indicates that the greater electronegativity or electron-attracting property of the chlorine atoms enhances the dissociation of trichloroacetic acid at comparable concentrations. The plot for HCl, which is shown as curve *D* in Fig. 1, is characteristic of an incompletely dissociated electrolyte. Owing to the impossibility of establishing accurate values of the limiting equivalent conduct-

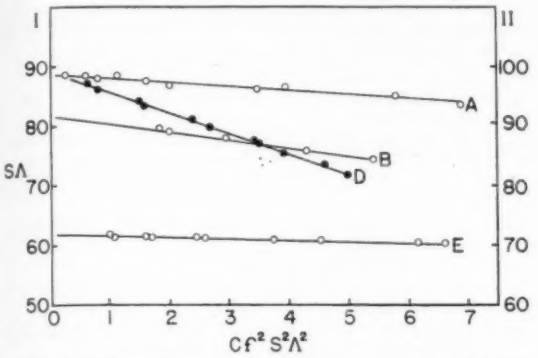

FIG. 2. Fuoss-Shedlovsky plots for some electrolytes in dimethylformamide. Ordinate I: A, HBr; D, Et_2NHBr; ordinate II: B, $EtNH_3Br$; E, HPi.

TABLE III. *Limiting equivalent conductances and dissociation constants for some electrolytes in DMF obtained by the Fuoss-Shedlovsky method*

Electrolyte	Λ_0	$K \times 10^3$
HBr	88.7	17
HPi	71.7	63
Et_2NHBr	89.1	3
$EtNH_3Br$	91.8	8

ances of acetic, trichloroacetic, and hydrochloric acids, no further treatment of the data was attempted.

In contrast to the behavior of the three acids which have been mentioned above, HBr and $C_6H_3O_7N_3$ (2,4,6-trinitrophenol) in DMF are characterized by linear Kohlrausch plots and are more completely dissociated. The weakening of the bond due to the increased size of the nonmetal atom more than compensates for the decrease in ionic character and gives corresponding greater acidity in DMF to HBr than to HCl. Hantzsch and Caldwell (6) and Kolthoff and Willman (7) have observed the same relative behavior for these acids in pyridine and acetic acid, respectively.

Data pertinent to the comparison of the experimental and the theoretical slopes of the plots of Λ vs. $\sqrt{C}$ for HBr and $C_6H_3O_7N_3$ and some other electrolytes are presented in Table II. The experimental slopes of the plots for the acids and the partially substituted ammonium bromides are numerically greater than the corresponding slopes calculated using the Onsager equation (8). Inasmuch as this behavior is usually typical of incomplete dissociation, data for these electrolytes were analyzed by the Fuoss-Shedlovsky method (9) (*see* Fig. 2). The resulting values of the dissociation constants and the limiting equivalent conductances are given in Table III.

It is interesting to note that the results provide evidence that $C_6H_3O_7N_3$ is stronger than HBr in DMF. The reversal of the dissociation constants for these two acids in water and in DMF probably can be attributed primarily to the bromide ion being relatively less solvated in DMF than in water whereas the picrate ion can be assumed to be a large unsolvated ion in both solvents. If this were the case, the bromide ions with their relatively smaller size and greater charge density may be sufficiently more susceptible

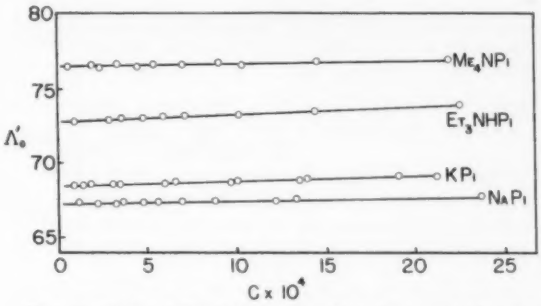

FIG. 3. Plots of Shedlovsky equation for some picrates in dimethylformamide.

TABLE IV. *Data obtained from plots of the Shedlovsky equation for some electrolytes in DMF*

Electrolyte	Λ_0	$B \times 10^3$
NaPi	67.3	1.5
KPi	68.5	3.0
Me_4NPi	76.4	1.9
Et_3NHPi	72.8	4.5

than picrate ions to ion-pair formation with solvated protons in DMF to reduce the degree of dissociation of HBr below that of $C_6H_3O_7N_3$. Although the results indicate that it is less dissociated, HBr may be more ionized than $C_6H_3O_7N_3$ in DMF.

Like other strictly electron-donor solvents such as acetone, methyl ethyl ketone, acetonitrile, nitrobenzene, and nitromethane (10–13), DMF exhibits differentiating properties toward partially substituted ammonium salts. Wynne-Jones (12) has made a reasonable postulation that these substances are partially covalent in nature and that in solution there exists an equilibrium between ions and un-ionized molecules formed through hydrogen bonding. Data in the literature concerning the conductances of partially substituted ammonium salts in electron-donor solvents show that picrates generally are more dissociated than bromides which, in turn, are much more dissociated than chlorides. The authors' results agree with this generalization inasmuch as monoethylammonium and triethylammonium bromides have dissociation constants of 8×10^{-3} and 3×10^{-3}, respectively, and triethylammonium picrate is dissociated completely in DMF. In most electron-donor solvents the partially substituted ammonium picrates are incompletely dissociated also; however, triethylammonium picrate is dissociated completely in acetonitrile as it is in DMF.

Slopes of the Kohlrausch plots for some of the electrolytes were found to be numerically less than the calculated Onsager slopes (*see* Table II). Data for these completely dissociated electrolytes were analyzed using the Shedlovsky equation (14) which may be written as follows:

$$\Lambda_0' = \frac{\Lambda + \beta\sqrt{C}}{1 - \alpha\sqrt{C}}\Lambda_0 + BC$$

The results are presented in Fig. 3 and in Table IV. The behavior of the picrates is very similar to that of the perchlorates and iodides in DMF (1, 2).

Utilizing data in this and earlier papers (1–3), the following series of decreasing relative cationic conductances in DMF may be established:

$$Me_4N^+ > EtNH_3^+ > Et_4N^+ > Et_3NH^+ > DMF \cdot H^+ > Me_3PhN^+ > K^+ > Na^+ > Pr_4N^+ > Bu_4N^+$$

Inasmuch as the cationic conductance is related inversely to the effective cationic size, this series suggests that several of the cations are solvated probably through hydrogen bonding or ion-dipole attraction or both.

Manuscript received January 25, 1956. The paper was taken from a thesis submitted by R. K. Wolford in partial fulfilment of the requirements for the M.S. degree. University of Kentucky, Lexington, Ky. The work was supported in part by a contract with the U. S. Army Signal Corps.

Any discussion of this paper will appear in a Discussion Section to be published in the June 1957 JOURNAL.

REFERENCES

1. D. P. AMES AND P. G. SEARS, *J. Phys. Chem.*, **59,** 16 (1955).
2. P. G. SEARS, E. D. WILHOIT, AND L. R. DAWSON, *ibid.*, **59,** 373 (1955).
3. P. G. SEARS, E. D. WILHOIT, AND L. R. DAWSON, *J. Chem. Phys.*, **23,** 1274 (1955).
4. G. R. LEADER AND J. F. GORMLEY, *J. Am. Chem. Soc.*, **73,** 5731 (1951).
5. F. D. ROSSINI, F. T. GUCKER, JR., H. L. JOHNSTON, L. PAULING, AND G. W. VINAL, *ibid.*, **74,** 2699 (1952).
6. A. HANTZSCH AND K. S. CALDWELL, *Z. physik. Chem.*, **61,** 227 (1908).
7. I. M. KOLTHOFF AND A. WILLMAN, *J. Am. Chem. Soc.*, **56,** 1007 (1934).
8. L. ONSAGER, *Physik. Z.*, **28,** 277 (1927).
9. R. M. FUOSS AND T. SHEDLOVSKY, *J. Am. Chem. Soc.*, **71,** 1496 (1949).
10. P. WALDEN AND E. J. BIRR, *Z. physik. Chem.*, **144,** 269 (1929); **153,** 1 (1931); **163,** 263, 281 (1933).
11. D. M. MURRAY-RUST, O. GATTY, W. A. MACFARLANE, AND H. HARTLEY, *Ann. Repts. Progr. Chem. (Chem. Soc. London)*, **27,** 342 (1930).
12. W. F. K. WYNNE-JONES, *J. Chem. Soc.*, **1931,** 795.
13. S. GLASSTONE, "The Electrochemistry of Solutions," pp. 172–177, D. Van Nostrand Co., Inc., New York (1937).
14. T. SHEDLOVSKY, *J. Am. Chem. Soc.*, **54,** 1405 (1932).

JUNE 1957 DISCUSSION SECTION

A Discussion Section, covering papers published in the July–December 1956 JOURNALS, is scheduled for publication in the June 1957 issue. Any discussion which did not reach the Editor in time for inclusion in the December 1956 Discussion Section will be included in the June 1957 issue. Those who plan to contribute remarks for this Discussion Section should submit their comments or questions in triplicate to the Managing Editor of the JOURNAL, 216 W. 102nd St., New York 25, N. Y., *not later than March 1, 1957.* All discussions will be forwarded to the author, or authors, for reply before being printed in the JOURNAL.

Technical Review

Rectifying Semiconductor Contacts

H. K. Henisch[1]

Research Laboratories, Sylvania Electric Products Inc., Bayside, New York

The behavior of rectifying contacts between metals and semiconductors constitutes a topic of major interest in the semiconductor field from theoretical as well as practical points of view. The literature of the subject contains well over a thousand publications, and it is now desirable to review the extent of knowledge and to discriminate between contributions which add to operational understanding and those which add only ingenious algebra. The present review is intended for readers who have not made the study of contacts their special field, but who would like to be acquainted with the present state of the art.

Barrier Concepts

The aim of this paper is the understanding of the behavior of single contacts as such, whereas practical systems nearly always include two contacts and some bulk material as well. There is a well-known method of separating these components, as illustrated on Fig. 1. By means of potential probe measurements, it is possible to determine the voltage distribution across the system for various currents. Accordingly, one can also distinguish (semi-quantitatively) between high resistance and low resistance contacts. Very little is known about the latter and the present review is therefore restricted to high resistance contacts. The probe measurements generally indicate a voltage step at the contact and it was soon realized that this voltage must exist across some definite layer of material, however thin. This is called the barrier layer. Its identification and characterization occupied many years of research. It was not found possible to identify the layer as a distinct new phase and this gave rise to the concept of a potential barrier, i.e., a region of high electrical potential for the charge carriers concerned. The high energy required for transmission of carriers across the region accounts for the high contact resistance, and the asymmetrical deformation of the barrier under the influence of an externally applied voltage is responsible for rectification. These simple concepts have survived numerous changes in the theoretical outlook on contacts and may thus be regarded as reassuringly stable. Geometrical features, e.g., the point-contact configuration, were at one time regarded as essential requirements of rectification, but are now known to play only a secondary role. They can enhance the effective rectification ratio, but are not themselves responsible for asymmetric conduction. Similarly, heating effects at contacts can be responsible for symmetrical nonlinearities of the voltage-current relation, but not for rectification as such. Fig. 1 shows that the achievement of pronounced rectification depends on eliminating as much bulk material as possible and on emphasizing electrical and structural differences between the two end contacts. This is the aim of the sophisticated manufacturing processes now in use, most of which have been developed by empirical methods.

Conditions encountered in practice are more complicated than Fig. 1 suggests. When a voltage is applied to a rectifier assembly, the current is not constant, but is generally a function of time. This is referred to as current creep and distinction is made between positive creep (corresponding to an increase of current with time) and negative creep (corresponding to a decrease of current). It follows that the voltage-current relation is not uniquely defined, except in operational terms. By using short voltage pulses instead of constant applied voltages, the processes which involve longer time constants can be rendered inoperative. On the other hand, electronic quasi-equilibrium is not necessarily established during short pulses; this may lead to a new difficulty in the interpretation of experimental results.

Contacts on Transistor Materials

Since potential probes always occupy some space, the experiment illustrated on Fig. 1 involves an extrapolation. To determine the voltage across the contact itself, one assumes that the bulk material is electrically homogeneous to within the immediate neighborhood of the barrier layer itself. This extrapolation is permissible as long as the bulk material remains unaffected by the current flowing. However, many types of contacts on transistor materials support the well-known process of carrier injection which is responsible for the appearance of additional charge carriers in the neighborhood of a contact passing a forward current. These additional carriers alter the electrical properties of the material and the above extrapolation is then no longer meaningful. Under these conditions, it is no longer helpful to regard the contact as being in any important sense "in series connection" with the bulk material. Instead, the system must be studied as a whole, the contact being regarded as the location in which the additional carriers originate, and the bulk material as the location in which they decay. One may thus distinguish between theoretical approaches to contacts on transistor specimens and on other (nontransistor) specimens. The distinction is above all a matter of degree and must be handled with care. Methods of detecting injection (and, indeed, various other effects, like exclusion, extraction, and accumulation) are of limited sensitivity, and it is

[1] On leave of absence from the University of Reading, Berks, England.

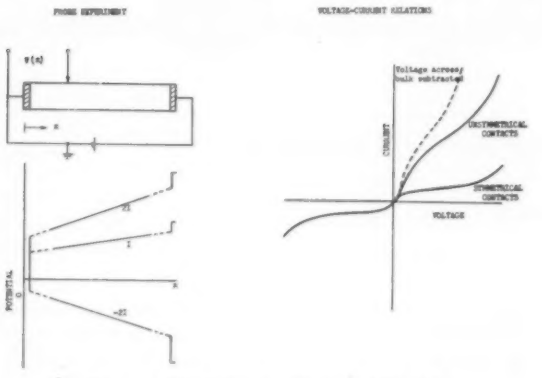

FIG. 1. Principle of contact rectification

therefore impossible to assert with complete confidence that any particular contact is definitely noninjecting.

NATURE OF THE BARRIER LAYER

Potential barriers of the kind referred to above can be envisaged as arising in many different heights and shapes, and it is plausible that the most important single parameter in this context is the barrier height. Many detailed theories are available which concern themselves with the effect of various barrier shapes on the voltage-current relation of the contact, but the models on which such theories are based can seldom be established by independent means. One learns about contact structure through experiments on contact behavior and alters the models to reach agreement with experimental results. Quite generally, modifications of the barrier height provide more sensitive corrections than almost any other modification of the theoretical model. The barrier height and its changes under the influence of the applied voltage are therefore our principal concern.

A barrier of the kind envisaged here can in principle arise from one of three causes: (*a*) because the semiconductor and the metal have different thermionic work-functions, (*b*) because the semiconductor surface is characterized by so-called surface states, and (*c*) because there is a thin foreign layer between the metal and the semiconductor which, in turn, involves contacts with barriers by way of mechanisms (*a*) or (*b*). Such a layer is called an artificial barrier layer. Thermionic work functions were given great prominence in theoretical treatments before the formulation of Bardeen's theory of surface states in 1947. There are few well-authenticated cases (although there appear to be some) in which thermionic work functions have been demonstrated definitely to play an important role, whereas there are many in which they have been shown to be irrelevant in practice. In view of this, most present-day theoretical accounts are based on models involving barriers arising from surface states. There is little systematic knowledge of the behavior of thin foreign layers at the interface, and models for barriers arising in this way have too many arbitrary features to make discussion desirable here. In any case, it is firmly established that distinct macroscopic foreign layers are not an essential requirement for rectification.

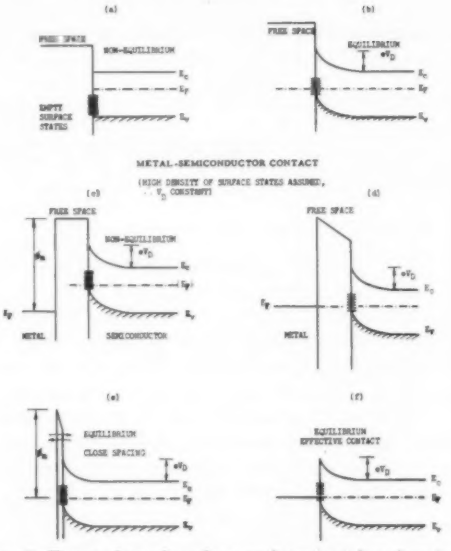

FIG. 2. Formation of surface and contact barriers in the presence of surface states.

The manner in which surface states, even in the absence of a metallic contact, can lead to the formation of a potential barrier is shown on Fig. 2 (*a*) and Fig. 2 (*b*). Use is made of the band structure model, subject to the additional and somewhat arbitrary hypothesis that the band structure which is characteristic of the material in bulk also applies in the immediate vicinity of the surface. Surface states are localized electronic states which are permitted within the otherwise forbidden band, and at least some of which are empty when the surface is neutral. When equilibrium is established these states become filled or partially filled; this gives the surface a negative charge. The corresponding positive charge of the double layer produced in this way resides primarily in the impurity centers of the semiconductor within a narrow region which, in fact, constitutes the barrier layer. The surface states thus act as one electrode of a capacitor and the adjoining semiconductor region acts partly as the other electrode and partly as the dielectric. A pictorial way to express the action of surface states is to consider that the semiconductor is covered by a two-dimensional metallic shield. If the density of surface states is large enough, the barrier layer is screened by this shield from all external electrostatic influences and thus is independent of the external contact material and its thermionic work function. Diagrams (*e*) to (*f*) of Fig. 2 illustrate the energetic conditions at and near the interface when a contact is established. The closest spacing between metal and semiconductor considered here is of the order of an interatomic spacing, as in (*e*). The thin part of the potential barrier which arises under these conditions can be neglected, since it can be shown to be transparent to electrons. It is therefore omitted on (*f*) which represents the essential features of the barrier when in equilibrium.

The barrier profiles of Fig. 2 are known as Schottky barriers and are based on an important simplification, already recognized by Schottky. These energy profiles

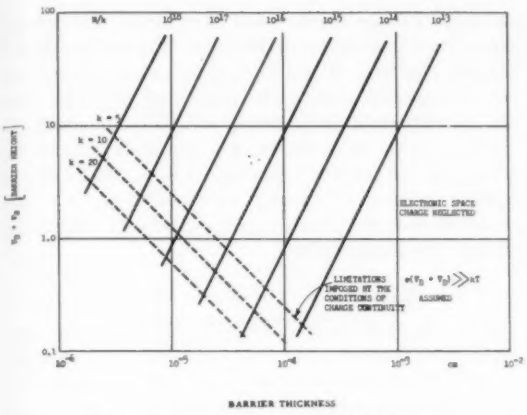

FIG. 3. Properties of a Schottky barrier

imply a continuous space charge, whereas any charge residing in discrete impurity centers must be discontinuous. The assumption of continuity is permissible as an approximation as long as the impurity centers are relatively closely spaced. It is not permissible when the thickness of the barrier layer extends over only a few inter-center distances. This limits the validity of theories based on the traditional profile of the Schottky barrier. Fig. 3 illustrates this limitation for various barrier heights, impurity contents, and dielectric constants. In this case the limitation has been based on the somewhat arbitrary but perhaps still plausible assumption that the barrier layer must be at least five times as thick as the inter-center distance, if the assumption of continuity is to be at all applicable. Some cases of considerable practical importance must be excluded from the simplified treatment under this heading. Satisfactory theories of discontinuous space-charge layers are difficult to formulate in view of the random distribution of impurity centers.

Charge Transport across a Barrier

The most general rectification theory would deal with the transport of both types of charge carriers (electrons and holes) through a contact on near-intrinsic semiconducting material of high carrier lifetime. The corresponding equations are those for the electron and hole flow, Poisson's equation, and the corresponding boundary conditions. They can be formulated without difficulty, but explicit solutions are not available. Simplifying assumptions must always be introduced and these may or may not be applicable to particular cases encountered in practice. The coarsest simplification is to assume that the current is carried either wholly by majority or wholly by minority carriers. The practical case in which holes and electrons participate in an arbitrary ratio has not yet been satisfactorily solved. In the remainder of this section only unipolar rectification is considered and the assumption is made that charge carriers are electrons in extrinsic n-type material.

There are two ways in which electrons can, in principle, move from one side of a potential barrier to the other: they can tunnel through the barrier (wave-mechanical tunnel effect) even though their energy may be small, or

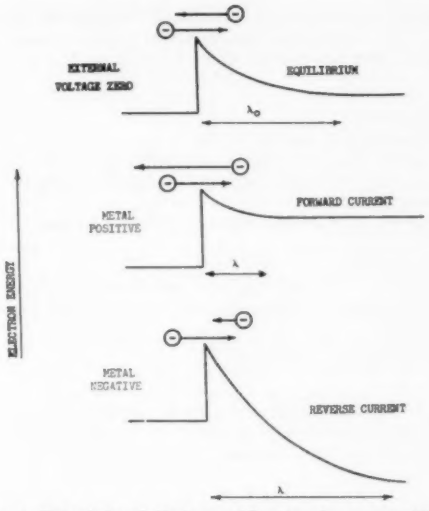

FIG. 4. Principle of diode rectification by a metallic contact of an n-type semiconductor.

they can pass over it, if their energy is sufficiently high. The first mechanism is known to play only a subsidiary role, since rectification theories based primarily on the tunnel effect predict rectification in the wrong direction. In any case, barriers which are of practical importance are known to be too thick for the tunnel effect to operate. The tunnel effect can, however, be operative near the thin top of a barrier and thus can modify rectification characteristics which depend essentially on the other mechanism. The concept of rectification by charge transport over a barrier lends itself to a simple pictorial representation (Fig. 4). The length of the horizontal arrows is intended to be a measure of the charge flow. The arrows pointing toward the right remain constant in (*a*), (*b*), and (*c*), since the barrier height as seen from the metal is assumed to remain constant. Those pointing to the left change in response to the applied voltage which alters the barrier height as seen from the semiconductor side. This process is in agreement with the observed direction of rectification.

In this context one may distinguish between two limiting cases: that in which the charge carriers make normal collisions while passing over the barrier, and that in which they make no collisions at all. The last case applies if the mean free path is greater than the barrier thickness. The current can then be calculated on the basis of streamline flow, using only classical kinetic gas theory. This is known as the diode theory of rectification. If, on the other hand, normal collisions are envisaged, diffusion terms must be taken into account in the usual way. This leads to the diffusion theory of contact rectification. It will be clear that the diode theory is, in a sense, contained in the diffusion theory, of which it represents a special case. If collisions within the barrier are postulated as being absent, the barrier shape cannot influence the rectification process. Accordingly, the diode theory is concerned only with the barrier height, whereas the diffusion theory is concerned with height and shape.

A straightforward comparison between the currents cal-

TABLE I. *Comparison of unipolar rectification theories* (Equations apply to *n*-type material before correction for image force and tunnel effect.) Based on $V_D + V_B >> kT/e$

Diode theory:
Independent of barrier profile
$j = ne(kT/2\pi m)^{1/2} \exp(-eV_D/kT)[\exp(-eV_B/kT)-1]$
Diffusion theory: (uncorrected for high field effects)
Schottky barrier
$j = ne\mu[(V_D + V_B)8\pi Ne/K]^{1/2} \exp(-eV_D/kT[\exp(-eV_B/kT)-1]$
Mott barrier
$j = ne\mu[(V_D + V_B)/\lambda_0] \exp(-eV_D/kT)[\exp(-eV_B/kT)-1]$
Diffusion theory: (with simplest correction for high field effects)
Independent of barrier profile
$j = nev_m \exp(-eV_D/kT)[\exp(-eV_B/kT)-1]$

V_D = diffusion potential; V_B = barrier voltage; v_m = maximum drift velocity of electrons in high fields; λ_0 = thickness of the Mott barrier; j = current density.

culated on the basis of the diode and the simplest diffusion theories, respectively, leads to an apparent paradox. For a given applied voltage, the current predicted by diffusion theory is greater than that predicted by the diode theory, whereas, by virtue of the collisions, it should be smaller. The reason for this discrepancy has been recognized only recently. The electric fields which prevail within a barrier may be (and usually are) very strong. Electrons in such a field can be accelerated to velocities which are comparable with thermal velocities, whereas the usual drift equation assumes that the energy gained from the field is negligibly small. Again, the usual diffusion equations postulate small concentration gradients, whereas the gradients applying within a barrier layer may be very large. For these reasons, the conventional formulation of drift and diffusion problems cannot be accepted as satisfactory when applied to rectifying barriers, and corrections must be introduced which take account at least of the strong electric fields. The simplest correction of this kind postulates that the electrons move throughout the barrier with a limiting drift velocity which remains constant and independent of the field as long as the field is high enough. The corresponding equations can be explicitly integrated. Results of various theoretical approaches are compared in Table I. It will be seen that the differences between them are not great on the whole, and that, in particular, the diode theory and the diffusion theory with the correction for strong fields lead to similar equations.

All rectification theories make some explicit or implicit assumption concerning the space charge density within the barrier layer and its dependence (or lack of it) on the current flowing. To simplify the mathematical treatments, it is usually postulated that the space charge due to majority carriers passing the barrier can be neglected, but this cannot be a good approximation for high forward currents and may also break down in the extreme reverse direction. Moreover, theoretical treatments of the voltage-current relation concern themselves nearly always with isothermal conditions, whereas Joule heating of the contact by the current flowing is known to be an important factor. At high reverse voltages, especially on point contacts, a voltage-turnover phenomenon is often observed, i.e., a maximum voltage which cannot be exceeded. For currents higher than the turnover current, the differential resistance becomes negative. It can be shown, e.g., by comparison with experiments under pulse conditions, that this turnover phenomenon is primarily thermal in character. However, as far as is known, no satisfactory theory has been developed yet which gives an adequate description of turnover in terms of thermal processes alone. It is now considered that electronic processes must play a secondary but not unimportant part.

Variations in Barrier Height

In the above discussion, the barrier height, at any rate as seen from the metal side, has been treated as a constant. In view of the great importance attached to this parameter, this particular assumption calls for special comment. An effective lowering of the barrier by the tunnel effect has already been envisaged. Most theoretical treatments also include some reference to the image force which acts on charges just outside a conductor and distorts the electric field in which the charges move. This image force would also lead to a smaller effective barrier height than otherwise expected. A more general reservation can be formulated as follows: if a barrier arises from a difference of thermionic work functions, it is plausible to assume that it should be of constant height and (except for the operation of tunnel effect and image force lowering) independent of the current flowing. Likewise, it should be practically independent of temperature. On the other hand, if the barrier arises from charges in surface states, there is no particular reason to believe that either of these conclusions necessarily applies. The charge in surface states may be temperature-dependent and it may increase and decrease in response to the density of charge flow across the barrier. As far as is known, no theoretical treatment is available at present which takes account of these very real possibilities. Uncertainties arising in this connection have an important bearing on the interpretation of experimental results, since most information on barrier heights is derived from procedures which assume this height to be firmly constant. These procedures indicate that most barrier heights (eV_D) encountered in practice are in the neighborhood of 0.3 ev. Results quoted to a large number of significant figures may safely be distrusted when encountered in the literature.

Inversion Layer and Injection

Fig. 2 gives profiles of barriers which are wholly characterized by a pronounced diminution in the concentration of majority carriers, in this case of electrons. However, it is possible to envisage barrier profiles which enable minority carriers (in this case positive holes) to play an important and even predominating role. Fig. 5(*a*) shows such a barrier. The hole concentration in the immediate vicinity of the metal interface is high by virtue of the fact that the barrier is high or that the forbidden band is narrow. Indeed, there is a region in which the hole concentration exceeds the electron concentration and this is called the inversion layer. This system has some of the features of a *p-n* junction, although some important differences remain. Fig. 5(*a*) shows the positive hole population in the full

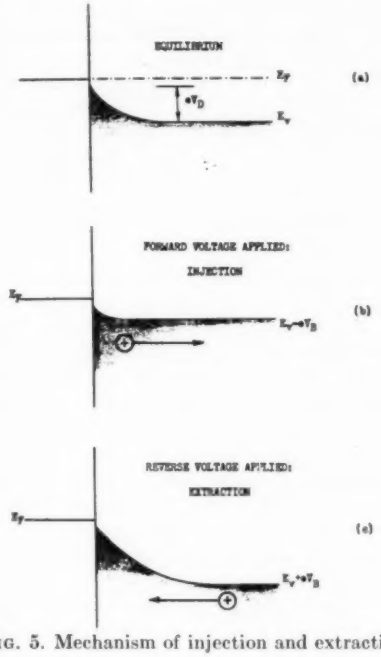

FIG. 5. Mechanism of injection and extraction

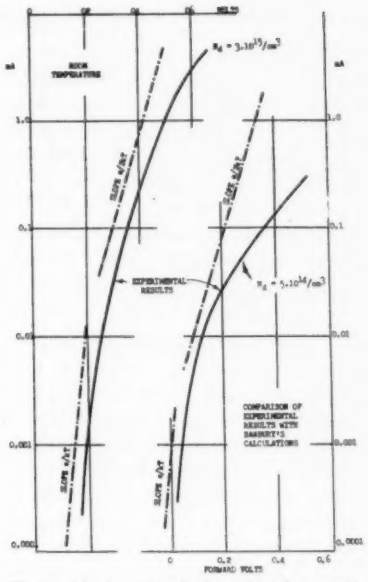

FIG. 6. Forward characteristics of point contacts on *n*-germanium.

band of the semiconductor within the barrier region. It can be shown that the presence of these minority carriers increases the effective field in the immediate vicinity of the metal and also makes it less dependent on the external voltage. When the barrier is distorted by the application of an external forward voltage, as in Fig. 5(*b*), the equilibrium evidently is disturbed and positive holes pass into the interior of the semiconductor. This is the process on minority carrier injection mentioned above. As long as the applied fields are small, the current is carried mainly by a diffusion process. With increasing field strength, drift effects tend to predominate over diffusion effects. The carriers that pass into the semiconductor decay in accordance with an approximately exponential law, the time constant of which is called the carrier lifetime. If the lifetime is high, these carriers may move through considerable distances before decaying. By so doing they modulate the resistivity of the bulk material adjoining the injecting barrier. If the adjoining material embodies a spreading resistance, as it does in the case of point contacts, this modulation may be very pronounced indeed. In general, the forward current is carried by both majority and minority carriers in a ratio which depends on the barrier height and probably on other factors. A quantity known as the current composition ratio which can be used to characterize the mechanism of current flow is defined. It denotes the fraction of the total current which is carried by minority carriers. In a near-intrinsic material, some of the current even within the bulk (far away from contacts) is carried by minority carriers. Thus, a further quantity that characterizes the injection properties of a contact is needed: the *injection "ratio"*. This is the difference between the current composition ratios at the contact interface and within the bulk material, respectively. A noninjecting contact is thus not one which is free from the participation of minority carriers, but one in which minority carriers contribute to the current flowing to the same degree as they do within the bulk material. It is then at once plausible that completely noninjecting contacts would represent a very special case which is not encountered often in practice. Experimental methods have been developed for the measurement of the injection ratio under a variety of conditions. Special interest attaches to the measurement of very low injection ratios, e.g., of base contacts on diodes, and to the measurement of high injection ratios for very small currents, since this is the condition best suited for a comparison between calculated and observed results.

On the basis of the injection mechanism illustrated above, it is possible to calculate the forward characteristic of the rectifier. Fig. 6 shows this for point contacts of two different specimens of germanium, at any rate as far as slopes are concerned. Slopes are calculated and the full lines represent experimental results. The agreement must be regarded as satisfactory, considering that certain special assumptions had to be introduced into the calculations, e.g., that recombination could be neglected because of the high fields present, and that the injection ratio is unity. Three general methods are available for the detection of injected charge carriers. They are illustrated on Fig. 7, which is largely self-explanatory. Each of these idealized experiments is also the basis of practical applications.

Fig. 5(*c*) shows the conditions that apply in the presence of an inversion layer when a reverse voltage is applied. The minority carriers then tend to move toward the metal, and to contribute to the reverse current. It is clear that this will result in a deficit of minority carriers just inside the semiconductor. This is the effect known as carrier extraction. The extraction current can be calculated on the basis of simple and well-known equations, and again on the assumption that minority carrier flow alone is of

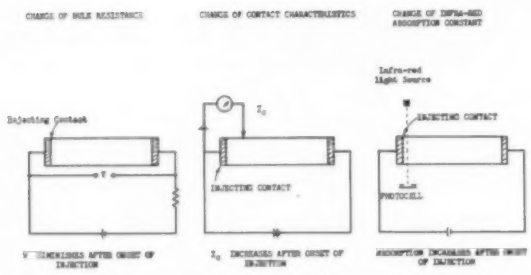

FIG. 7. Three methods of detecting carrier injection

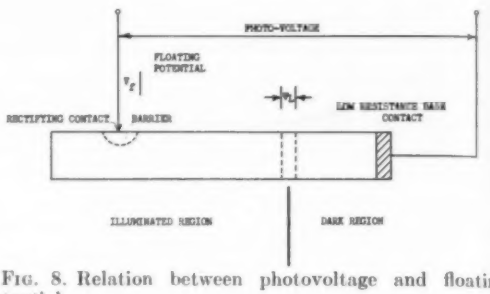

FIG. 8. Relation between photovoltage and floating potential.

concern; but when the calculated results are compared with actual observations, they tend to be too low. The precise origin of the higher currents observed is not yet certain, although one may well suppose that additional minority carriers are generated at the surface of the semiconductor in the immediate vicinity of the contact. Once generated, they would augment the reverse extraction current. Calculations of the extraction current are handicapped by lack of precise understanding of the phenomenon of current gain. It is known that a certain amount of current multiplication takes place when minority carriers pass through a contact in the reverse direction. The extent of this current multiplication must be intimately related to the mechanism whereby the space charge within the barrier tends to be neutralized by charge carriers of opposite sign.

Corresponding to the two phenomena of injection and extraction already discussed, two other processes can be envisaged and have been observed in practice. They are: (*a*) carrier exclusion, corresponding to a negative "injection ratio" (in this case a misnomer, of course), and forward current, and (*b*) carrier accumulation, corresponding to a negative "extraction ratio" (again a misnomer when applied to this case) and reverse current. These four phenomena can be analyzed by a single set of equations, subject to various changes in signs. They can be detected by the methods illustrated on Fig. 7, except of course, that extraction and exclusion lead to a diminution in the concentration of charge carriers near the contact. Experimental methods have recently been developed whereby the extraction ratio can be estimated. As discussed above, the phenomenon of injection is governed by (among other things) the carrier lifetime; in a similar way, exclusion and extraction are governed by carrier generation time. For infinitesimal displacements from equilibrium these times must be identical, but for large displacements the situation may be much more complicated. All current composition ratios are somewhat dependent on the current itself, and their behavior in this respect is generally in accordance with theoretical expectations.

Effect of Additional Charge Carriers

The foregoing discussions concern contact systems that are in equilibrium in the absence of any current flowing. It is of interest to consider how the various contact properties are changed when the semiconductor is permanently in a nonequilibrium state, e.g., if it is continuously illuminated. The illumination produces electron and hole pairs, and these pairs affect the conduction processes through contacts. This problem can be dealt with as if the illumination produces only minority carriers, as long as the native majority carriers predominate sufficiently over the native minority carriers and as long as the displacement from equilibrium is quite small. These are then the minority carriers which are described as being "additional". Fig. 8 shows such a system. The field in the barrier at the rectifying contact draws positive holes into the contact where they eventually decay. Since their decay requires a certain amount of time, these carriers constitute a net positive charge and the metal point thus becomes positive with respect to the semiconductor. When a metal is positive with respect to an *n*-type specimen of transistor material, injection of minority carriers occurs and this clearly counteracts the original drift of additional minority carriers into the barrier. A steady state arises when this drift and the injection just balance. The metal contact is then somewhat positive and the voltage which exists across the barrier under these conditions is called the floating potential. It is not the voltage measured (even for zero current) in the external circuit; this is the photovoltage. The two voltages differ by the amount V_L, as indicated in Fig. 8; V_L is a diffusion voltage which, in principle, must always arise between illuminated and nonilluminated portions of a semiconductor. This diffusion voltage can be negligibly small if the contact under test is highly rectifying and has a high floating potential, but it need not be so. If it is negligibly small the external photovoltage can be regarded as equal to the floating potential. Fortunately, V_L can be calculated with confidence from existing equations. The floating potential itself exists whenever there are additional charge carriers in the neighborhood of a contact, independent of how these carriers are produced, whether by illumination or by injection from another contact. The voltage V_L cannot be eliminated or even modified by illuminating the specimen as a whole. It has been found possible to calculate the floating potential explicitly, but only for contacts of unit injection ratio. In other cases a semi-empirical treatment must be used.

The change in contact properties in the presence of additional charge carriers, e.g., change of conductance near the origin or change of saturation current in the reverse direction, can be used as a measure of the additional minority carrier concentration. Care must be taken when these methods are used in the context of other investigations. Simple tests show that point contacts are nonlinear

detectors of additional carriers. They are in fact more sensitive to low than to high concentrations. When this method is used in the course of certain forms of lifetime determinations, it tends to produce fictitiously high lifetimes which arise from this nonlinearity.

Fig. 8 shows a situation in which there is no external voltage applied to the system. However, in other contexts, the conditions are of special interest when the rectifying contact carries a reverse voltage. In this case the migration of minority carriers is enhanced, and this is the phenomenon known as carrier collection. It is concerned primarily with additional carriers, as compared with extraction which concerns resident minority carriers. Again, theoretical calculations of the collection current depend on the assumptions made with regard to the mechanism of current gain and the extent to which space charge compensation can be achieved by having carriers of opposite sign within the barrier region.

Outstanding Problems

Many important contact problems are still in need of theoretical clarification, such as the detailed relation between contact structure and the current composition ratio, the relation between surface generation of charge carriers and contact characteristics, the nature of transient phenomena observed during measurements on contacts, the dependence of contact characteristics on the surrounding gas atmosphere, the mechanism of various relaxation effects observed at ultra-high frequencies, and so on. Most of these problems are complicated, and it seems likely that their solution will occupy semiconductor physicists for a long time to come.

Manuscript received April 21, 1956. This paper was prepared for delivery before the San Francisco Meeting, April 29 to May 3, 1956.

Any discussion of this paper will appear in a Discussion Section to be published in the June 1957 Journal.

MANUSCRIPTS AND ABSTRACTS FOR SPRING MEETING

Papers are now being solicited for the Spring Meeting of the Society, to be held at the Statler Hotel in Washington, D. C., May 12, 13, 14, 15, and 16, 1957. Technical Sessions probably will be scheduled on Electric Insulation, Electronics (including Luminescence, Semiconductors, Oxide Cathodes, Instrumentation, and possibly Screen Applications), Electrothermics and Metallurgy, Industrial Electrolytics, and Theoretical Electrochemistry (including a special symposium on electrolytes).

To be considered for this meeting, triplicate copies of abstracts (*not to exceed 75 words in length*) must be received at Society Headquarters, 216 West 102nd St., New York 25. N. Y., *not later than January 2, 1957. Please indicate on abstract for which Division's symposium the paper is to be scheduled.* Complete manuscripts should be sent in triplicate to the Managing Editor of the Journal at the same address.

* * *

The Fall 1957 Meeting will be held in Buffalo, N. Y., October 6, 7, 8, 9, and 10, 1957, at the Statler Hotel. Sessions will be announced in a later issue.

A TRIUMPH OF TELEPHONE TECHNOLOGY

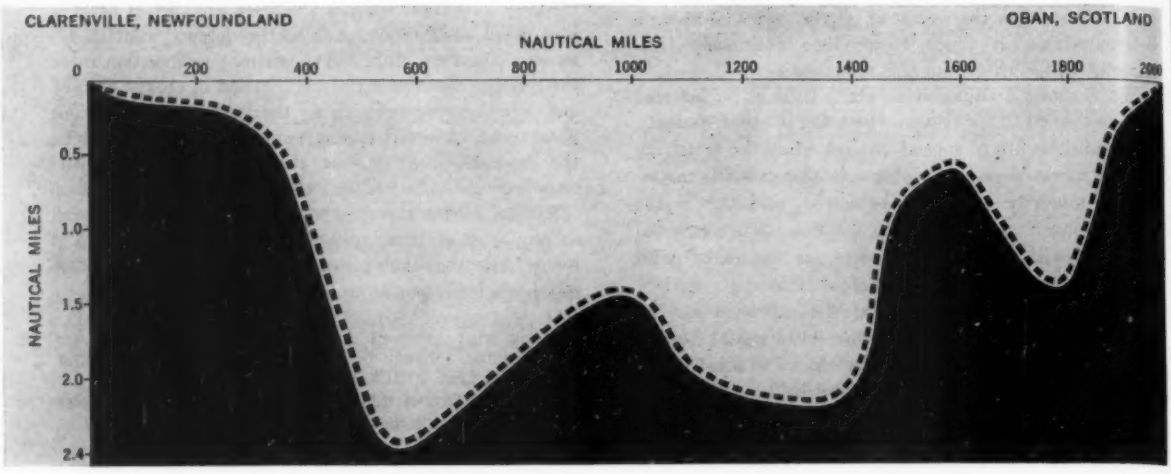

Contour of ocean bed where cable swiftly and clearly carries 36 conversations simultaneously. This is deep-sea part of system — a joint enterprise of the American Telephone and Telegraph Company, British Post Office and Canadian Overseas Telecommunications Corporation.

A great new telephone cable now links North America and Europe—the first transoceanic cable to carry voices.

To make possible this historic forward step in world communications, Bell Laboratories scientists and engineers had to solve formidable new problems never encountered with previous cables, which carry only telegraph signals.

To transmit voices clearly demanded a much wider frequency band and efficient ways of overcoming huge attenuation losses over its more than 2000-mile span. The complex electronic apparatus must withstand the tremendous pressures and stresses encountered on the ocean floor, far beyond adjustment or servicing for years to come.

Here are a few of the key developments that made this unique achievement possible:

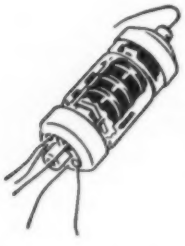

More than 300 electron tubes of unrivaled endurance operate continuously, energized by current sent from land.

Precisely designed equalizing networks and amplifiers compensate for the loss in the cable every 40 miles and produce a communication highway 144 kc. wide.

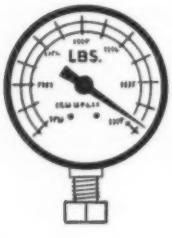

A unique triple watertight seal protects the amplifiers from pressures as high as 6500 pounds per square inch.

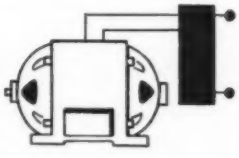

Power supplies of exceptional reliability send precisely regulated current along the same coaxial that carries your voice to energize the amplifying units.

BELL TELEPHONE LABORATORIES

World center of communications research and development

FUTURE MEETINGS OF

The Electrochemical Society

Washington, D. C., May 12, 13, 14, 15, and 16, 1957

Headquarters at the Statler Hotel

Sessions probably will be scheduled on

Electric Insulation, Electronics (including Luminescence, Semiconductors, Oxide Cathodes, Instrumentation, and possibly Screen Applications), Electrothermics and Metallurgy, Industrial Electrolytics, and Theoretical Electrochemistry (including a special symposium on electrolytes)

* * *

Buffalo, October 6, 7, 8, 9, and 10, 1957

Headquarters at the Statler Hotel

* * *

New York, April 27, 28, 29, 30, and May 1, 1958

Headquarters at the Statler Hotel

* * *

Ottawa, September 28, 29, 30, October 1, and 2, 1958

Headquarters at the Chateau Laurier

* * *

Papers are now being solicited for the meeting to be held in Washington, D. C. Triplicate copies of each abstract (*not exceeding 75 words in length*) are due at the Secretary's Office, 216 West 102nd St., New York 25, N. Y., *not later than January 2, 1957* in order to be included in the program. *Please indicate on abstract for which Division's symposium the paper is to be scheduled.* Complete manuscripts should be sent in triplicate to the Managing Editor of the JOURNAL at the same address.

News Notes in the Electrochemical Field

New Sustaining Members

The Boeing Airplane Co., Seattle, Wash., and the Reynolds Metals Co., Richmond, Va., recently became Sustaining Members of the Society.

Hydrogen in Semiconductors

Dissolved hydrogen does not affect the apparent electrical properties of some semiconductors, but markedly increases the conductivity of others. Zinc oxide is of the latter type. D. G. Thomas and J. J. Lander of Bell Telephone Labs. have proposed that electron donating centers are formed by union of the dissolved hydrogen atoms with lattice oxygen ions, a chemically probable process. Since the resulting hydroxyl groups are sufficiently large, under the influence of the dielectric constant (12) of the oxide lattice they are easily ionized and the hydrogen electron is freed to participate in the conduction process. This mechanism accounts successfully for the experimentally observed diffusional behavior of hydrogen in zinc oxide and is consistent with the observed dependence of conductivity on hydrogen pressure.

The conductivity of pure germanium, however, is not increased by dissolved hydrogen. Howard Reiss of Bell Labs. suggests that this is because the interstitial vacancies are so large in the germanium lattice that a hydrogen atom in one of them is effectively in free space. Thus its ionization potential is not decreased by the high dielectric constant (16) of the lattice: it is not ionized and so does not contribute its electron to the conduction process. Although similar interstitial holes exist in the zinc oxide lattice, the formation of hydroxyl groups results in quite different behavior.

Since its external pressure may be readily controlled, it appears that hydrogen will prove to be a valuable tool in semiconductor research. Furthermore, the concept of hydroxyl impurity centers is expected to be important in understanding such widely different phenomena as the working of oxide-coated cathodes, electronic conduction in organic crystals, and chemical reactions in catalysis.

Mass Production of Transistors

A new technique for the mass production of high-speed and ultra-high-frequency transistors, announced by the Philco Corp., represents a major advance in semiconductor technology. Two new types of transistors, a Micro-Alloy Transistor (MAT) and a Surface-Barrier Diffused Transistor (SBDT), the direct result of this technique, are now in engineering development.

Developed at Philco's Research Labs. in cooperation with the Navy, Army Signal Corps, and Air Force, the new devices will be produced by the Landsdale Tube Co., a division of Philco, at its new semiconductor plant at Spring City, Pa. The MAT and SBDT may be used in electronic "brains," guided missiles, communications, radar, and other military equipment.

The MAT and SBDT devices are fabricated from germanium, utilizing Philco's unique Surface Barrier technique. This process, now highly mechanized, permits the mass production of transistors requiring precision control of critical dimensions. It avoids the necessity of manually assembling the germanium and the electrode material and alloying them in a furnace.

Radioactive Tracers Aid Corrosion Studies at New National Carbon Research Lab.

Radioactive elements, sent from Oak Ridge in hermetically sealed containers, will be used increasingly in research at the new Parma, Ohio, laboratories of the National Carbon Co., a Division of Union Carbide and Carbon Corp. The atoms of the materials are "tagged," that is, they emit signals in the form of radiation that can be detected by Geiger counters and other instruments.

A typical use of radioactive techniques has been in establishing the major causes of shelf corrosion in flashlight batteries and the development of effective corrosion preventatives. A similar application in the field of corrosion chemistry is in the investigation of corrosion of automotive cooling systems under all conditions of use and abuse. As manufacturers alter the materials used, continual research is required to maintain corrosion protection. Radioactive tracer techniques will form an important tool at Parma in the investigation of new radiator materials such as aluminum.

Much the same techniques will be used in the investigation of various types of carbon products where the tracing of the radioactive C^{14} atom will lead to a better knowledge of the site of reactions and to improvements in processing.

The new Parma laboratory, dedicated on September 18, is designed primarily for basic research in chemical and solid state physics.

Society of Plastics Engineers National Technical Conference

"Fifteen Years of Plastics Progress" is the theme of the forthcoming 13th Annual National Technical Conference to be presented by the Society of Plastics Engineers, Inc., January 16–18, 1957, at the Hotel Sheraton-Jefferson in St. Louis, Mo.

Technical sessions will be held covering most phases of plastics engineering and research. Each day's sessions are planned to avoid any conflicts in major interests. An interesting program for the ladies is scheduled.

Individual advance registration will be acknowledged prior to the Conference; registration at the Conference will be handled at separate registration desks. Individual registration fees are: members SPE, $10.00; nonmembers SPE, $15.00. Company registration fees are in accordance with classification. Facilities for accommodation at St. Louis' leading hotels have been confirmed.

Information in reference to registration should be directed to the Registration Chairman, Mr. Harold A. Holz, Bakelite Co., 122 No. Kirkwood Rd., Kirkwood 22, Mo.

Phosphoric Acid Unit

Construction of a phosphoric acid unit by Monsanto Chemical Co. has begun at the Pueblo, Col., plant of The Colorado Fuel and Iron Corp. The phosphoric acid unit, the first of its

particular kind and size, has been engineered to meet the needs of the CF&I coal chemicals operation.

Electric furnace elemental phosphorus will be shipped from Monsanto's plant at Soda Springs, Idaho, to Pueblo, where it will be burned in the new unit to make phosphoric acid. This acid will then be pumped directly into the CF&I plant system for use in the production of diammonium phosphate, a high analysis fertilizer material being marketed by CF&I under the trade name of DAP.

The use of phosphoric acid, instead of sulfuric acid, for recovery of ammonia from coke oven gas was pioneered by CF&I in January 1955.

Olin Revere Metals Corp.

Olin Mathieson Chemical Corp. and Revere Copper and Brass Inc. have announced the formation of a jointly owned company to produce 180,000 tons a year of primary aluminum. The company is to be called the Olin Revere Metals Corp. President will be Walter F. O'Connell, who will also continue as Executive Vice-President in charge of Olin Mathieson's aluminum program.

Earlier in the year, Olin Mathieson announced plans to enter the primary aluminum industry (*See* May 1956 JOURNAL, p. 117*C*). These are superseded by the new plans establishing the Olin Revere Metals Corp.

Olin Mathieson has contracted with Olin Revere on a long-term basis for 120,000 tons of primary aluminum a year. Revere has made a similar contract with the new company for 60,000 tons a year.

Facilities of the Olin Revere Metals Corp. will include: (*a*) An alumina plant with a capacity of 350,000 tons per year, to be built on a site still to be selected near the Gulf Coast on deep water transportation. (*b*) A reduction plant with a capacity of 180,000 tons per year, which is now under construction near Clarington, Ohio. Capacity production is expected to begin late in 1958 with some production before then. (*c*) A new power subsidiary wholly owned by Olin Revere, which will own two 225,000-kw generating units in a new power plant at Cresap, W. Va. These units will supply power to the reduction plant. A third 225,000-kw unit at the power plant will be owned by the Ohio Power Co., a subsidiary of the American Gas and Electric Co. All three units will be operated by Ohio Power.

Arrangements have been made to provide the bauxite supplies required by an aluminum operation nearly three times the size of that originally planned. Bauxite will be furnished from the Surinam, Dutch Guinea, mines of N. V. Billiton. Bauxite will be processed into alumina at Olin Revere's plant on the Gulf Coast. Alumina will be transported by barge up the Mississippi and Ohio Rivers to the Clarington plant, where it will be reduced to aluminum.

Zone Refining Technique for Uranium

Zone refining, a technique in wide use as a method of preparing ultra-high-purity germanium, has been successfully applied to the purification of uranium, it has been announced by Sylvania Electric Products Inc.

C. I. Whitman, V. B. Compton, and R. B. Holden of Sylvania's Atomic Energy Division developed the new application of zone refining as a simple means of purifying uranium for research purposes. By causing a molten zone, created by induction heat, to move slowly along a uranium bar, the Sylvania engineers achieved extensive purification from boron, iron, nickel, and other impurities.

The effectiveness of the method is indicated by the fact that nine zone passes resulted in a concentration of 15 parts of iron per million of uranium at one end of the bar, and 200 ppm of iron at the other end. Additional passes would be expected to produce even better results.

Stackpole Carbon Celebrates Fiftieth Anniversary

On August 8, the Stackpole Carbon Co. of St. Marys, Pa., completed its first 50 years in business. It was founded in 1906 as the Stackpole Battery Co. and six years later, when carbon brushes and other carbon graphite specialties were added to the company lines, the name was changed to the present form.

Today, in addition to more than 30 carbon-graphite specialties, the Stackpole Electronic Components Division is a leading producer of fixed and variable resistors, powdered iron and ferromagnetic cores, Ceramagnet magnetic ferrites, slide switches, low-value capacitors, and coil forms.

Stackpole's main offices and two plants are in St. Marys, Pa. In addition, there are three plants in nearby Kane, Pa., and one in Johnsonburg, Pa. In 1953, electronic component manufacturing was begun by Canadian Stackpole Ltd. in Toronto.

Gordon Research Conferences Anniversary Dinner

A commemorative dinner to mark the Silver Anniversary of the founding of the Gordon Research Conferences will be held at the Hotel Commodore, New York City, on December 27. The date of the dinner was selected to coincide with the Annual Meeting of the American Association for the Advancement of Science, scheduled for the same week in New York.

The principal speaker at the dinner will be Nobel Prize winner Glenn T. Seaborg. His topic will be "The Future Through Science."

Reservations for the Silver Anniversary Dinner, at $10 per person, can be made by writing to Dr. W. George Parks, Director, Gordon Research Conferences, University of Rhode Island, Kingston, R. I.

Central Scientific Moves Newark Branch to Mountainside

Central Scientific Co., Chicago, has moved its Newark branch to a new building at 237 Sheffield St., Mountainside, N. J., a Newark suburb.

The New Jersey branch serves the metropolitan New York area and adjacent states including the District of Columbia, Delaware, Maryland, New Jersey, Pennsylvania, Virginia, and lower New York state.

The new building will also house Central Scientific's Export Division, including Cenco International Cia which handles export business in Western Hemisphere countries, and will be the company's Eastern headquarters for the Petroleum Specialty Sales Division.

Highly Alkaline *p*H Standard

To increase the accuracy of *p*H measurements in the highly alkaline range, the National Bureau of Standards is recommending a sixth *p*H standard for use with the five *p*H standards previously established.

The new *p*H standard is a solution of calcium hydroxide saturated at 25°C. This reference solution is easily prepared. No weighings are necessary, as a solution of reproducible composition can be made merely by shaking finely granular calcium hydroxide with water. The calcium hydroxide is prepared by igniting calcium carbonate conforming to American Chemical Society specifications for the reagent grade low in alkalies. The solid material must not be contaminated with soluble alkalies,

but the presence of carbonate is of no concern since calcium carbonate will precipitate from the solution at the time of preparation. The filtered solution of calcium hydroxide supersaturates readily and can normally be used over a wide range of temperatures without separation of the solid phase.

The *p*H of this solution is 12.45 at 25°C and is a rather sensitive function of temperature. Values of *p*H on the NBS conventional activity *p*H scale have been assigned at intervals of 5 degrees from 0° to 60°C. Although standard samples of calcium hydroxide are not yet available from the Bureau, highly pure preparations can be readily made from commercially available grades of calcium carbonate.

Enthone Expands Marketing Program

Enthone, Inc., has announced a marketing program designed to increase service to customers in the New England-Middle Atlantic States area. In the first phase of this program Mr. Derick S. Hartshorn, Jr., has been promoted from Sales and Service Engineer to District Manager of the New York City, Westchester, and Long Island area. In his new capacity Mr. Hartshorn will be in charge of all sales and service work and personnel in his area. He will also be available personally for service and consultation.

"The Petrified River"

"The Petrified River—The Story of Uranium" is the title of a new motion picture sponsored by Union Carbide and Carbon Corp. in cooperation with the U. S. Bureau of Mines. This 16 mm color and sound film which has a running time of 28 min covers the story of uranium in the United States from prospecting for ore to the peaceful uses of atomic energy and radioisotopes.

The film derives its name from the prehistoric rivers whose beds now lie buried in the mesas of the Colorado Plateau. Over 150 million years ago the precious uranium was deposited in these ancient river beds. Much of the film footage was taken in that colorful area of flat-topped mesas and strange rock formations.

An animated sequence shows how the elements of nature were created, the formation and splitting of the uranium atom, and the way an atomic power station works. Scenes taken at the Oak Ridge National Lab. show the loading of a uranium graphite reactor, the irradiation of isotopes, and the incredibly complex manipulating equipment being used to handle radioactive materials. Also described are various ways of using radioisotopes in medicine, food preservation, agricultural research, and industry.

Requests to borrow prints of the film should be addressed to Graphic Services Section, U. S. Bureau of Mines Experiment Station, 4800 Forbes St., Pittsburgh 13, Pa.

Bound Vol. 102 Available

Copies of bound Vol. 102 (1955) of the JOURNAL are available from Society Headquarters, 216 W. 102 St., New York 25, N. Y.

The Price is $12.00 to members of the Society and $18.00 to nonmembers.

Addendum

J. S. Prener and F. E. Williams, authors of the paper "Activator Systems in Zinc Sulfide Phosphors" which appeared in the June 1956 JOURNAL, wish to make the following acknowledgment of cooperation in the preparation of the manuscript: The authors would like to thank Mr. Louis Stang and his group at the Hot Laboratory of the Brookhaven National Laboratory for their help in the preparation of the zinc sulfide from the highly radioactive ZnO. They also wish to thank the Phillips Petroleum Co. and the staff at the Idaho Falls Reactor for irradiation of the sample of zinc oxide.

Notice to Subscribers

Your subscription to the JOURNAL of The Electrochemical Society will expire on *December 31, 1956*. Avoid missing any issue. Send us your remittance now in the amount of $18.00 for your 1957 subscription. (Subscribers located outside the United States must add $1.00 to the subscription price for postage, and payment must be made by Money Order or New York draft, not local check.) An expiration notice has been mailed to all subscribers.

A bound volume of the 1957 JOURNALS can be obtained at a prepublication price of $6.00 by adding this amount to your remittance. However, no orders will be accepted at this rate after *December 1, 1956*, when the price will be increased to $18.00 subject to prior acceptance. Bound volumes are not offered independently of your JOURNAL subscription.

SECTION NEWS

India Section

The Sixth Annual Meeting of the Section was held on August 27 at the Indian Institute of Science, Bangalore, with Dr. N. R. Srinivasan presiding in the absence of the Chairman. After the minutes of the previous business meeting were approved, the Secretary-Treasurer presented the Sixth Annual Report covering the activities of the Section for 1955–56.

The following officers were elected to serve for the 1956–57 term:

Chairman—M. S. Thacker
Vice-Chairman—P. S. Narayana
Vice-Chairman—K. Rajagopal
Treasurer—T. L. Rama Char
Secretary—J. Balachandra, Indian Institute of Science, Bangalore 3, India

J. BALACHANDRA, *Secretary*

San Francisco Section

At the August 1 meeting of the Section, the following officers were elected for the 1956–57 term:

Chairman—H. F. Myers
Vice-Chairman—Bernard Porter
Treasurer—J. F. Aicher
Secretary—R. A. Zimmerly, Columbia-Geneva Steel Div., U. S. Steel Corp., Pittsburg, Calif.
Representatives on Council of Local Sections—S. H. Dreisbach and C. D. Hunt
Membership Chairman—T. R. Beck

R. A. ZIMMERLY, *Secretary*

NEW MEMBERS

In September 1956 the following were approved for membership in The Electrochemical Society by the Admissions Committee:

Active Members

DAVID BAKALAR, Transitron Electronic Corp., 407 Main St., Melrose 76, Mass. (Electronics)

By action of the Board of Directors of the Society commencing January 1, 1956, all prospective members must include first year's dues with their applications for membership.

Also, please note that, if sponsors sign the application form itself processing can be expedited considerably.

MARIO D. BANUS, Metal Hydrides Inc., Beverly, Mass. (Electrothermics & Metallurgy)

LOUIS H. BERKELHAMER, Ohmite Manufacturing Co., 3601 W. Howard St., Skokie, Ill. (Electronics)

PHILIP E. BOCQUET, Continental Oil Co.; Mail add: 716 Marland Drive, Ponca City, Okla. (Theoretical Electrochemistry)

HANS H. BODE, Accumulatorenfabrik AG. and University of Hamburg; Mail add: Forsthausstr. 101a, Frankfurt a.M., Germany (Battery, Theoretical Electrochemistry)

JOHN W. BRODHACKER, Automotive Div., Electric Storage Battery Co., P. O. Box 6266, Cleveland 1, Ohio (Battery)

WILLIAM L. BRUCKART, Universal-Cyclops Steel Corp.; Mail add: 85 Inglewood Drive, Pittsburgh 28, Pa. (Electrodeposition, Electrothermics & Metallurgy)

EDWARD S. CANDIDUS, National Research Corp.; Mail add: 25 Ware St., Cambridge 38, Mass. (Electronics, Electrothermics & Metallurgy)

JOSEPH E. CHILTON, JR., Stanford Research Institute; Mail add: 134 Graham St., Apt. 3, San Jose, Calif. (Electrodeposition, Electro-Organic, Theoretical Electrochemistry)

C. H. DE MINJER, Research Lab., N. V. Philips Gloeilampenfabrieken, Kastanjelaan, Eindhoven, Holland (Corrosion, Electrodeposition)

ROBERT J. FABIAN, Materials &, Methods, Reinhold Publishing Co., 430 Park Ave., New York 22, N. Y. (Electrodeposition)

LORING R. FRAZIER, Metal Hydrides Inc.; Mail add: 71 Walnut Rd., Swampscott, Mass. (Electrothermics & Metallurgy)

ARTHUR J. FREEDMAN, Engineering Research Dept., Standard Oil Co. (Indiana), 2400 New York Ave., Whiting, Ind. (Corrosion)

MILTON GENSER, International Business Machines Corp.; Mail add: 5 Homer Place, Greenvale Farms, Poughkeepsie, N. Y. (Electronics)

ARTHUR L. GINSBURG, La Cartoucherie Francaise, 8–10 rue Bertin-Poirec, Paris I, France (Battery, Industrial Electrolytic)

THOMAS C. HALL, Pacific Semiconductors Inc.; Mail add: 217 Montreal St., Playa del Rey, Calif. (Electronics)

J. DEAN HERMAN, Lithium Corp. of America, Inc., 2500 Rand Tower, Minneapolis 2, Minn. (Industrial Electrolytic)

CHRISTOPHER G. A. HILL, Levy-West Labs. Ltd.; Mail add: 86 Gallows Hill Lane, Abbots Langley, Watford, Herts, England (Electronics)

ROGER W. HOFFMANN, American Potash & Chemical Co.; Mail add: 2121 So. 15 St., Las Vegas, Nev. (Battery, Electrodeposition, Industrial Electrolytic)

GEORGE L. JACOBS, Sperry Gyroscope Co.; Mail add: 123 Cushing Ave., Williston Park, N. Y. (Electrodeposition)

WARTAN A. JEMIAN, Westinghouse Semiconductor Dept.; Mail add: 726 Eastmont Drive, Greensburg, Pa. (Electronics)

HAROLD F. JOHN, Research Labs., Westinghouse Electric Corp., Churchill Boro, Pittsburgh 35, Pa. (Electronics)

EUGENE L. JORDAN, Radio Corp. of America; Mail add: 44 Main St., Orange, N. J. (Electronics)

FRANKLIN H. KILPATRICK, Minneapolis Honeywell Regulator Co.; Mail add: 5550 Glenwood Ave., Minneapolis 22, Minn. (Electronics)

MELVIN KLEIN, Radio Receptor Co., Inc.; Mail add: 19 S. 10 St., Newark 7, N. J. (Electronics)

HOWARD E. KREMERS, Lindsay Chemical Co., West Chicago, Ill. (Electrothermics & Metallurgy)

JOHN B. LITTLE, Research Lab., International Business Machines Corp., Poughkeepsie, N. Y. (Electronics)

BERNARD LOVE, Research Chemicals, Inc.; Mail add: Box 431, Burbank, Calif. (Electrothermics & Metallurgy)

BYRON W. NEHER, Minnesota Mining & Manufacturing Co., 2301 Hudson Rd., St. Paul 6, Minn. (Electrodeposition)

PETER N. NOTWICK, Atlas Supply Co. Lab., 226 Mt. Pleasant Ave., Newark, N. J. (Battery)

GO OKAMOTO, Faculty of Engineering, Hokkaido University, Kita 12 Jo, Nishi 8 chome, Sapporo, Japan (Corrosion, Electrodeposition, Theoretical Electrochemistry)

HARRY J. PAULUS, Pittsburgh Plate Glass Co.; Mail add: 813 No. Meadowcroft, Pittsburgh 16, Pa. (Battery)

EDWARD P. PEARSON, Basic Refractories Inc., 845 Hanna Bldg., Cleveland 15, Ohio (Electrodeposition)

THOMAS G. PEARSON, Research Labs., British Aluminium Co., Chalfont Park, Gerrards Cross, Bucks, England (Electrothermics & Metallurgy, Industrial Electrolytic, Theoretical Electrochemistry)

ALFRED POE, General Electric Co.; Mail add: 102 So. Main St., North Syracuse, N. Y. (Corrosion, Electro-

1956 Directory

The 1956 Directory of Members of the Electrochemical Society is now available. The Directory contains an alphabetical and geographical list of members of the Society as of March 1, 1956, and a list of Patron and Sustaining Members, Past Presidents, and winners of Society prizes and awards.

Members who wish to receive the Directory are requested to fill in and return the order form below, accompanied by check, to Society Headquarters, 216 West 102 St., New York 25, N. Y.

Please send_____copy(ies) of the 1956 Membership Directory to:

Name_____

Company_____

Street_____

City_____ Zone____ State_____

Attached is check for $_____ for Directory. (Single copies cost $2.00.)

deposition, Electronics, Theoretical Electrochemistry)

ROBERT E. RALSTON, P. R. MALLORY & Co., Inc.; Mail add: 9004 E. 18 St., Indianapolis, Ind. (Battery)

JOHN N. REDING, JR., Dow Chemical Co.; Mail add: 707 North St., Midland, Mich. (Electrothermics & Metallurgy)

PAUL H. ROBINSON, Lincoln Lab., Mass. Institute of Technology, P. O. Box 73, Rm. C-221, Lexington 73, Mass. (Electronics, Theoretical Electrochemistry)

JOHN W. ROSS, Texas Instruments, Inc., 6000 Lemmon, Dallas, Texas (Electronics)

PETER C. ROSSIN, JR., Universal-Cyclops Steel Corp., Bridgeville, Pa. (Electrothermics & Metallurgy)

H. GUNTHER RUDENBERG, Transitron Electronic Corp., 168 Albion St., Wakefield, Mass. (Electronics)

ROBERT F. SHURTZ, Basic, Inc., 845 Hanna Bldg., Cleveland, Ohio (Electrothermics & Metallurgy)

EARL S. SNAVELY, JR., Defense Research Lab.; Mail add: 1207 Ridgemont Drive, Austin 5, Texas (Corrosion, Theoretical Electrochemistry)

ALFONS H. SZKUDLAPSKI, Ronson Corp. of Pennsylvania; Mail add: 201 Washington St., East Stroudsburg, Pa. (Electrodeposition, Electro-Organic, Theoretical Electrochemistry)

F. CORT TURNER, Arthur D. Little, Inc.; Mail add: 111 Mayo Rd., Wellesley, Mass. (Industrial Electrolytic)

MURRAY C. UDY, Strategic-Udy Processes, Inc.; Mail add: 818 Cayuga Drive, Niagara Falls, N. Y. (Electrothermics & Metallurgy)

GEORGE D. VINCENT, Eppley Lab., Inc.; Mail add: 260 Gibbs Ave., Newport, R. I. (Theoretical Electrochemistry)

CHARLES P. WALES, Naval Research Lab.; Mail add: 4107 Old Mt. Vernon Rd., Alexandria, Va. (Battery)

MALCOLM E. WASHBURN, Norton Co.; Mail add: Winn St., Northboro, Mass. (Electrodeposition)

IRVING R. WEINGARTEN, Radio Corp. of America; Mail add: 672 W. Seventh St., Plainfield, N. J. (Electronics)

ROBERT D. WILSON, Special Tubes Div., Raytheon Manufacturing Co., 55 Chapel St., Newton 58, Mass. (Electrodeposition, Electronics)

Student Associate Members

CARTER N. BROWN, P. R. Mallory & Co., Inc. and Butler University; Mail add: 882 Whittier Place, Indianapolis 19, Ind. (Battery)

S. SATHYANARAYANA, General Chemistry Dept., Indian Institute of Science, Bangalore 3, India (Battery, Corrosion, Electrodeposition, Electro-Organic, Industrial Electrolytic)

Associate Member

GREGORY H. PARKER, Electro Metallurgical Co.; Mail add: 137 47th St., Niagara Falls, N. Y. (Electrothermics & Metallurgy)

Reinstatements to Active Membership

ALVIN G. HELLFRITZSCH, Naval Ordnance Lab.; Mail add: C13 Norbeck Rd., Rockville, Md. (Battery, Corrosion, Electrodeposition)

EHRLICH M. EILAND, Aluminum Co. of America; Mail add: 129 Washington Drive, New Kensington, Pa. (Industrial Electrolytic)

VICTOR F. HRIBAR, Hughes Aircraft Co.; Mail add: 452 So. San Vicente Blvd., Los Angeles 48, Calif. (Corrosion, Electrodeposition, Theoretical Electrochemistry)

Deceased Member Reported During June 1956

JULES BEBIE, St. Louis, Mo.

1957 Bound Volume

Members and subscribers who wish to receive bound copies of Vol. 104 (for 1957) can receive the volume for the low, prepublication price of $6.00 if their orders are received at Society Headquarters, 216 West 102nd St., New York 25, N. Y., by *December 1*. After that date members will be charged $12.00 and nonmembers, including subscribers, $18.00.

BOOK REVIEWS

GLASS by G. O. Jones. Published by J. Wiley & Sons, Inc., New York, N. Y., 1956. vi + 119 pages, $2.00.

This pocket-size book (it is one of the Methuen series of monographs on physical subjects) is intended to bridge the gap between the empirical approach of the glass technologist and the fundamental theories of the modern physicist and chemist. The existence of the glassy state, the properties of glasses, and the behavior of glasses under mechanical stress are discussed from the point of view of crystallography, atomic and electronic structure, mechanics, and thermodynamics. The treatment is essentially qualitative and should be clear and interesting to anyone with a basic grounding in physical chemistry. The general insight and information that would be acquired by study of this well-written book would be of value to all who have occasion to use glass apparatus under the range of conditions encountered nowadays in chemical research.

S. Z. LEWIN

THE HISTORICAL BACKGROUND OF CHEMISTRY by Henry M. Leicester. Published by John Wiley & Sons, Inc., New York, N. Y., 1956. viii + 260 pages, $6.00.

The basic concepts and theories of chemistry are traced in highly condensed form from their earliest beginnings in ancient Mesopotamia, Egypt, Greece, and China through the Middle Ages to the first decades of the present century. Every era and theory is treated with brevity and succinctness; e.g., the development of the ideas of atomic combination (the work of Richter, Berthollet, Proust, Dalton, Berzelius, Gay-Lussac, Avogadro, Prout, and many others) is disposed of in 13 pages. However, the general picture of the roots and heritage of modern chemistry is successfully conveyed.

S. Z. LEWIN

DIE TECHNISCHE ELEKTROLYSE DER NICHTMETALLE by Jean Billiter. Published by Springer-Verlag, Vienna, Austria, 1954. xii + 401 pages, $16.40.

This book is the latest in a series on applied electrochemistry, extending over many years, by Professor Billiter.

After a short introduction, the following subjects are discussed: electrolytic manufacture of oxygen and hydrogen, manufacture of heavy water, electro-

(*Continued on page 252C*)

Notice to Members

By now you have received your official voting ballot from Society Headquarters. If you have not already done so, please return the ballot by *December 15* so that your vote may be included in the final election count.

Officers of Local Sections of the Society

Boston
F. C. BENNER, Chairman
L. B. ROGERS, Vice-Chairman
CHARLES LEVY, Sec.-Treas.
61 Central St.
Auburndale 66, Mass.
Representatives on Council of Local Sections:
H. BANDES AND C. W. JEROME

Chicago
ROBERT MISCH, Chairman
D. V. LOUZOS, Vice-Chairman
RALPH HOVEY, Treasurer
WILLIAM COLNER, Secretary
Armour Research Foundation
10 W. 35th St.
Chicago 16, Ill.
Representatives on Council of Local Sections:
C. A. HAMPEL (1 yr) AND H. T. FRANCIS (2 yr)

Cleveland
K. S. WILLSON, Chairman
P. S. BROOKS, Vice-Chairman
R. A. POWERS, Treasurer
D. E. KINNEY, Secretary
General Electric Co.
1099 Ivanhoe Road
Cleveland 10, Ohio
Representatives on Council of Local Sections:
N. C. CAHOON AND K. S. WILLSON

Detroit
G. V. KINGSLEY, Chairman
MANUEL BEN, 1st Vice-Chairman
SAM PIKEN, 2nd Vice-Chairman
MANUEL SHAW, Sec.-Treas.
Chrysler Corp., Engineering Div.
Dept. 487, 12800 Oakland Ave.
Highland Park 3, Mich.
Representative on Council of Local Sections:
FRANK PASSAL

Midland
P. R. JUCKNIESS, Chairman
H. W. SCHMIDT, Vice-Chairman
P. F. GEORGE, Sec.-Treas.
Dow Chemical Co.
Midland, Mich.
Representatives on Council of Local Sections:
F. W. KOERKER AND R. C. KIRK

New York Metropolitan
C. V. KING, Chairman
K. B. MCCAIN, Vice-Chairman
FRANCES LANG, Sec.-Treas.
Research Labs.
International Nickel Co., Inc.
Bayonne, N. J.
Representatives on Council of Local Sections:
A. C. LOONAM (1 yr) AND M. F. QUAELY (2 yr)

Niagara Falls
R. B. MACMULLIN, Chairman
L. A. STOYELL, Vice-Chairman
W. E. KUHN, Sec.-Treas.
Research & Development Branch
Carborundum Co.
Niagara Falls, N. Y.
Representatives on Council of Local Sections:
M. S. KIRCHER AND W. D. SHERROW

Pacific Northwest
G. H. KISSIN, Chairman
E. C. PITZER, Vice-Chairman
J. F. MURPHY, Sec.-Treas.
Dept. of Metallurgical Research
Kaiser Aluminum & Chemical Corp.
Spokane 69, Wash.
Representatives on Council of Local Sections:
G. H. KISSIN AND J. F. MURPHY

Philadelphia
E. L. ECKFELDT, Chairman
G. F. TEMPLE, Vice-Chairman
A. A. WARE, Treasurer
G. W. BODAMER, Secretary
Rohm & Haas Co.
Philadelphia, Pa.
Representatives on Council of Local Sections:
J. F. GALL AND J. F. HAZEL

Pittsburgh
A. J. CORNISH, Chairman
J. J. STOKES, JR., Vice-Chairman
LING YANG, Sec.-Treas.
Metals Research Lab.
Carnegie Institute of Technology
Pittsburgh 13, Pa.
Representatives on Council of Local Sections:
E. A. GULBRANSEN AND R. A. WOOFTER

San Francisco
H. F. MYERS, Chairman
BERNARD PORTER, Vice-Chairman
J. F. AICHER, Treasurer
R. A. ZIMMERLY, Secretary
Columbia-Geneva Steel Div.
U. S. Steel Corp.
Pittsburg, Calif.
Representatives on Council of Local Sections:
S. H. DREISBACH AND C. D. HUNT

Southern California-Nevada
THOMAS BLAIR, Chairman
WILLIAM HETHERINGTON, Vice-Chairman
L. J. DROEGE, Sec.-Treas.
7943 Haskell Ave.
Van Nuys, Calif.

Washington-Baltimore
D. T. FERRELL, JR., Chairman
JEANNE BURBANK, Vice-Chairman
DAVID SCHLAIN, Treasurer
GWENDOLYN B. WOOD, Secretary
National Bureau of Standards
Chemistry Bldg., Rm. 115
Washington 25, D. C.
Representatives on Council of Local Sections:
D. T. FERRELL, JR., AND J. C. WHITE

Ontario-Quebec
A. W. WHITAKER, JR., Honorary Chairman
JOHN SUMNER, Chairman
T. S. GAMBLE, Vice-Chairman (Programs)
R. R. ROGERS, Vice-Chairman (Membership)
J. U. MACEWAN, Chairman Junior Members Committee
H. A. TIMM, Sec.-Treas.
Dominion Magnesium Ltd.
Haley, Ont., Canada
Representatives on Council of Local Sections:
R. R. ROGERS (1 yr) AND E. A. HOLLINGSHEAD (2 yr)

India
M. S. THACKER, Chairman
P. S. NARAYANA, Vice-Chairman
K. RAJAGOPAL, Vice-Chairman
T. L. RAMA CHAR, Treasurer
J. BALACHANDRA, Secretary
Indian Institute of Science
Bangalore 3, India
Representatives on Council of Local Sections:
B. K. RAM PRASAD AND V. M. DOKRAS

(*Continued from page 250C*)

lytic oxidation and reduction of organic and inorganic compounds, anodic manufacture of ozone, electrolysis of sodium sulfate; electrophoresis, electroendosmosis, desalting of water by means of the electric current; manufacture of chlorine and alkali, and of chlorine from aqueous hydrochloric acid, electrolytic manufacture of hypochlorites, chlorates and perchlorates; and ion exchange materials. In addition, uses of products of electrolyses in the chemical industry are described, for example the manufacture of 80–99% hydrogen peroxide.

The author has written historical and theoretical introductions to the various subjects, and has then taken up cell design and operation in detail. Most attention has been given to processes of greatest industrial importance, including European practices.

The book is recommended to those interested in industrial electrochemistry.

SHERLOCK SWANN, JR.

ANNOUNCEMENTS FROM PUBLISHERS

SELF-DIFFUSION IN CRYSTALLINE SOLIDS AND IN LIQUIDS by N. H. Nachtrieb, University of Chicago, for Wright Air Development Center, Dec. 1954. Available as report PB 121066.* 72 pages, $2.00.

INVESTIGATION OF METHODS OF PRODUCING SINGLE CRYSTALS OF NON-METALLIC FERROMAGNETIC SUBSTANCES by J. Koenig, Brush Labs., for Air Force Cambridge Research Center. Available as report PB 111934.* 66 pages, $1.75. (Available also on microcards from Photoduplication Service, Library of Congress, Washington 25, D. C., price $2.40.)

ATOMS AND ENERGY by H. S. W. Massey. Published by Philosophical Library, New York, N. Y., 1956. 174 pages, $4.75. Nontechnical.

CATALYSIS, Vol. IV. Hydrocarbon Synthesis, Hydrogenation and Cyclization. Paul H. Emmett, Editor. Published by Reinhold Publishing Corp., New York, N. Y., 1956. vi + 570 pages, $12.50.

SODIUM, Its Manufacture, Properties, and Uses. By Marshall Sittig. ACS Monograph No. 133. Published by Reinhold Publishing Corp., New York, N. Y., 1956. viii + 529 pages, $12.50.

THE PETROLEUM REFINERY ENGINEER'S HANDBOOK by J. F. Strachan. Published by Philosophical Library, New York, N. Y., 1956. xv + 168 pages, $15.00.

CZECHOSLOVAK FINE CHEMICALS STANDARDS, Vol. I. Compiled by a committee of the Czechoslovak Standard Institution. Published by Chemapol, Prague, Czechoslovakia, 1955. 540 pages (in English).

*Order from Office of Technical Services, U. S. Dept. of Commerce, Washington 25, D. C.

LITERATURE FROM INDUSTRY

FILTER PUMP UNITS. Newly designed filter pumps for highly corrosive solutions are described in Bulletin 102. Various plastics, Lucite, rigid P.V.C. polyethylene, etc., and corrosion-resistant metals are used. Pumps are self-priming, leakproof, centrifugal type, all plastic, and incorporate backwashing features. Particles down to 1 μ can be removed from solutions. Specific filtration equipment is described for solving special problems. Complete price sheets are enclosed. *Sethco Mfg. Co.*, 70–78 Willoughby St., Brooklyn 1, N. Y.

ETUDES SUR LE GALLIUM. Booklet describes a new method for extracting gallium from the aluminate liquors of the Bayer process for the production of alumina. The new process yields gallium of a minimum purity of 99.95% which is available in pound lots at reasonable prices. Intermetallic compounds of gallium offer new possibilities in the semiconductor field. *Aluminium-Industrie-Aktien-Gesellschaft*, Research Labs., Neuhausen a/Rhf., Switzerland.

"DOW SODIUM ORTHOSILICATE." New booklet discusses various metal cleaning and laundry applications of the chemical, and concisely presents physical and chemical properties, packaging, and safety precautions. Sections on electrolytic and spray cleaning point up advantages of the chemical with special attention drawn to sodium orthosilicate's high electrical conductivity, good emulsification and saponification characteristics, and its high *p*H and acid capacities. Dip and soak cleaning is also reviewed. Copies available at all Dow sales offices or from *Chlor-Alkali Sales, The Dow Chemical Co.*, Midland, Mich.

EXIDE BATTERY CATALOGUE describes improvements in stationary batteries which are expected to extend service life up to 10% and reduce maintenance requirements. Devoted to Exide-Tytex flat-plate batteries, the catalogue features a new battery grid alloy and plastic containers. When writing for the catalogue, specify Form 5907. *The Electric Storage Battery Co.*, Dept. TC, Exide Industrial Div., Box 8109, Philadelphia 1, Pa.

EMPLOYMENT PRACTICES CRITERIA. Printed copies of the employment practices criteria adopted by the National Society of Professional Engineers are available. Printed in check-list format, the criteria cover specific categories of engineering career development. Topics included are recruitment, indoctrination, professional development of the individual, salaries, engineering titles, personnel practices, and termination policies. Price: single copies, 25¢ each; quantity orders, 10–49 copies, 20¢ each; 50–99 copies, 15¢ each; 100 or more, 1¢ each. *National Society of Professional Engineers*, 2029 K St., N. W., Washington, D. C.

To receive further information on any New Product or Literature from Industry listed write directly to the company at the address given in each item.

ADVERTISERS' INDEX

Bell Telephone Laboratories, Inc. 64
Dow Chemical Company 242C
E. I. du Pont de Nemours & Company, Inc. 244C
Enthone, Incorporated ... Cover 4
Great Lakes Carbon Corporation ..... Cover 2
National Carbon Company ...238C–239C
Stackpole Carbon Company . 241C
John Wiley & Sons, Inc. 240C